# Alternative fuel application on high-speed pilot vessels

## Technical feasibility study

Msc. Thesis report

Thomas Havenga

Delft University of Technology

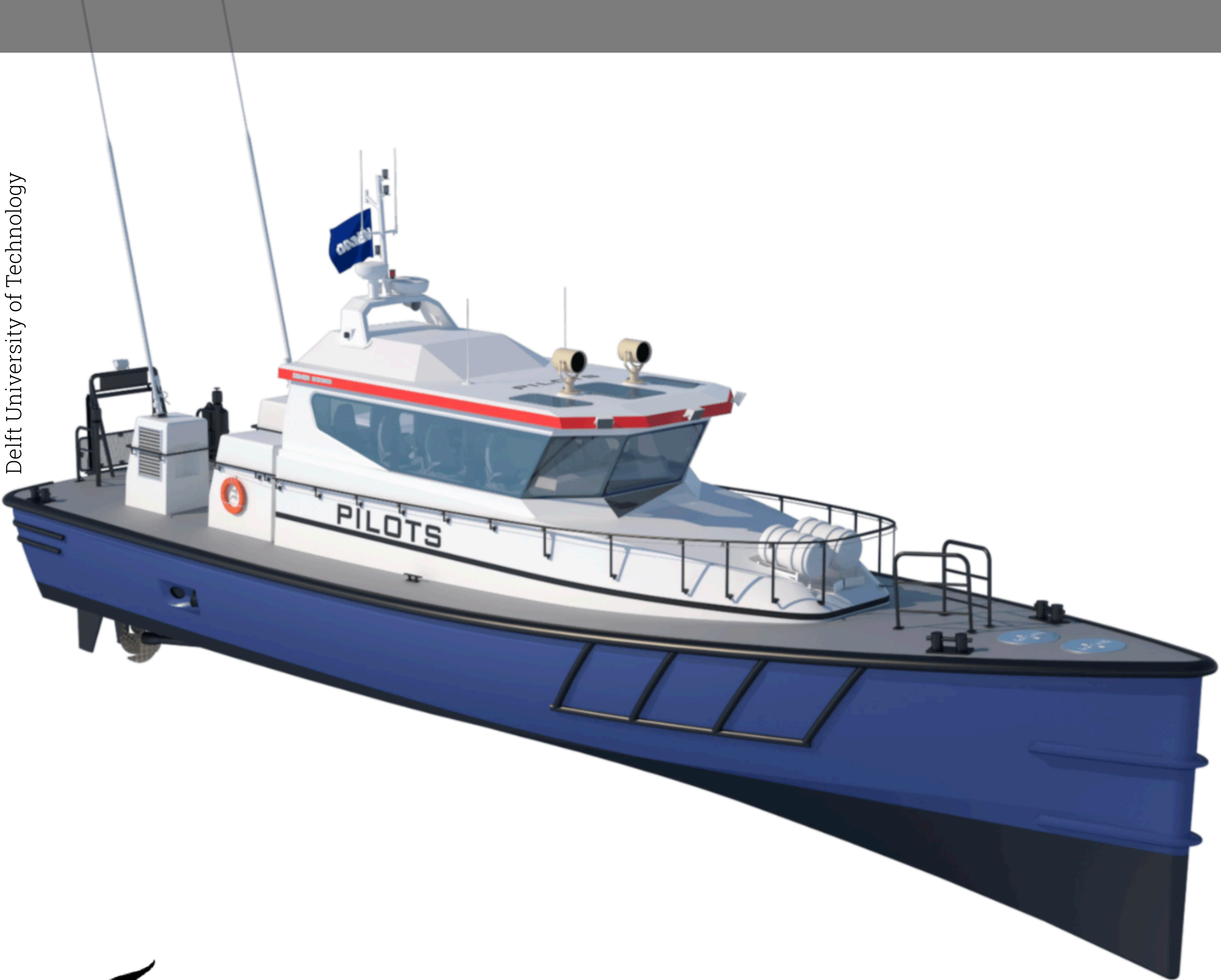

Thesis for the degree of MSc in Marine Technology in the specialisation of Ship Design

# Alternative fuel application on high-speed pilot vessels

## Technical feasibility study

by

Thomas Havenga

Performed at

Damen Shipyards

This thesis **MT.24/25.007.M** is classified as confidential in accordance with the general conditions for projects performed by the TUDelft.

Delft, Tuesday $15^{th}$ October, 2024

**Company supervisors**

| | |
|---|---|
| Responsible supervisor: | ir. T. Boxma |

**Thesis exam committee**

| | |
|---|---|
| Chair/Responsible Professor: | Dr. ir. P. de Vos |
| Staff Member: | ir. J. Gelling |
| Staff Member: | Dr. ir. A. Coraddu |
| Company Member: | ir. T. Boxma |

# Preface

When I started studying seven years ago, I had yet to learn what the study included. With ups and downs, I managed to work my way through the courses quite successfully, apart from the first year. After my first year I understood the trick of studying, resulting in not a single retake until my final master course in economics...

Then, when I was ready to start with my thesis, I again had no clue how to tackle this process. With some courage and luck, I managed to do my thesis at the RD&I department of Damen Shipyards, resulting in the following research: A technical feasibility study into alternative fuel application on high-speed pilot vessels in the Rotterdam harbour.

I want to thank the development workboats team, especially Timo, for their support, help, and helpful criticism. In addition to their help and the created workspace, the ambience made it fun to go to the office. Insight into their work principles gave me a peek preview into the 'real world'.

I also wish to extend my sincere thanks to Jaap Gelling. His willingness to assist me with my thesis project at Damen, despite it being already set in principle, was a significant turning point. His expertise in the design of the SPi 2206 FRP and the use of high-speed pilot vessels profoundly influenced my understanding of these vessels' potential. His feedback on my work was not just helpful, but instrumental in shaping my perspective. I want to thank Peter de Vos for being my graduation chairman; even though he was not very involved in my process, he had critical notes on my thesis, helping me achieve a better result.

Finally, I want to thank my family, friends, and roommates for their continuous support and tolerance. Their feedback, jokes, and distractions made my 10-month journey a truly memorable event. After my graduation, I'm happy to stay with the Damen family and explore the future ahead of me!

*Thomas Havenga*
*Delft, October 2024*

# Summary


In every major port, pilot vessels operate to transport pilots to and from seagoing vessels. This is done using small, high-speed diesel-powered vessels. Given that these vessels primarily operate within ECAs, reducing their emissions is increasingly critical. Consequently, this study investigates the technical feasibility of applying alternative fuel driven technologies and operational measures for pilot vessels that limit the formation of harmful emissions.

The considered fuels to reduce emissions are methanol, ammonia, and hydrogen. With all three, the emission of $SO_x$ and PM are diminished, $CO_2$ and $NO_x$ are reduced. Ammonia and hydrogen emit no $CO_2$ as these fuels are carbon-free. The storage method of alternative fuels is essential to increase energy density .In contrast to diesel, methanol, ammonia, and hydrogen can be converted into energy by both an ICE and a FC. In the ICE designs, due to the ongoing development of high-speed engines, the original diesel ICE has been used as a benchmark for size, weight, and power output. Consequently, both systems have been utilized for every fuel, resulting in six designs.

To adapt the designs for operation in the Port of Rotterdam, the use of pilot boats in the Rotterdam harbor has been analyzed. To align with the current operational profile of the Lynx, a maximum speed of 29 knots and 1800 liters of diesel equivalent energy seem necessary. However, the maximum speed can be reduced while keeping the operational profile equal. By lowering the maximum speed to 25 knots, the distance covered decreases by only 0.26%, while fuel consumption is reduced by 20% due to a lower required installed power. The operational profile can therefore be sustained with a maximum speed of 25 knots and a fuel capacity of 1400 liters diesel equivalent. With the application of alternative fuels safety requirements need to be implemented that influence the layout. A cofferdam surrounding the tanks to limit leaks is mandatory. Additionally, a fuel preparation room must be established, in which all fuel systems are located. This space is air and water-tight and is separated from the fuel cell or fuel storage room.

The necessary system components for the six designs have been assembled based on the required power, range, and class regulations. Due to varying efficiencies, each design has a different amount of fuel and corresponding energy installed. To compare the ICE and FC designs, the power on the propeller shafts is matched. The FC designs are equipped with electrically propelled rotating pods, improving the maneuverability at high and low speeds. The identified components, combined with the stripped SPi 2205 FRP hull, determine the new ship weight. To maintain the vessel's performance characteristics similar to the original design, preserving trim is crucial. Using Rhinoceros, all components were modeled within the hull, allowing for center of gravity calculations to ensure trim stability in the layout. The resistance of the designs changes due to the new ship weight. The installed power must be sufficient to overcome the increased resistance.

The ICE hydrogen design is not technically feasible as the required fuel capacity cannot be installed. All other designs meet the design requirements, match the trim, have sufficient installed power and transverse stability. The ship weight across the six designs varies by no more than 6% compared to the original, the trim varies by a maximum of 7 cm, and the GM is above 1.6 meters for all designs. The main difference is the presence of an accommodation or small bathroom. There is no best solution; the owner's preference, the shipyard's experience, and the availability of the fuel influence the specific design choice. The ammonia designs are yet not possible due to the low TLR. The FC hydrogen design is realistic on the short term. However, the ICE methanol design will result in the best design if the methanol single fuel ICEs are developed for this application.

# Contents

# List of Figures

# List of Tables

# Nomenclature

## Abbreviations

| Abbreviation | Definition |
|---|---|
| AIS | Automatic Identification System |
| CCS | Carbon Capture and Storage |
| CHP | Combined Heat and Power |
| CI | Compression-Ignited |
| CFD | Computational fluid dynamics |
| CO | Carbon monoxide |
| $CO_2$ | Carbon dioxide |
| DI | Direct Injection |
| ECAs | Emission Control Areas |
| EFD | Energy Flow Diagram |
| EGTS | Exhaust Gas Treatment Systems |
| FEM | Finite Element Method |
| FC | Fuel cell |
| GHG | Greenhouse gas |
| GM | Metacentric Height |
| GWP | Global warming potential |
| HCCI | Homogeneous Charge Compression Ignition |
| HVO | Hydrotreated Vegetable Oil |
| HVAC | Heating, Ventilation and Air Conditioning |
| HT | High Temperature |
| ICE | Internal Combustion engine |
| IMO | International Maritime Organisation |
| LCB | Longitudinal Center of Buoyancy |
| LCG | Longitudinal Center of Gravity |
| LFP | Lithium FerroPhosphate (Battery) |
| LHV | Lower Heating Value |
| LNG | Liquid Natural Gas |
| LT | Low Temperature |
| MSR | Methanol Steam Reformer |
| NMC | Nickel Manganese Cobalt (Battery) |
| $NO_x$ | Nitrogen oxide |
| PCCI | Premixed Charge Compression Ignition |
| PEMFC | Proton Exchange Membrane Fuel Cell |
| PM | Particulate Matter |
| PTO | Power Take-Off |
| PSD | Propulsion Selection Diagram |
| RCCI | Reactivity controlled compression ignition |
| rpm | rounds per minute |
| SCR | Selective Catalytic Reduction |
| SI | Spark-Ignited |
| SLD | Single Line Diagram |
| SoG | Speed over Ground |
| SoW | Speed over Water |
| $SO_x$ | Sulfur oxide |
| SOFC | Solid Oxide Fuel Cell |

| Abbreviation | Definition |
|---|---|
| STP | Standard Temperature and Pressure |
| TRL | Technical Readiness Level |
| UHC | Unburned Hydrocarbons |
| VCG | Vertical Center of Gravity |
| WtT | Well-to-Tank |
| WtW | Well-to-Wheel |

# Symbols

| Symbol | Definition | Unit |
|---|---|---|
| $P_b$ | brake power | [kW] |
| $\dot{m}_f$ | mass flow | [g/s] |
| $h^L$ | lower heating value | [MJ/kg] |
| $\eta$ | Efficiency | [%] |

# 1 Introduction

The piloting of seagoing vessels has been practiced since the Greek era. During that period, sailing ships were guided by fishermen to safely reach harbors that were unfamiliar to the captains. While this was originally done using small rowing or sailing boats, it is now carried out by fast, diesel-powered pilot boats. The size and operational speed of these boats have evolved alongside the increasing scale of modern seagoing vessels. These pilot boats are designed and constructed by companies such as Damen. The Damen designed vessels can sail at high speed and have excellent seakeeping performance due to their Axe Bow concept design. The operation speed of 30 knots requires a high power output, resulting in serious fuel consumption and corresponding emissions as these vessels sail on diesel. To address this issue, the required operational speed and range can be optimized based on data collected from pilot vessels operating in the Rotterdam harbor. To further reduce emissions during operation, enhancements in energy generation are necessary. A substitute power generation system, distinct from diesel fueled, would necessitate increased spatial allocation due to the lower density of the alternative fuel, the requisite adjustments in the fuel storage infrastructure and possible lower engine or fuel cell efficiencies. Consequently, modifications to the hull design may be imperative within the design process. Implementation of greenhouse gas (GHG) reducing fuels has been done with several vessel types, such as electric sailing ferries or hydrogen fuelled barges. However, for small high-speed vessels like a pilot vessel fuels other than diesel have yet not been implemented.

Given that GHG - reducing fuels occupy more space than the original diesel configuration, the investigation will encompass possible modifications to the hull design. Small changes in hull dimensions might enable the implementation of alternative fuels, which will yield distinct water resistance profiles, thereby influencing propulsion efficiency differentially. Identifying the optimal alignment between hull design, propulsion system, and fuel type, while adhering to an acceptable range and speed, poses a significant challenge.

## 1.1. Problem definition

As Dutch pilot vessels operate in Emission Control Areas (ECAs), their operator 'het Loodswezen' feels the responsibility to reduce their fuel consumption and strive for a switch towards zero emission sailing as they are a key player in their main port Rotterdam. The elimination of sulfur oxide ($SO_x$) and particle matter (PM) and the significant reduction of nitrogen oxide ($NO_x$) and carbon dioxide ($CO_2$) is critical in sailing towards zero emission. The relatively small pilot vessels sail at a Froude number above 1.5, this requires an energy-dense propulsion system and results in limited space for fuel storage. Integrating an alternative fuel with a lower energy density requires a critical review of vessel usage and the corresponding load profile. Compared with conventional seagoing vessels, the fuel storage is already limited. However, as pilot vessels operate close to shore, a more frequent bunker schedule is possible.

## 1.2. Research objectives

To address the problem statement, a research question has been formulated. This main question will be answered through sub-questions categorized by subtopic.

**Is it technical feasible to integrate alternative fuel based technologies in pilot vessels, with a particular emphasis on the technical aspects and layout design considerations, using the Stan Pilot 2205 design as a framework for investigation?**

### Alternative fuels

- What is the energy density, and how are the storage conditions of the possible alternative fuels?
- What are the emissions related to the possible alternative fuels?
- How is the Technical Readiness Level (TRL) of the possible alternative fuels?

### Power generation systems

- What are the operational principles of Internal Combustion Engines (ICE) and fuel cells (FCs)?
- What are the energy conversion efficiencies associated with ICEs and FCs for alternative fuels?

### Design inputs

- What is the energy demand based on the load profiles of the 'Loodswezen' pilot vessels?
- How do the necessary safety regulations affect the vessel design?

### System and layout design

- What is the effect an alternative fuel propulsion system on the speed and range?
- What is the size and weight of an alternative fuel propulsion system for a required power and range?
- What is the impact of an alternative fuel propulsion system on the resistance and speed of the pilot vessel?

The sub-questions will be answered throughout the report to support the research question. The first three sub-questions regarding alternative fuels will be answered in chapter 2. With this better understanding of possible fuels and the associated power generation systems, the next two sub-questions will be answered in chapter 3. The first five sub-questions form the basis for the initial literature study. The following two sub-questions determine the design inputs for the new design; the results are gathered in chapter 6 but are answered in chapters 4 and 5, respectively. The last three sub-questions guide the design method and evaluate decisions made in the process; these questions are answered in chapters 7 and 8.

## 1.3. Scope

It is essential to frame the scope of this feasibility study to construct an executable research in the given timetable. Therefore, several aspects are excluded. The limitations of this research are given below:

- End-of-pipe emission reducing technologies. Although some are described in the literature, these technologies are not included in the final designs.
- Vessel dimension changes, the Stan Pilot 2205 FRP is used with its original dimensions. Changing the vessel dimensions might lead to a different resistance and seakeaping behaviour.
- Dynamic simulation of power across all system components during operation.
- The financial aspects are excluded as this study focuses on the technical feasibility. Furthermore, the fuel and machinery costs are challenging to predict because of the rapid development in technology and availability.
- Auxiliary systems, these systems are assumed as a constant factor in the preliminary design.

- Computational Fluid Dynamics (CFD) resistance and Finite Element Method (FEM) hull calculations will not be executed. CFD calculations are relevant for hull design optimization, FEM calculations determine the hull strength. Both are not part of the preliminary design but are relevant for further design stages.
- Well-to-tank (WtT) emissions, this study focuses on the fuel processing on board of the vessel.
- In this research a distinction in emissions is made, $CO_2$, $NO_x$, $SO_x$ and PM are elaborated. More emissions as $CH_4$, $N_2O$, CO and VOC are not taken into account to compare possible alternative fuels but are mentioned when significant for that fuel.
- Complex power generation system with combinations of ICEs and FCs are not taken into account due to the complexity and limited research time. However, integrating these systems might lead to an higher overall efficiency

## 1.4. Gap analysis

Implementing alternative fuels on high-speed vessels of roughly 20 meters has yet to be done; no vessels are sailing with another fuel than diesel or diesel hybrid. Furthermore, there are few publications on design concepts in this category. This results in a wide gap to fill. There are designs for smaller hydrogen or electric sailing vessels and larger electric, methanol, and hydrogen sailing vessels. Despite the gap, the developments in both larger and smaller high-speed vessel types show the possibilities for alternative propulsion implementation. Especially a study in Sweden where a 13-meter pilot vessel is retrofitted with a methanol internal combustion engine [66]. One of two engines in this vessel is replaced, leaving a diesel engine onboard. This study gives insight into the required system components and safety aspects for sailing on methanol with a small vessel.

# Part I

# Literature study

# 2 Alternative fuels

A wide range of fuels has been researched over the last decades as possible substitutes for diesel. In this study, this spectrum is narrowed to a few fuels with the best potential: Bio-diesel, Liquid Natural Gas (LNG), Methanol, Ammonia, Hydrogen, and batteries. Some fuels can be stored at different densities based on the storage conditions, the most promising conditions will be discussed. The implementation of alternative fuels for diesel is a difficult task as storage requirements, energy density, safety, and energy conversion differ from diesel. Therefore, each alternative fuel is reflected in three research questions:

- What is the energy density, and how are the storage conditions of the possible alternative fuels?
- What are the emissions related to the possible alternative fuels?
- What is the Technical Readiness Level (TRL) of the possible alternative fuels

Given the numerous alternative fuels currently under research, a comprehensive analysis of all options falls outside the scope of this study. Consequently, the selection of fuels deemed suitable and most favorable includes HVO, LNG, Methanol, Ammonia, and Hydrogen. Diesel is used as a benchmark against which all other fuels are compared. Another viable solution for reducing emissions is the integration of a battery pack with an electric motor. Emissions are categorized into GHGs and pollutant emissions. Examples of GHGs include $CO_2$, carbon monoxide (CO), and methane, while $O_x$, $NO_x$, and PM are considered harmful local pollutants. To accurately assess a fuel's emissions, the entire life cycle must be considered. However, this study focuses on vessel design, and therefore WtT emissions are excluded from the analysis. Zero emission is achieved when no carbon is present in the fuel cycle. Neutral emission occurs when the carbon in the fuel is offset by its removal from the air during production. For each fuel, a TRL is assigned based on the European Union standard. Although TRL definitions for some fuels may not be explicitly detailed in the literature, they are determined according to EU standards.

## 2.1. Marine gas oil/ Diesel oil

Marine gas oil or diesel oil is currently the most commonly used fuel in high-speed marine engines. The favourable energy density, accessible storage, and low bunker prices resulted in world domination. The combustion of diesel results in significant emissions worldwide. To reduce the impact of the marine sector on the global GHG emissions diesel usage needs to be reduced. As diesel is a liquid with a density of 840 kg $m^{-3}$ at standard temperature and pressure (STP), storage on board is straightforward and without energy losses. As the chemical composition of diesel variates between $C_{10}H_{20}$ and $C_{15}H_{28}$ [10], the combustion efficiency will differ with various types of diesel. As carbon atoms are present, carbon dioxide will be produced during combustion. However, the usage of a single type of diesel is created by diesel standards (the EN590 in Europe). As a result, extensive information is available on emissions and engine efficiency. Diesel has a high gravimetric and volumetric Lower Heating Value (LHV) of 43 MJ $kg^{-1}$ and 36.1 MJ $dm^{-3}$ respectively [10]. The combustion of diesel results in the emission of $CO_2$, $NO_x$, PM, and small amounts of $SO_x$. The safety aspects regarding diesel usage are well known, therefore, diesel safety, storage, and conversion efficiency will be used as a reference for other fuels.

## 2.2. Hydrotreated Vegetable Oil

Hydrotreated Vegetable Oil (HVO) is a renewable diesel based on various fats and oils. As a renewable diesel, storage is at STP. As these oils differ in molecular structure, the resulting HVO structure is unstable with $C_nH2_{n+2}$ [80]. HVO does not contain aromatics or sulfur, which results in clean combustion without producing $SO_x$. However, $CO_2$, PM, and $NO_x$ are still emitted. HVO, with a density of 780 kg $m^{-3}$, can be stored in fuel tanks like diesel without extra space needed. The gravimetric and volumetric LHV are comparable with diesel with 44 MJ $kg^{-1}$ and 34.3 MJ $dm^{-3}$ respectively. In the production of HVO, hydrogen reacts with the oil to remove oxygen at high pressure. HVO is still produced on a limited scale compared to diesel. HVO can be used in conventional diesel engines without alterations, resulting in a quick implementation. Volvo approved the usage of HVO in marine applications, resulting in a reduction of 90% $CO_2$ emission [64]. HVO as fuel has a TRL of 9 but the implementation into marine applications is not yet in the trial stage resulting in a TRL of 6.

## 2.3. Liquid Natural Gas

Liquid Natural Gas is a combination of gasses, mainly Methane ($CH_4$) and some butane and propane. Methane is voluminous at STP. Therefore, it is stored in liquid form at 111 Kelvin in cryogenic tanks to achieve a higher density of 430 kg $m^{-3}$ [10]. At this density a gravimetric and volumetric energy density of 49 MJ $kg^{-1}$ and 21.1 MJ $dm^{-3}$ is reached. Storing fuel at such low temperatures presents significant technical and safety challenges. Metals can lose their strength and functionality due to embrittlement at low temperatures [79]. LNG can result in cold burn when it is in contact with the skin, inhaling the cold vapour can cause freezing of the lungs and airways. However, since LNG began being used on vessels in 2000, particularly on LNG tankers utilizing the boil-off principle, the technology for storing and converting LNG into energy has become well-established and widely adopted over the past decades. Therefore, the TRL of LNG is 9 [89]. Natural gas is extracted out of the ground, similar to diesel. Methane can be produced carbon neutral with green hydrogen and carbon dioxide, it then becomes E-Methane.

Methane is a strong GHG as it has a Global warming potential (GWP) rating of 27.2 with a non-fossil origin, so controlling the methane slip is essential [38]. Methane has a higher H/C ratio than diesel, creating a lower $CO_2$ emission per kWh. Methane combusts at a higher temperature than diesel, resulting in a possible higher $NO_x$ emission as these are formed at high temperatures and pressures. The PM emission is reduced as well by the high H/C ratio, and $SO_x$ emission is eliminated by using LNG. Burning the boil-off gasses of the abundant storage onboard those vessels increases energy efficiency. Unburned methane poses a risk as it contributes to GHG emissions; therefore, a sufficiently robust engine design is required. Bio-LNG can be produced with Liquefied Bio Gas made by compressing biomass. A carbon-neutral method to produce methane combines $CO_2$ and hydrogen ($H_2$) from electrolysis based on green electricity. Besides ICEs, LNG can be used directly inside a Solid Oxide Fuel Cell (SOFC).

## 2.4. Methanol

Methanol is the simplest alcohol structure ($CH_3OH$) and has similarities to methane. Methanol is flammable and toxic. Accidentally ingesting small concentrations of methanol can result in blindness, at higher concentrations methanol is lethal [79]. As there is an oxygen atom, the extra hydrogen bonding on top of the standard Van Der Waal connection results in a liquid form at STP and a density of 790 kg $m^{-3}$ [87]. Methanol has a significantly lower gravimetric and volumetric LHV than LNG with 20.1 MJ $kg^{-1}$ and 15.9 MJ $dm^{-3}$ respectively. Methanol can reduce $SO_x$, $NO_x$ and PM emissions with respectively 99%, 80%, and 85% compared to HFO [36]. Methanol can be used in an ICE as a single or dual fuel. Furthermore, methanol can be used directly or after hydrogen extraction in a FC. With a Proton Exchange Membrane Fuel Cell (PEMFC), hydrogen cracking is necessary, inside a SOFC direct use is possible. Like methane/LNG, methanol is currently produced from fossil fuels, but with electrolysis and green electricity, it can be produced in a carbon-neutral way [10]. The TRL of Methanol as dual fuel is 8 with a proven and qualified concept in marine application, taking into account that this is still with fossil-based methanol [89]. Soon, various vessels will be constructed using methanol as fuel, leading to a higher TRL [52] [29]. In contrast, the use of fuel cells remains at a lower TRL. Methanol can be produced in various ways, as shown in figure 2.1. The production methods are ranked based on their carbon footprint; for methanol to be a clean alternative fuel green methanol is necessary. Therefore, E-methanol and Bio-methanol are the best types of methanol. However, it is acceptable to use the more polluting but available methanol production methods to stimulate the development of methanol vessels, as the production of green methanol is still limited.

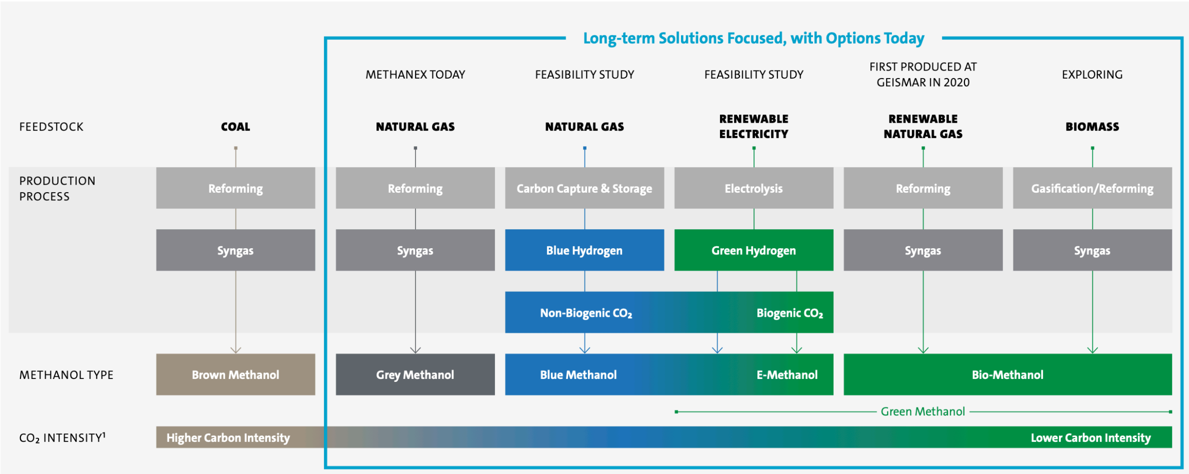


**Figure 2.1:** Production methods methanol [55]

The GreenPilot project in Sweden investigated the feasibility of methanol combustion onboard of a 12-meter pilot vessel [67]. One of the two diesel engines was replaced by a methanol-fueled engine, three different engines were tested. This resulted in a high emission reduction and an engine efficiency of 37-40%. The necessary safety aspects were taken into account as this vessel did sea trails, providing an excellent example of alternative fuel system implementation. However, the vessel size difference between the GreenPilot and the Damen Stan Patrol 2205 is significant, a direct comparison between the two vessels is difficult.

## 2.5. Ammonia

Ammonia ($NH_3$) is a carbon-free fuel that can be used in an ICE or FC. It performs well as a hydrogen carrier with a mass percentage of 17 wt% [23] when stored at 239.9 Kelvin. Ammonia has a density of 682 kg $m^{-3}$ and a gravimetric and volumetric LHV of 18.8 MJ $kg^{-1}$ and 12.8 MJ $dm^{-3}$ at 239.9 Kelvin [51]. As ammonia is used as fertilizer in the agricultural sector, the storage and transportation of ammonia have been well-established for many years. No carbons are present in the fuel, resulting in a complete $CO_2$-free combustion in an ICE. Ammonia can be burned in a spark-ignited (SI) ICE and combustion-ignited (CI) ICE; the results, however, differ. Pure ammonia performs well in an SI-ICE, but in a CI-ICE, small amounts of, for example, diesel are needed for acceptable performance [23]. In both engine configurations, injection timing is crucial in reducing the fuel slip, as ammonia is toxic. Furthermore, burning ammonia still results in large amounts of $NO_x$; exhaust gas after treatment is therefore required. Ammonia can be used in SOFC and High Temperature PEMFC (HT-PEMFC). In a SOFC direct injection is possible, for PEMFC applications hydrogen cracking is required. Ammonia has severe safety concerns as it is highly toxic. Liquified ammonia can lead to caustic irritations and severe burns to the skin. Ammonia vapour can enter the deeper airways and damage the lungs [79]. The TRL of ammonia is still at level 5 as the first marine application still has to be built. Similar to methanol, the production methods of ammonia are color-categorized based on the carbon footprint as shown in figure 2.1. Therefore, applying green ammonia results in the largest impact on emission reduction.

## 2.6. Hydrogen

The research into hydrogen as an energy source is older than diesel as the first hydrogen fuel cell was investigated in 1843 [33]. Hydrogen is the cleanest form of alternative energy, as no carbon or sulfur atoms are present. However, the production determines the level of emission. The production of hydrogen is categorized by color into Grey, Blue, and Green hydrogen [39]. Grey hydrogen production encompasses all methods that rely on fossil fuels, such as coal, oil, or natural gas, and this process results in the release of $CO_2$. Using the same process but with carbon capture and storage (CCS), the grey hydrogen transforms to blue hydrogen and becomes carbon neutral. Hydro, solar, or wind energy used to produce electricity for electrolysis is called green hydrogen and produces the cleanest hydrogen without emissions. However, the current production of green hydrogen is nearly negligible, amounting to just 35 kt (0.004%) out of a total of 900 Mt of hydrogen produced in 2021 [2]. The future outlook shows significant growth in green production as the production will rise to 27 Mt in 2030 [3].

Hydrogen can be converted into mechanical energy using an ICE or electricity with a FC. Pure hydrogen usage is possible in a SI-ICE but not in a CI-ICE. However, using hydrogen in addition to diesel in a dual-fuel CI-ICE does reduce emissions significantly [13]. Hydrogen usage in a FC eliminates emissions; both PEMFC and SOFC are suitable. The small molecular size of hydrogen results in poor storage conditions at STP with 0.0824 g $L^{-1}$ [82]. The density can be improved by storing hydrogen using various techniques, as shown in figure 2.2. With a lower heating value of 120 MJ $kg^{-1}$, hydrogen shows potential as an energy carrier. This study will discuss the physical-based storage techniques and storage in complex hydrates ($NaBH_4$). Hydrogen is non-toxic but flammable, colourless, and burns with a hardly visible flame [79].

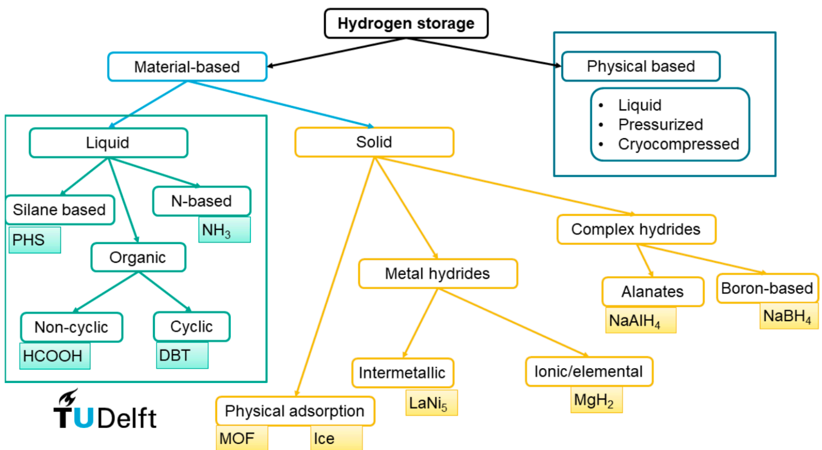


**Figure 2.2:** Various hydrogen storage principles. [85]

### Compressed hydrogen

The most straightforward technique of hydrogen storage is compression. The compression pressure increased over the years from 100 up to 700 bar. The most common storage conditions are 350 and 700 bar, these two will be investigated. As pressure increased, storage tanks were engineered to contain hydrogen, which, due to its status as the smallest molecule, demands highly precise and robust techniques. The currently used tanks for storage at 700 bar are classified as Type III and Type IV. The type III tank uses a metal liner with a composite overwrap, whereas the type IV is all composite [71]. The hydrogen storage at 350 bar has a density of 23 kg $m^{-3}$ and volumetric LHV or 2.7 MJ $dm^{-3}$, increasing the pressure up to 700 bar provides in a density of 39 kg $m^{-3}$ and volumetric LHV or 4.7 MJ $dm^{-3}$. However, compressing hydrogen results in a loss of 24 MJ $kg^{-1}$ of the original energy [44]. Furthermore, storing hydrogen in tanks results in additional required space and added weight. The cylindrical tanks require more volume, therefore the gross volumetric energy density decreases, the specifications for the storage at 350 and 700 bar are given in table 2.1.

**Table 2.1:** Hydrogen storage tank specifications for both compressed and liquid storage

| | **350 bar** [18] | **700 bar** [19] | **Liquid** [20] | **Unit** |
|---|---|---|---|---|
| Net mass | 6.2 | 10.4 | 40 | kg |
| Gross mass | 132 | 250 | 400 | kg |
| Net density | 23 | 39 | 71 | kg $m^{-3}$ |
| Gross density | 294 | 555 | 358 | kg $m^{-3}$ |
| Length tank | 2.6 | 2.6 | 2.5 | m |
| Net volume | 0.27 | 0.27 | 0.57 | $m^3$ |
| Gross volume | 0.47 | 0.47 | 1.26 | $m^3$ |
| Net gravimetric energy density | 120 | 120 | 120 | MJ $kg^{-1}$ |
| Gross gravimetric energy density | 9.11 | 3.84 | 10.9 | MJ $kg^{-1}$ |
| Net volumetric energy density | 2.7 | 4.7 | 8.5 | MJ $dm^{-3}$ |
| Gross Volumetric energy density | 1.58 | 2.68 | 3.80 | MJ $dm^{-3}$ |

Compressed hydrogen is a proven concept on small scale, producing a TRL of 8 [14]. High-pressure storage is effective at all scales, the size of the tanks is limited, therefore tanks are stacked to achieve larger storage capacity and the tanks keep their original efficiency.

### Liquefied hydrogen

A more compact method of hydrogen storage is liquefying hydrogen. Cooled down to 20 Kelvin, hydrogen becomes liquid, resulting in a storage capacity of 71 kg/$m^{-3}$ and a volumetric LHV of 8.5 MJ $dm^{-3}$; this process requires 36 MJ $kg^{-1}$ but is expected to improve up to 21.6 MJ $kg^{-1}$ [9]. However, similar to compressed hydrogen the required tank reduces the volumetric and gravimetric energy densities as shown in table 2.1. The boil-off principle, similar to LNG, keeps the temperature in the tank constant. Therefore, additional cooling is not necessary. Liquefied hydrogen is a proven concept similar to compressed hydrogen, resulting in a TRL of 9 in the automobile industry [14]. However, as liquefied hydrogen is not yet used on a large scale in marine applications, a TRL of 8 is achieved. The storage of liquefied hydrogen is more effective at a large scale as the tank size is scalable.

### Sodium Borohydride

The storage of hydrogen can also be done at STP, using Sodium Borohydride, for example. Using sodium borohydride as a hydrogen carrier results in a circular process. Hydrogen is bound to the salt and released by adding water as shown in formula 2.1. In this formula, sodium metaborate combined with water is the byproduct [60].

$$NaBH_4 + (2+x)H_2O \rightarrow NaBO_2 \cdot xH_2O + 4H_2 \tag{2.1}$$

Sodium Borohydride is non-toxic, non-flammable, and non-explosive when kept dry [58]. In this carrier, a mass percentage of 10.7% is reached, resulting in a gravimetric energy density of 25.6 MJ $kg^{-1}$ and a volumetric energy density of 27.5 MJ $dm^{-3}$ [84]. The by-product can be re-used, by adding hydrogen under pressure $NaBH_4$ is recreated, and the process starts again. Therefore, the residual needs to be stored on board. This onboard storage asks for profound design alterations as twice as many storage tanks are needed or an intelligent re-use of fuel tanks is needed. Sodium Borohydride is a solid powder; its storage conditions can influence factors such as particle size distribution and surface characteristics. When stored in an increased moisturized environment, the material can change from a flowing powder to a non-flowing solid [84]. Most mechanical characteristics are still unknown, resulting in a low TRL of 6. This system is currently used in a concept design vessel, as an Amsterdam saloon boat is equipped with a Sodium Borohydride system in the EU subsidized project H2SHIPS [7].

## 2.7. Batteries

Batteries onboard are used as an electrical energy storage method. This electricity can be generated onboard using a FC, generator, or power take-off (PTO) on a gearbox. When charged by an onshore installation, the battery can be used as the primary energy source. For example, the Damen Ferry 2306 E3 has an electric motor with only batteries as energy storage [30]. Larger electrified vessels such as Sparky, an RSD Tug 2513 Electric, still have backup generators to guarantee their operational profile

[72]. Sailing with batteries as a primary energy source results in total zero-emission shipping. However, when looked at the holistic side, this is not the case [40]. Batteries as secondary energy sources can reduce fuel usage by peak shaving.

Battery technology has improved rapidly over the last decades. Whereas lead acid batteries were the known standard, Lithium-ion batteries made rapid technological improvements in specific energy density. Various compositions are developed for battery usage; most differences are at the cathode, as shown in table 2.2. Lithium FerroPhosphate (LFP) and Nichel Manganese Cobalt (NMC), in bold in table 2.2, are the most suitable candidates [8].

**Table 2.2:** Most common Lithium - Ion batteries [77]

| Type | Anode | Cathode | Energy Density (Wh/kg) |
|---|---|---|---|
| LCO | Graphite | Lithium Cobalt Oxide | 110-190 |
| **LFP** | **Graphite** | **Lithium Iron Phosphate** | **90-115** |
| LMO | Graphite | Lithium Manganese Oxide | 100-120 |
| LTO | Lithium Titanate | Graphite | 60-75 |
| NCA | Graphite | Lithium Nickel Cobalt Aluminium Oxide | 100-150 |
| **NMC** | **Graphite** | **Lithium Nickel Manganese Cobalt Oxide** | **100-170** |

State-of-the-art batteries expose the differences between lead-acid and lithium-ion, shown in table 2.3. The energy density of lead acid is both gravimetric and volumetric inferior to Lithium-ion. Still, lead-acid batteries are cheaper and safer as lithium-ion batteries are fragile and sensitive to water damage. Water damage to lithium-ion batteries can result in short circuits and fires that are difficult to extinguish. Furthermore, Lithium-ion charges faster but requires better temperature management as high temperatures can result in a thermal runaway and damage the battery extensively.

**Table 2.3:** State-of-the-art batteries specifications

| | Lead Acid AGM | LFP | NCM |
|---|---|---|---|
| Brand | Power Sonic [76] | AYK Energy [26] | EVOY [28] |
| Type | PDC-122000 | Aries+ | Evoy 69 |
| Energy (kWh) | 2.57 | 17.6 | 69.3 |
| Weight (kg) | 62.5 | 130 | 385 |
| Volume (L) | 35.1 | 84.3 | 312 |
| Gravimetric Energy Density (Wh $kg^{-1}$) | 41.1 | 135 | 180 |
| Volumetric Energy Density (Wh $L^{-1}$) | 73.2 | 209 | 222 |
| Cooling method | ambient | air | liquid |
| Continuous discharge | 0.1 C | 0.43 C | 2 C |
| Peak discharge | 10 C | 1.3 C | 4 C |

The NCM battery performs better on both gravimetric and volumetric density. The pilot vessel requires a high energy load as it sails at high speeds; therefore, the cooling of the battery is essential. The NCM has a higher cooling capacity with liquefied cooling. The difference in cathode material and energy density determines the batteries' stability. The LFP battery has a lower density but is safer as it is thermally and mechanically more stable and reacts less by overload or penetration than the NCM battery [61]. Still, in 2022 NCM batteries dominated the EV batteries with a 60% share proving acceptable safety risks [1]. The discharge rates between LFP and NCM differ, NCM can deliver more power at both continuous and peak discharge rate. The TRL of NCM batteries is 8, it is a proven concept in operation on a small scale in marine applications.

## 2.8. Bunkering

The bunker frequency of high-speed vessels is high compared with regular sea-going vessels. Therefore, bunker speeds are essential for pilot vessel operations. For Diesel, HVO, LNG, and Ammonia a speed of above 400 $m^3$ $h^{-1}$ is assumed possible [79]. For hydrogen, an acceptable bunker speed is more difficult to achieve due to the high pressure, low temperature, and small molecular size. However, a bunkering speed of 300 g $s^{-1}$ for gaseous hydrogen at 350 and 700 bar is expected in the automotive industry [35]. Liquid hydrogen can be bunkered at an indicated speed of 400 to 500 kg $h^{-1}$. The bunker time of gaseous hydrogen can be reduced by interchangeable containers placed on deck, creating a more flexible operational profile [31]. This principle is used in inland barges with similar operational profiles regarding bunker options.

## 2.9. Fuel overview

The described fuels in paragraphs 2.1 to 2.6 differ in chemical composition, storage conditions, safety aspects, and energy conversion. Therefore, these fuels are summarized and compared. Table 2.4 shows the chemical composition, storage conditions and TRL. The absence of carbon in ammonia and hydrogen is noticeable. The storage conditions require, in most cases, compressing or cooling, resulting in energy losses; the liquefaction process requires significantly more energy than compression. However, as this study focuses on the feasibility of alternative fuels on board, the energy losses in compressing or liquefying the fuel are not considered as this process is not done onboard the vessel. Of course, looking at the total well-to-wheel (WtW) energy consumption, these losses should be considered. The technical readiness level of all fuels is above level 5. Therefore, all fuels can be considered in the concept design stage.

**Table 2.4:** Chemical composition, storage conditions, and TRL of the investigated alternative fuels

| Fuel | Formula | Temperature (K) | Pressure (kPa) | TRL |
|---|---|---|---|---|
| Diesel | $C_{10}H_{20}$ - $C_{15}H_{28}$ | 298 | 101 | 9 |
| HVO | $C_nH_{2n+2}$ | 298 | 101 | 6 |
| LNG | $CH_4$ | 111 | 101 | 9 |
| Methanol | $CH_3OH$ | 298 | 101 | 8 |
| Ammonia | $NH_3$ | 239.9 | 101 | 5 |
| Hydrogen (g) | $H_2$ | 298 | 350000<br>700000 | 8 |
| Hydrogen (l) | $H_2$ | 20 | 101 | 8 |
| $NaBH_4$ | $NaBH_4$ | 298 | 101 | 6 |
| Batteries | NCM | 298 | 101 | 8 |

The volumetric- and gravimetric energy and energy conversion efficiency density are essential indicators of fuel performance. Table 2.5 shows the investigated fuels' density and LHV. The low volumetric energy density of both compressed and liquefied hydrogen shows the challenge of implementing hydrogen as more space is required. Methanol, ammonia and hydrogen can be used inside a FC. In all cases, hydrogen is necessary, and all other atoms in the fuel are residual. The hydrogen percentage in all fuels directly indicates the effective energy density; the losses in hydrogen extraction are, in this case, not taken into account but will be part of conversion efficiency.

**Table 2.5:** The density, lower heating value, and hydrogen substitute of the investigated alternative fuels

| Fuel | Density (kg $m^{-3}$) | LHV (MJ $kg^{-1}$) | LHV (MJ $dm^{-3}$) | $H_2$ wt% |
|---|---|---|---|---|
| Diesel | 840 | 43 | 36.1 | 13.96 |
| HVO | 780 | 44 | 34.3 | 15.01 |
| LNG | 430 | 49 | 21.1 | 25.13 |
| Methanol | 790 | 20.1 | 15.9 | 12.58 |
| Ammonia | 682 | 18.8 | 12.8 | 17.76 |
| Hydrogen 350 bar (g) | 294 | 9.11 | 1.58 | 100 |
| Hydrogen 700 bar (g) | 555 | 4.84 | 2.68 | 100 |
| Hydrogen (l) | 348 | 10.9 | 3.8 | 100 |
| $NaBH_4$ | 1074 | 25.6 | 27.5 | 10.66 |
| Batteries | 1234 | 0.648 | 0.799 | |

The current fuel standard in marine applications is diesel. Therefore, a direct comparison to diesel gives an understanding of the alternative fuels. Table 2.6 shows the investigated fuels' density, weight, and volume scaled to diesel. In this comparison, the volume needed for the same energy in diesel is the best indicator. Most fuels require more space than diesel for the same energy. However, LNG achieves a higher energy concentration per volume. Methanol and Ammonia are more than twice as voluminous, and pure hydrogen storage requires even more space. The indicated energy densities for hydrogen include the weight and volume of the storage tanks for a realistic comparison. Sodium Borohydride requires twice the storage space as there is a rest product that needs to be stored onboard, this is not included in the energy density.

**Table 2.6:** Density, weight, and volume of alternative fuels compared to diesel

| Fuel | Density (kg m$^{-3}$) | LHV (MJ kg$^{-1}$) | LHV (MJ dm$^{-3}$) |
|---|---|---|---|
| Diesel | 1.00 | 1.00 | 1.00 |
| HVO | 0.93 | 1.02 | 0.95 |
| LNG | 0.51 | 1.14 | 0.58 |
| Methanol | 0.94 | 0.47 | 0.44 |
| Ammonia | 0.81 | 0.44 | 0.35 |
| Hydrogen 350 bar (g) | 0.35 | 0.21 | 0.04 |
| Hydrogen 700 bar (g) | 0.66 | 0.11 | 0.07 |
| Hydrogen (l) | 0.41 | 0.25 | 0.11 |
| $NaBH_4$ | 1.28 | 0.60 | 0.76 |

## 2.10. Alternative fuel conclusion

Methanol, ammonia, and hydrogen densities are significantly lower than diesel. At the same time, these three fuels result in GHG and local harmful emissions. The use of HVO or LNG is not a clean and sustainable option in the long term but a short-term interim solution. Methane, as a substitution for LNG, can be produced with green energy, similar to methanol. However, methanol is preferred as the storage conditions are better; thus, energy losses are less than methane. The feasibility of batteries as single energy storage is deemed unattainable due to insufficient energy density. The application of $NaBH_4$ is not effective for high-speed vessel use because twice as much storage space is required to accommodate the residual slush. Liquid hydrogen is more effective for large-scale applications as the tank size increases. For gaseous hydrogen, the scaling towards larger applications is done by stacking multiple pressure tanks. Therefore, the implementation of gaseous hydrogen on a pilot vessel is relatively more effective than liquid hydrogen. Given the drawbacks of HVO, LNG, liquid hydrogen, and $NaBH_4$, methanol, ammonia, and gaseous hydrogen appear to be better suited for use in high-speed pilot vessels.

# 3 Power generation systems

In this chapter, the general working principles of all critical parts of the energy conversion onboard are analyzed. Paragraph 3.1 elaborates the ICEs, both CI- and SI-engines are taken into account. PEMFC and SOFC are discussed in paragraph 3.2. The essential auxiliary systems for the ICEs and FCs; the exhaust gas treatment system and extraction principles are examined in paragraphs 3.3 and 3.4 respectively. To obtain an overview of the conversion differences of the different fuels the following questions are answered:

- What are the operational principles of Internal Combustion Engines (ICE) and fuel cells (FCs)?
- What are the energy conversion efficiencies associated with ICEs and FCs for alternative fuels?

The research is restricted to single usage of an ICE or FC. Various alternative ignition principles like Homogeneous Charge Compression Ignition (HCCI), Premixed Charge Compression Ignition (PCCI), and Reactivity controlled compression ignition (RCCI) that reduce the combustion temperature and reduce $NO_x$ emissions are considered but out of the scope. Combinations of both ICE and FC such as the Ammonia drive or a PEMFC with a turbine are considered but out of scope.

## 3.1. Internal Combustion Engine

The ICE is used on all types of marine vessels, varying from high-speed tenders to slow sailing deep sea vessels. The difference in operational profile, vessel size, and cruise speed demands a different power output, resulting in different engine sizes. The engine's rounds per minute (rpm) is determined by the required power output. Diesel engines are divided into low, medium, and high-speed engines, the power output decreases as the engine's rpm increases. [78]. The general working principle of an internal combustion engine is converting chemical energy in the fuel to thermal energy during combustion and then to mechanical energy with piston movement.

**Table 3.1:** The definition of general diesel engine types [78].

| Type | RPM | Stroke Type |
|---|---|---|
| Low speed | 80 - 300 | 2-stroke |
| Medium speed | 300 - 1000 | 4-stroke |
| High speed | 1000 - 3500 | 4-stroke |

The current pilot vessels are sailing with heavy-duty, high-speed diesel engines. Therefore, low and medium-speed diesel engines are out of the scope of this study. The known diesel and petrol engines operate based on a different working principle. Diesel (and derivatives) reacts in a so-called diesel cycle, also known as CI-combustion. Alternative fuels such as LNG, methanol, ammonia, and hydrogen can also burn in an otto cycle, known as SI-combustion. These different working principles will be discussed in paragraphs 3.1.1 and 3.1.2.

$$\eta_e = \frac{P_b}{\dot{m}_f \cdot h^L} \tag{3.1}$$

The general combustion efficiency is approximated by equation 3.1; in this equation, $P_b$ is the brake power, $\dot{m}_f$ the mass flow, and $h^L$ the lower heating value. In general, high-speed diesel engines' efficiency is around 40%, and the resulting energy is lost in heat and friction. The engine block is cooled for controlled operation as elevating temperatures lead to piston jamming by metal expansion; this is done by cooling water in a closed loop with a heat exchanger for seagoing applications. Keeping the cooling water in a closed loop protects the engine against corrosion by salt water. Smaller inland vessels use an open loop cooling water system as this system is cheaper than a closed loop, and the influence of external pollution is limited.

The operational usage of an ICE is strongly influenced by the ramp rate during power output variations. The ramp rate is determined by the engine specifications and fuel properties. The ramp rate or throttle response is an important parameter for the controlled operation of a high-speed vessel. For high-speed engines, the throttle response is higher than for other engine types because of the lower moment of inertia on the crankshaft. Turbocharging influences the throttle response drastically. During turbocharger spool-up, the response is delayed. At high turbo pressure, the compression ratio is high leading to a quick throttle response. Furthermore, the ignition speed influences the response, quick igniting fuels with high octane numbers result in an optimal throttle response. The fuel's evaporation time determines the ignition speed. Based on these properties, hydrogen performs better than diesel, methanol has a slower ramp rate than diesel, and ammonia performs similarly to diesel.

### 3.1.1. Compression Ignited

The most used principle in ICEs is the 4-stroke CI diesel engine, which works on the self-ignition of fuel at high temperatures induced by compressed air. Figure 3.1 shows the four stages in the combustion cycle. Air enters the cylinder by the blue-colored inlet (pressurized and cooled) and starts the cycle in the most right scenario. The work of the crankshaft and other cylinders or the inertia of a flywheel then compresses the air in the closed cylinder. When the top dead center is almost approached, fuel is injected, combusting and creating work on the cylinder head. The exhaust gasses are pushed out of the cylinder in the third figure, and the cycle restarts in the fourth figure.

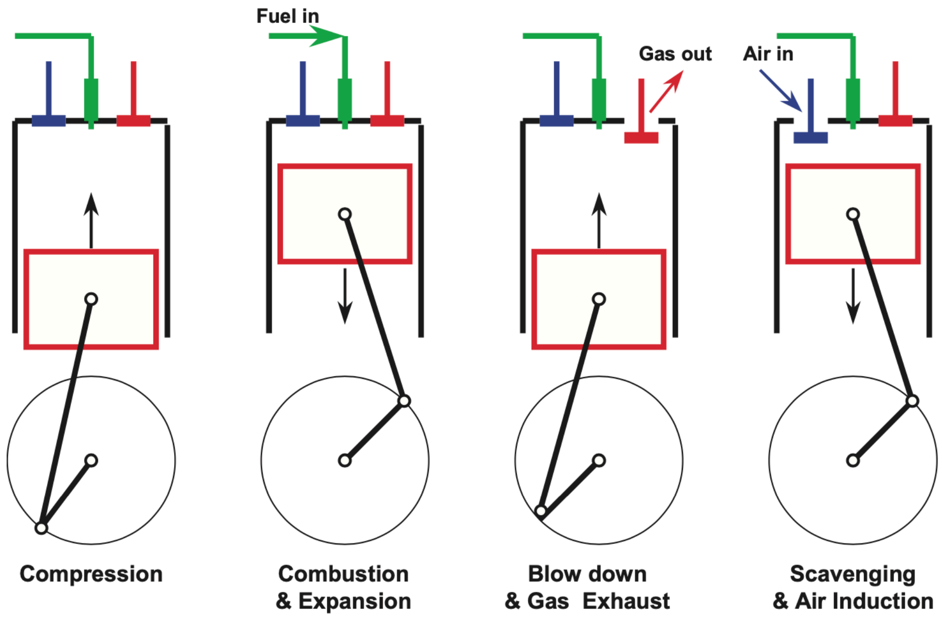


**Figure 3.1:** Working principle of a 4-stroke diesel engine [78]

**Diesel & HVO**

As discussed in chapter 2, some alternative fuels are applicable for CI engines with or without alterations. The currently used engine in the Damen Stan patrol 2205, the MTU 10V2000M72, consumes 231 l hr$^{-1}$, producing 900 kW, resulting in an engine efficiency of 39% based on the LHV [57]. The similar molecule structure of HVO to diesel results in comparable combustion characteristics; no alterations to the diesel engines are needed. A parallel dual fuel system is preferred as HVO as single fuel usage still needs to be classified due to the uncertainty of HVO availability. The LHV of HVO is comparable to diesel. Therefore, the engine efficiency can be assumed to be comparable as well.

**LNG**

LNG can be directly used in a CI engine despite the higher auto-ignition temperature than diesel. Dual fuel with diesel can be used to increase the temperature in the cylinder. Before LNG injection, diesel is used as a pilot fuel to increase the temperature. In this scenario, 90% of the diesel is replaced. The LNG replacement creates a higher H/C ratio, resulting in lower $CO_2$ and PM emissions. The evaporation of LNG gives in a better fuel-air mix than diesel resulting in better engine performance [12]. The thermal efficiency of LNG in an ICE is around 40% [48].

**Methanol**

Methanol cannot be used directly in a conventional diesel CI engine. The different chemical properties of methanol require alterations to the piping, cylinder head, and fuel injection system [91]. Like LNG, methanol has a high auto-ignition temperature with a high combustion ratio as a requirement for efficient combustion. This can be overcome using a dual-fuel system with diesel as pilot fuel. For example, the methanol is injected separately after the diesel injection to have a better fuel-to-air mix and higher temperature induced by diesel combustion [87]. The pilot injection creates turbulence in the cylinder improving the mixing between fuel and air. Methanol as a single fuel reaches a thermal efficiency of 45% in an ICE based on the specifications of the Wärtsilä 6L32M with a total energy consumption of 7970 kJ kWh$^{-1}$ [88]. Larger engines have in general a higher efficiency than smaller engines, therefore the efficiency of 45% might be optimistic. The diesel variant, the Wärtsilä 6L32, operates at a similar efficiency. Therefore the methanol efficiency for high-speed engines will be equal to diesel. Dual fuel engines have a lower efficiency as the geometric specifications are not optimized for a single fuel. However, the usage of dual-fuel engines is asked by classification as methanol has limited availability.

**Ammonia**

Ammonia can combust as a single fuel in a CI engine at a high compression ratio of 35:1 due to the high auto-ignition characteristic similar to LNG and methanol [23]. Combustion at such high compression rates results in higher temperatures and thus elevated $NO_x$ emissions, especially as ammonia is a nitrogen-based fuel. The combustion of pure ammonia is unpredictable; to obtain a more stable process, a pilot injection of ammonia is used to create a premixed mixture before compression inside the cylinder. This process is shown in the most left situation in figure 3.2. After this air mixture with little ammonia is compressed, the main fuel injection and combustion occurs.

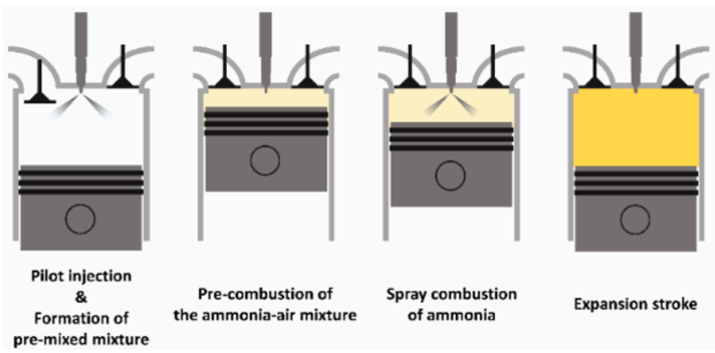


**Figure 3.2:** Ammonia pilot injection process [45]

Dual fuel combustion with ammonia and diesel can reduce the combustion ratio significantly from 35:1 to 15.2:1, resulting in lower $NO_x$ emissions. To overcome the high auto-ignition of ammonia, diesel is injected before ammonia to start the combustion [23]. The brake thermal efficiency of ammonia dual-fuel engines is low at 29.4% compared with an efficiency of 31.8% using bio-diesel as a single fuel [59].

**Hydrogen**
The low volumetric density of hydrogen results in a lower energy density inside the cylinder and a lower engine power density when hydrogen is injected at low pressure. To improve the energy density hydrogen injection is done at high pressure, taking into account that the fuel-to-air ratio is optimal. The direct injection (DI) principle can improve the power density as air is compressed by piston movement after intake, and hydrogen is injected into the cylinder at high pressure; this system has the best efficiency with compressed hydrogen storage as hydrogen is already compressed as no efficiency is lost by the vaporization of liquid hydrogen. A severe problem with hydrogen-fueled engines is knock. With port fuel injection, the time to create this knock is more extensive; using direct injection reduces this risk. Hydrogen as a single fuel in CI engines is still difficult to manage. Therefore, using a dual-fuel with diesel has the preference [13]. The high molecular thermal capacity of hydrogen changes the combustion phase in comparison with diesel as a single fuel, resulting in less efficient combustion. However, adding hydrogen does accelerate the combustion time but results in higher fuel consumption and brake-specific fuel consumption. The added hydrogen reduces the CO and increases the H/C percentage in the fuel, and therefore, less carbon dioxide is emitted per kg of fuel. The dual fuel operates at higher pressure and temperature at combustion, reducing the unburned hydrocarbons (UHC) but increasing the $NO_x$ emissions; this can be prevented by adding a selective catalytic reduction (SCR) system. The thermal efficiency of dual fuel CI combustion reduces 5% averaged over all measured rpms [41].

### 3.1.2. Spark Ignited

An alternative method for ICEs is SI-combustion. The working principle of the SI engine differs from the CI engine, mainly in the fuel injection system. The working principle is shown in figure 3.3. The fuel is mixed with air and enters the cylinder as a fuel-air mix in the first sketch. In the second scenario, the mixture is compressed. Then, the spark plug ignites the mixture with a spark and combustion occurs. This spark ignites the fuel before self-ignition temperatures are reached, resulting in a lower compression ratio in the engine.

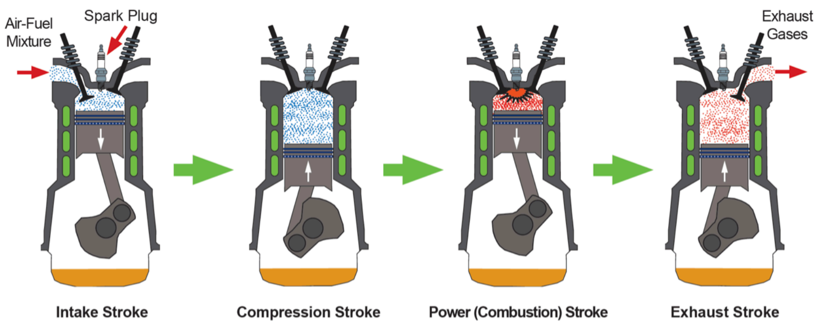


**Figure 3.3:** Working principle of a spark ignited engine [4]

The lower compression ratio limits the $NO_x$ emissions because of the lower combustion temperature. The CI engines have a compression ratio of 14:1 up to 22:1; using a SI engine, the compression ratio is reduced to 8:1 up to 12:1 [75]. The spark ignition creates a more precise and better controllable engine, resulting in the possibility of higher RPMs to make up for the lower power density per stroke due to a lesser fuel-air mix density. Generally, fuels with a high auto-ignition temperature are suited for spark-ignited engines [56]. As diesel and HVO have a relatively low self-ignition temperature, the application in an SI is inefficient and, therefore, not considered.

**LNG**

An SI engine is suitable for LNG usage; Scania designed a natural gas engine with a comparable kg per kW range as the MTO 10V2000 M72 and a mechanical efficiency of 39% [73]. This engine gives a power density indication, but direct marine application is not intended as this engine is air-cooled and designed for the automotive industry. Dual fuel usage with hydrogen addition in an ICE can increase the brake thermal efficiency at lower brake mean effective pressure. The resulting higher H/C ratio reduces $CO_2$ emissions [49].

**Methanol**

Implementing methanol in an SI engine is possible; with state-of-the-art turbocharging, an engine efficiency of 44% can be achieved at an indicated mean pressure of 17 bar. The significant benefits of methanol are best projected on large engine geometry in comparison to automotive engines; this is favourable for marine applications [34].

**Ammonia**

Ammonia is suitable for single-fuel combustion in modern spark-ignited engines with little or no design modifications. The indicated efficiency of 37% single fuel ammonia can be increased by adding 5% of hydrogen to 39% [46]. The small amount of hydrogen acts as an ignition promoter, resulting in better performance and combustion stability. The performance of single-fuel ammonia can be improved by cracking amounts of ammonia and injecting this into the airflow in the carburetor to stabilize the combustion process. This cracking of ammonia breaks the $NH_3$ into $H_2$ molecules and is discussed in paragraph 3.4. This study shows an induced efficiency of 34% with an addition of a molar hydrogen fraction of 0.375 [54].

**Hydrogen**

Single-fuel hydrogen spark-ignited engines are developed for marine applications; The 'Hydrotug 1' sails both on dual fuel with diesel as on pure hydrogen in the harbour of Antwerp, engine efficiencies are not provided yet [27]. A SI gasoline engine can be improved on efficiency and emissions by adding hydrogen; mixing 80% gasoline with 20% hydrogen results in an improvement of the brake thermal efficiency of 28% compared with the base fuel of 24%. Furthermore, if the hydrogen partition is increased further to 25%, the hydrocarbon content and CO content decrease by 22.8% and 40.26% respectively [25]. Single-fuel hydrogen engines are available in the automotive industry in the pilot phase. A port fuel-injected 7.8L hydrogen engine achieves a peak efficiency of 44.5% [43].

### 3.1.3. ICE overview

The obtained efficiencies for all fuels are summarised in table 3.2. Methanol achieves the highest efficiency in both CI and SI engines. The accented CI efficiency of ammonia is dual fuel. In this comparison measured efficiencies from diesel and methanol are compared with theoretical or simulated efficiencies. Therefore, these efficiencies are not complete trustful numbers but approximations for further applications. The difference between the measured efficiencies of diesel and Methanol can be explained by the engine size; smaller high-speed engines have a lower efficiency than medium or slow-speed engines in general. The diesel efficiency is calculated based on a high-speed engine as the methanol efficiency is calculated using an already existing medium-speed engine. Furthermore, that same medium-speed engine operates at a similar efficiency using diesel as methanol.

**Table 3.2:** Engine efficiencies for CI and Si applications

| Fuel | CI | SI |
|---|---|---|
| Diesel | 39% | N/A |
| HVO | 39% | N/A |
| LNG | 40% | 38% |
| Methanol | 39% | 44% |
| Ammonia | 29%* | 37% |
| Hydrogen | N/A | 44% |

The application of alternative fuels on high-speed four-stroke engines as installed in the Stan Patrol is yet not commercialized. Therefore, the size- and weight-to-power ratio of the installed MTU10V2000M72 are assumed to be the same for all engines on alternative fuels with the same power output and load factor, these are shown in table 3.3. The specific fuel conversion efficiency is taken for each fuel.

**Table 3.3:** Specifications of the MTU 10V2000 M72 [57]

| Specification | Value | Unit |
|---|---|---|
| Power | 900 | kW |
| Speed | 2250 | rpm |
| Cylinders | 10 | - |
| Displacement | 22.3 | L |
| Weight | 2820 | kg |
| Volume | 3,22 | m3 |
| Weight | 0,319 | kW kg$^{-1}$ |
| Volume | 280 | kW m$^{-3}$ |

## 3.2. Fuel Cell

The conversion of chemical energy in fuels to mechanical energy for propulsion can be done without combustion, using a FC with an electric motor. FC technology developed rapidly in a journey towards zero-emission. The development of one of the first FCs by Ludwig Mond with Charles Langer took already place before 1900 [65]. After the rapid rise of the combustion engine, the development of the FC diminished. A wide range of FCs is investigated; the most promising FCs are the PEMFC and the SOFC, which will be elaborated on more. Figure 3.4 shows the different operating temperatures of the FCs and corresponding advantages and disadvantages. The direct differences between the SOFC and PEMFC are the operation temperature, the tolerance to reformed fuel and the start-up time.

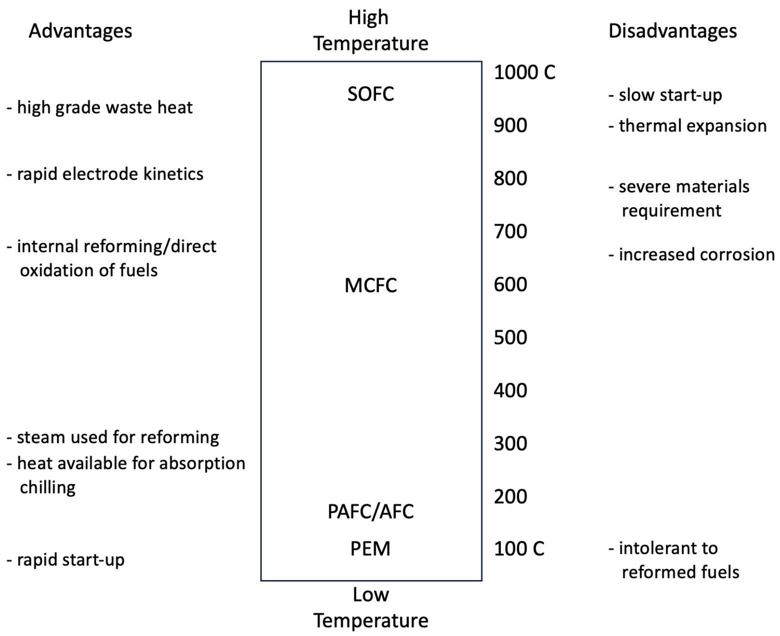


**Figure 3.4:** Types of FCs with temperature based advantages and disadvantages [65]

Load swings in FC operation reduce efficiency. The load transients create a low-reactant condition inside the FC that compromises the performance. Furthermore, during partial load operation as a result of load swings polarization losses occur. Therefore, the optimum FC performance is at a constant output. A battery pack is necessary to obtain similar or better usability regarding power output variations compared with a diesel engine. Direct load changes can be achieved with the mechanical power output towards the propeller delivered by an electrical motor. These required extra components harm the propulsion system's total weight and size, resulting in a lower total efficiency.

### 3.2.1. Proton Exchange Membrane Fuel Cell

When fueled with green hydrogen, the proton exchange membrane FC generates electricity without GHG emissions. As no combustion is used, a FC is a quiet system; only cooling equipment produces some noise. The working principle is displayed in figure 3.5; three plates are pressed together: the Anode, the membrane, and the Cathode.

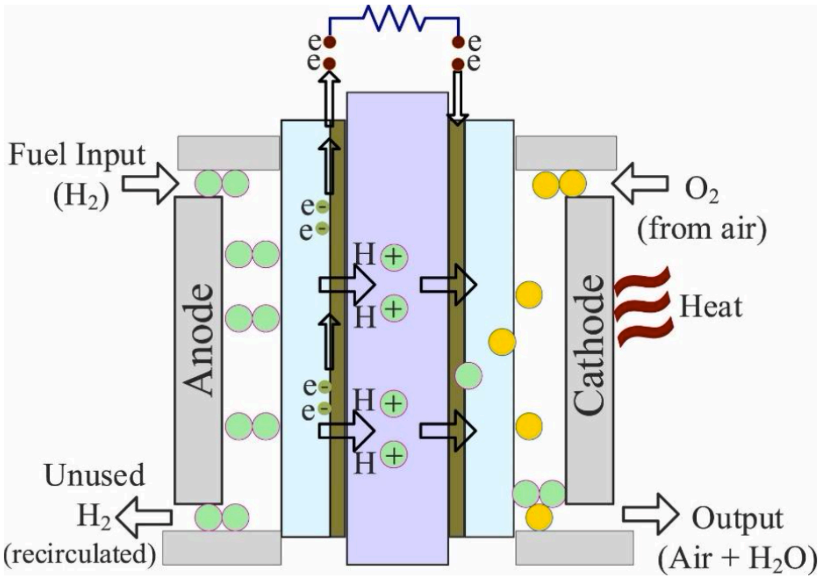


**Figure 3.5:** Working principle PEM FC [69]

The reaction of the FC can be divided into three stages. In the first stage, the hydrogen is split into electrons and protons at the anode formulated in equation 3.2. The electrons are used for electricity; the protons travel to the cathode through the proton exchange membrane. At the cathode, oxygen from the outside air reacts with the protons into water, as shown by equation 3.3, producing heat. The overall process of the PEMFC, shown in equation 3.4, only requires hydrogen and air and emits heat and water.

$$\text{Anode:} \quad 2H_2 \leftrightarrow 4H^+ + 4e^- \tag{3.2}$$
$$\text{Cathode:} \quad O_2 + 4H^+ + 4e^- \leftrightarrow 2H_2O \tag{3.3}$$
$$\text{Overall:} \quad 2H_2 + O_2 \leftrightarrow 2H_2O \tag{3.4}$$

The energy reaction in a FC is given by equation 3.5, $\Delta$H is the total heat energy or the change in reaction enthalpy, $\Delta G_{cell}$ is the maximum electrical work that the FC can generate, and T$\Delta$S is the maximum heat release with T as Temperature and $\Delta$S the change in reaction enthalpy [94]. Then, the theoretical electrical energy efficiency can be calculated using equation 3.6.

$$\Delta H = \Delta G_{cell} + T\Delta S \tag{3.5}$$
$$\eta_e^o = \frac{\Delta G_{cell}}{\Delta H} \cdot 100\% \tag{3.6}$$

The PEMFC operates at low temperatures and is called the LT-PEMFC. This low temperature is required for optimal membrane conditions; at higher temperatures, the humidity and permeability are reduced. The FC has a high power density, high energy conversion efficiency, and fast start-up compared with a SOFC [94]. However, the PEMFC has downsides such as the hydrogen purity; the membranes are sensitive to impurities, resulting in a hydrogen level of above 99%. Therefore, only pure hydrogen is suitable for LT-PEMFCs. The LT-PEMFC is a more compact FC requiring fewer external systems than the SOFC and reaches an efficiency of 45-55% [24]. A LT-PEMFC provides better dynamic loads and a lower cost per kW than a SOFC [86].

Besides the low-temperature PEMFC, a high-temperature PEMFC is also developed and has several benefits. The impurity tolerance of the membrane is higher, the electrode kinetics are improved, and the heat management is less critical. The major downside is the higher degradation of the FC. The higher impurity tolerance enables methanol and ammonia to be suitable fuels for HT-PEMFC. However, hydrogen has to be extracted from these fuels before usage in the FC; this principle is elaborated in paragraph 3.4. An integrated methanol steam reformer (MSR) with a high-temperature PEM FC (HT-PEMFC) achieves an electrical efficiency of 41%, combining a small Combined Heat and Power (CHP) system, the overall system efficiency can reach 87% [47]. After hydrogen decommissioning, ammonia reaches a total electrical efficiency of 40% [17]. In principle, methanol and ammonia are with a hydrogen extraction system suitable for LT-PEMFC. In practice, this is not done as the purity level in these extraction systems is not high enough.

### 3.2.2. Solid Oxide Fuel Cell

The operating temperature of the Solid Oxide FC is between 800 and 1000 Celcius, reducing the need for electrocatalysts [42]. Furthermore, CO is possible as fuel in addition to hydrogen because of the high operating temperature. In an SOFC, oxygen transfers through the membrane from the cathode towards the anode, which differs from the PEMFC, whereas protons travel from the anode to the cathode.

$$\text{Anode:} \quad 2H_2 + 2O^{2-} \leftrightarrow 2H_2O + 2e^- \tag{3.7}$$

$$\text{Cathode:} \quad O + 4e^- \leftrightarrow 2O^{2-} \tag{3.8}$$

$$\text{Overall:} \quad 2H_2 + O_2 \leftrightarrow 2H_2O \tag{3.9}$$

The fuel tolerance of SOFC increased over the years, as shown in figure 3.6. In the left figure, a separate external reformer creates hydrogen and carbon monoxide. Newer techniques use an internal reformer; the newest FCs can use natural gas directly. The most significant difference with the PEMFC is carbon dioxide emission. A SOFC reduces the $SO_x$, $NO_x$, and PM emissions compared to an ICE, but $CO_2$ is still emitted when carbon-based fuels are used.

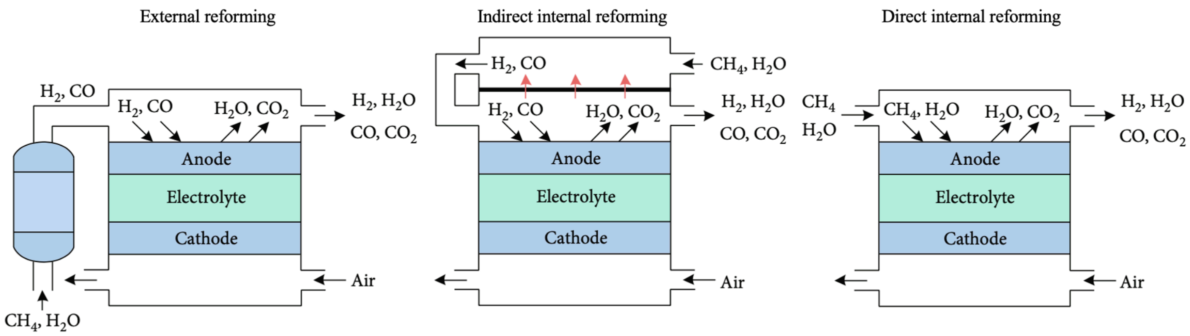


**Figure 3.6:** Development in fuel reforming requirements [16]

In general, SOFC has a high fuel efficiency ability and is suitable for a CHP system. The heat produced by the FC can be used in the Heating, Ventilation and Air Conditioning (HVAC) system on board. However, the high temperature creates corrosion and breakdown of cell components, this is still a challenge for SOFC application. LNG in an SOFC reaches an efficiency of 50%, which is higher than an ICE on LNG [50]. As a single SOFC has low efficiency, combining it with a heat and power system, an electrical efficiency of 54% can be reached [95] as the technology is further developed. In a SOFC, ammonia is injected directly, and the electrical efficiency is 52% [68]. In the ShipFC project, the Viking Energy is converted with a SOFC installation. Alma power tested a 6 kW SOFC with an electrical efficiency of 61 to 67% that will be scaled up to 2MW for commercial applications [6]

### 3.2.3. Fuel cell overview

FC research and development remains ongoing, with much to explore. Despite numerous publications, a significant portion of the data still relies on theoretical models rather than comprehensive full-scale tests. However, pioneering companies are already building FCs for full-scale application; table 3.4 presents the current most promising FCs. The LT-PEMFC has the highest power density but requires a high level of hydrogen purity. The HT-PEMFC has a low absolute power output but is in the range of power density with the LT-PEMFC. The SOFC has the most comprehensive application but has a significantly lower power density. The efficiency of PEMFC and SOFC is almost similar. The HT-PEMFC has a higher efficiency. However, this efficiency is given in a press release, so it is not clear if the electrical efficiency or overall efficiency is stated.

**Table 3.4:** Currently available FC specifications

| | **LT-PEMFC** | **HT-PEMFC** | **SOFC** |
|---|---|---|---|
| Brand | Zepp.Solutions [93] | Blue.World [81] | Bloomenergy [11] |
| Fuel | Hydrogen | Hydrogen | Natural gas |
| Power (kW) | 150 | 18 | 300 |
| Efficiency (%) | 51 | 65 [53] | 52 |
| Volume ($m^3$) | 0.595 | 0.052 | 27.67 |
| Weight (kg) | 355 | 57 | 15800 |
| | | | |
| Volume ($kW\ m^{-3}$) | 252.1 | 346.3 | 10.84 |
| Weight ($kW\ kg^{-1}$) | 0.423 | 0.316 | 0.0190 |

An ICE achieves the highest efficiency above 75% power output. A FC obtains the highest efficiency at a constant partial load. Figure 3.7 shows the decreasing system efficiency curve of the Zepp Solution X150.

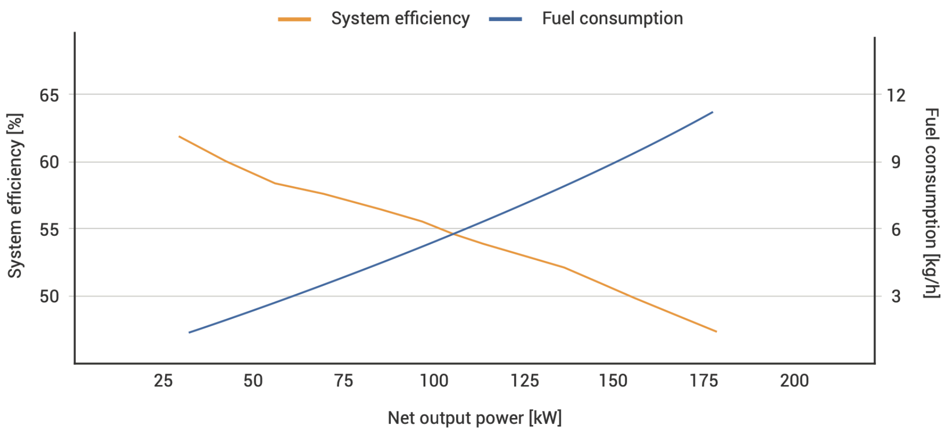


**Figure 3.7:** FC efficiency and fuel consumption curve [93]

## 3.3. Exhaust gas treatment system

Another method to reduce emissions is treating the exhaust gasses. The International Maritime Organisation (IMO) has set several rules to limit marine emissions. The MARPOL annex VI regulation determines the maximum sulfur and nitrogen oxide emissions, these emissions are rated in three tiers. If a newly built vessel will be operational in the ECAs, it has to meet the Tier III regulation. For a combustion engine with a RPM of 2250, as the MTU 10V2000 M72, this results in a maximum emission of 0.50 % m/m and 2.00 g/kWh for sulfur and nitrogen oxides [62] [63]. The emissions can be reduced using various types of exhaust gas treatment systems (EGTS).

$SO_x$ can be removed from exhaust gases using scrubbers. Scrubbers can use an open loop with seawater combined with a caustic chemical or a closed loop with a sodium hydroxide solution to absorb $SO_x$. Scrubbers are most effective on vessels sailing on heavy oils such as HFO or MDO. High-speed engines on EN590 diesel produce almost no $SO_x$ because the fuel contains very little to no sulfur. Therefore installing a large scrubber installation is not effective on vessels like high-speed pilot vessels.

$NO_x$ can be removed from exhaust gasses using SCR. This system uses ammonia to react with the exhaust gasses resulting in nitrogen and water as emissions, the reactions are given in equation 3.10 [74]. This principle is developed and used by shipbuilders and engine manufacturers. For example, Damen developed their '$NO_x$ reduction system' that can reduce $NO_x$ emissions by 80% to achieve Tier III emissions [21].

$$4NH_3 + 4NO + O_2 \rightarrow 4N_2 + 6H_2O \tag{3.10a}$$
$$4NH_3 + 2NO + 2NO_2 \rightarrow 4N_2 + 6H_2O \tag{3.10b}$$
$$8NH_3 + 6NO_2 \rightarrow 7N_2 + 12H_2O \tag{3.10c}$$

A CCS system can reduce the emitted $CO_2$ by 90%, using an inventive heat exchange system this can be done without energy losses [5]. The combustion of 1 kg of diesel results in 2.6 kg of $CO_2$. The problem with a CCS is that it takes a lot of space and the carbon needs to be stored onboard, especially for high-speed vessels as pilot vessels this is a serious issue. Value Maritime implements this principle on short sea vessels with a power of 3-10 MW with swappable $CO_2$ batteries [83].

## 3.4. Hydrogen extraction

Methanol and ammonia as hydrogen carriers can both be burned in an ICE or used in a FC. For HT-PEMFC application hydrogen needs to be extracted from the carrier, this can be done by MSR and ammonia cracking. Methanol with water is cracked to $CO_2$ and hydrogen, as shown in equation 3.11.

$$CH_3OH + H_2O \rightarrow CO_2 + 3H_2 \tag{3.11}$$

Figure 3.8 displays the working principle of an MSR system and the interaction with an HT-PEMFC. First, the methanol and water mixture has to evaporate before it enters the reformer. The unreacted hydrogen-rich gas is burned to heat-up the reformer process, this results in a more efficient process. The same principle is used in the evaporator where the hot air exiting the FC heats up the methanol and water mixture. This system achieves a methanol-reforming efficiency of 96% [70].

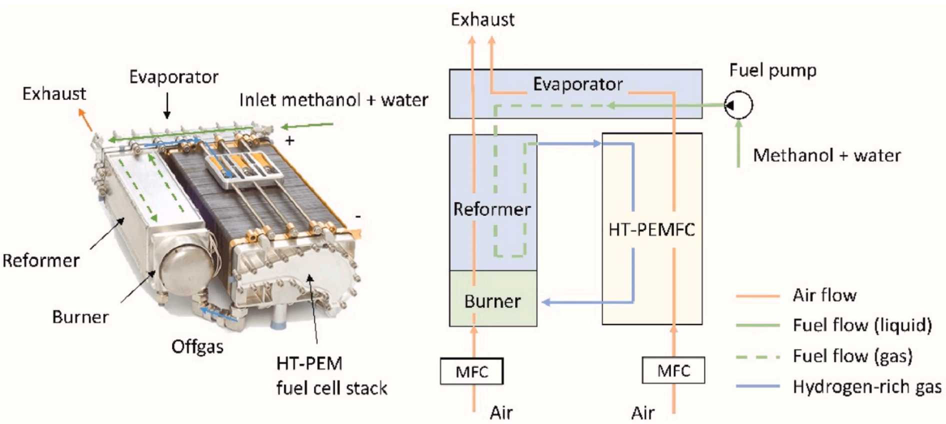


**Figure 3.8:** A combined HT-PEM FC with MSR system [47]

Ammonia cracking can be done with two methods effectively; thermochemical and electrochemical cracking. Thermochemical cracking requires heat, a catalyst, and separation for high hydrogen purity. At temperatures above 400 Celcius a conversion of above 99% is reached [92], the required heat can be obtained by heat exchanging with the high-temperature FCs similar to the MSR interaction in figure 3.8. Electrochemical cracking does not require the need for thermochemical cracking but is done using electricity that has to be generated onboard and reduces the overall efficiency.

## 3.5. Power generation conclusion

Implementing a FC will be the best solution to achieve maximum emission reduction. However, an ICE provides flexibility in load conditions and robust operation. Furthermore, the mechanical output of an ICE can be directly used to propel the vessel by propeller or water jet. The FC requires a battery pack to overcome load swings and an electric motor for mechanical energy. Still, an ICE requires an EGTS to obtain acceptable local harmful emissions. The most energy-dense FC is the LT-PEMFC by Zepp.Solutions, it has comparable energy densities to the MTU 10V2000M72. When the auxiliary systems are taken into account, the required power density of the FC propulsion system will reduce drastically. Still, both systems are taken into account as the usage per fuel results in different efficiencies. The hydrogen purity requirement of the LT-PEMFC results in only hydrogen being investigated in low-temperature FC applications. The HT-PEMFC will be used for methanol and ammonia because it tolerates fuel impurities that still can occur after hydrogen extraction. The SOFC will not be considered due to the low energy density. Methanol, ammonia, and hydrogen will be investigated in an ICE as a single fuel; this will be a CI-ICE for methanol, while ammonia and hydrogen will be used in a SI-ICE. The six combinations that will be investigated are summarised as follows:

- Methanol + CI-ICE
- Methanol + HT-PEMFC
- Ammonia + SI-ICE
- Ammonia + HT-PEMFC
- Hydrogen + SI-ICE
- Hydrogen + LT-PEMFC

# Part II

# Design input based on operational data and class regulations

# 4 Operational input based on piloting analysis in Rotterdam

The installed power and fuel capacity must align with the vessel's operational profile. Therefore, it is crucial to map the ship's usage, as discussed in chapter 1, since alternative fuel systems occupy more space and weight than the conventional diesel fuel system. Therefore this chapter will address the following question:

- What is the energy demand based on the load profiles of the 'Loodswezen' pilot vessels?

Currently, Dutch pilots operate 20-meter pilot tenders with a design speed of approximately 30 knots. It is uncertain whether this speed is used and if it is effective during daily use. Reducing the operational speed has significant effects on the required power and fuel consumption of the pilot vessels, leading to smaller installed fuel tank. A clear operational profile of the pilot tenders is determined through onboard measurements.

The pilot service operates a large fleet of tenders in all major ports of the Netherlands. This fleet includes various types of vessels: the H-class, Aquila-class, Discovery-class, L-class, and M-class. For a significant portion of the fleet, two types of measurements have been conducted; Automatic Identification System (AIS) data and engine data have been collected. Table 4.1 presents the type class and the collected measurements for each vessel.

**Table 4.1:** Measured pilot tenders

| Vessel | Class | AIS Data | Engine-Data |
|---|---|---|---|
| Mira | M-Class | Yes | No |
| **Lynx** | **L-Class** | **Yes** | **Yes** |
| Lacerta | L-Class | No | Yes |
| Lesath | L-Class | No | Yes |
| Libra | L-Class | No | Yes |
| Lucida | L-Class | Yes | No |
| Aquila | Aquila-Class | No | Yes |
| Draco | Aquila-Class | No | Yes |
| Orion | Aquila-Class | No | Yes |
| Hydra | H-Class | Yes | Yes |
| Hercules | H-Class | No | Yes |

From the measured fleet, only the Lynx and Hydra have both sets of measurements. The Hydra, designed as an ice-class vessel for the Wadden Sea, provides measurements that are less relevant for comparison with a pilot boat in the Port of Rotterdam. The Lynx is a typical pilot vessel for the Rotterdam area. All other vessels, except the H-class, are similar vessels. The H-class vessels are designed with a steel hull, making the vessels heavier and slower than the other class types. The data gathered from the Lynx will be projected on the Damen Stan Pilot 2205 FRP. As can be seen in table 4.2, the vessel specifications are comparable.

**Table 4.2:** General specification pilot tenders

| | Lynx | Damen Spi 2205 |
|---|---|---|
| Design | Camarc | Damen |
| $Length_{overall}$ | 22.47 | 22.70 |
| Power | 2*969 kW | 2*900 kW |
| Engine | Cat C32 Accert | MTU 10V2000 M72 |
| Fuel consumption | 2*243.6 l/hr | 2*231.0 l/hr |
| Design speed | 29 kn | 30 kn |
| Range | 261 NM @29 kts | 300 NM @30 kts |

## 4.1. Operational area

The pilot boats from Rotterdam operate in one of the busiest maritime regions in the world. The area surrounding the Port of Rotterdam has distinctive characteristics. For instance, there is almost always wind, with speeds exceeding 17 knots 25% of the time during autumn and winter. Moreover, the wind is predominantly onshore, as illustrated in figure 4.1. Combined with the constant outflow of water from the Maas river and relative shallow water, this results in unique sea conditions. The interaction between the wind and opposing current creates short, steep, and sometimes standing waves. While these waves are not a significant issue for larger short- and deep-sea vessels, they pose a challenge for 20-meter pilot boats in achieving their design speed. According to personal communications, the hull design of the L-class vessels limits their speed to 13 knots in wave heights exceeding 1.5 meters to keep vertical accelerations within 1.5 G. Accelerations in this magnitudes results in unpleasant conditions for crew onboard, with a risk of serious injury.

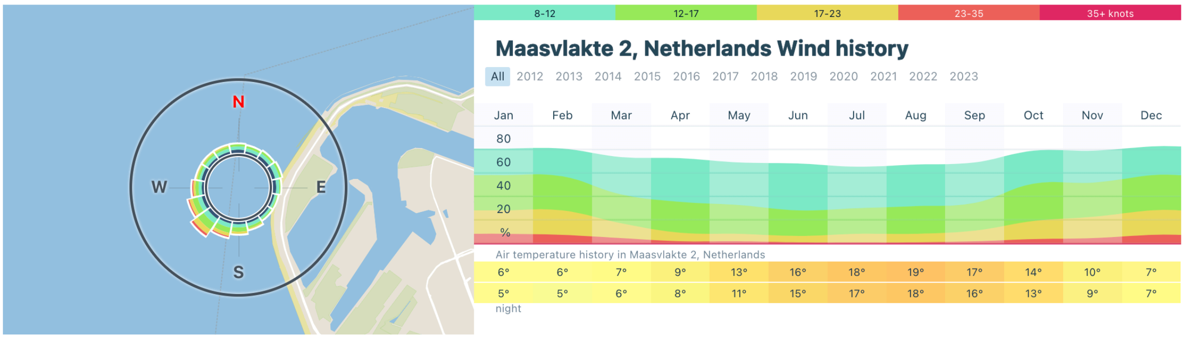


**Figure 4.1:** Wind statistics Maasvlakte 2, Rotterdam 2012-2023 [90]

## 4.2. Method

Both datasets contain information about the ship's characteristics and the conditions in which it operates. By combining these datasets, a comprehensive dataset is created, presenting all relevant data on a per-minute basis. The dataset was collected from January to November 2022. The following data have been collected:

- Speed over ground
- Current
- Significant wave height
- Wind
- GPS location
- Engine rpm
- Sailed distance
- Fuel consumption

Each of these parameters defines a different aspect of the operational profile. Speed over ground (SoG), in combination with the current, yields the speed over water (SoW). The measured wind and wave height provide information about the sea state, which influences the achievable speed and contextualizes the measured speed relative to the applied engine power. The fleet operates throughout the year at all piloted ports, and thus the GPS location offers two insights: the sailing area and the trip configuration. This data can distinguish whether the ship is sailing far offshore, piloting multiple vessels, or merely traveling to the pilot station at sea. The engine RPM can be converted into engine power in kW using the engine envelope and propeller openwater diagram. The resulting SoW, location, engine power, sailed distance, and fuel consumption provide a comprehensive understanding of the fleet's operational profile. To construct acceptable trips out of the data set, an off-time between trips of 45 minutes is set. A new trip starts, when a vessel is longer than 45 minutes in the harbour. The 45 minutes are set to provide the necessary bunker time with alternative fuels. With this pause time, the ship may remain stationary for about 30 minutes in between. The sailing before and after this shorter pause is still considered a single trip.

## 4.3. Results

The collected data for the Lynx in Rotterdam have been extracted from the overall dataset, providing a clear overview of the vessel's navigation behavior. Since the data points are logged at one-minute intervals, only a rough outline can be produced. Detailed dynamic navigation behavior or precise pilotage cannot be determined from the data points. However, the travel time and fuel consumption per trip can be determined. Fuel consumption is measured in liters per minute, and any potential variations in consumption between measurement points will average out over the periods. Figure 4.2 shows a histogram of all trip durations; the maximum and average trip times are provided in table 4.3. The fuel consumption per trip is depicted in figure 4.3, with the maximum and average values also listed in table 4.3. The histograms for fuel consumption and trip duration have similar shapes, indicating that the travel time and fuel consumption per trip correspond with each other. This is illustrated in figure 4.4, where the data points align linearly.

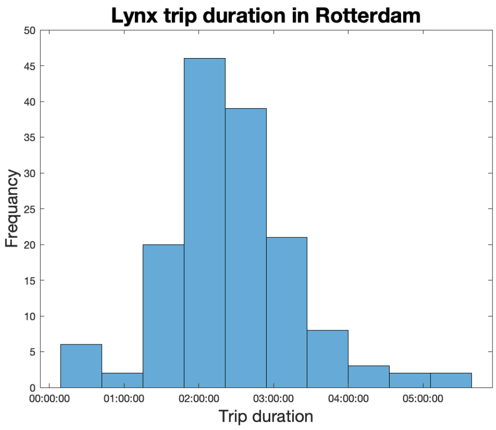


**Figure 4.2:** Trip durations Lynx in Rotterdam

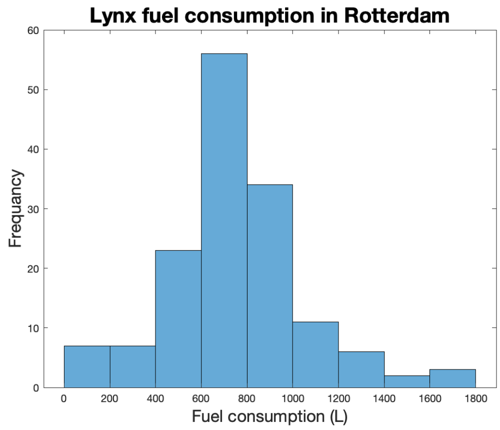


**Figure 4.3:** Fuel consumption Lynx in Rotterdam

With an average trip time of roughly two and a half hours, the Lynx is briefly at sea compared with the originally installed fuel capacity capable of sailing at full speed for nine hours. The trip duration and consumed fuel are related in table 4.3. The full gas percentage and maximum speed represent individual trips.

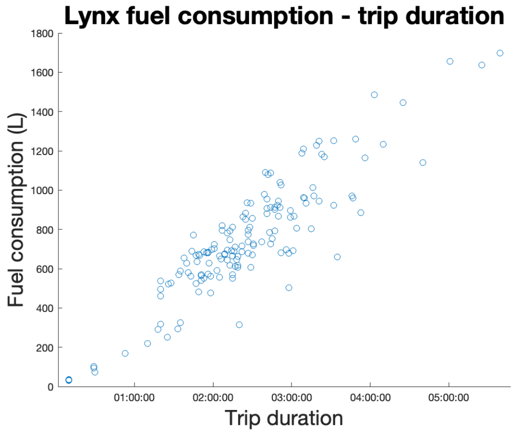


Figure 4.4: Relation between fuel consumption and trip duration

Table 4.3: mean and maximum values of the sailed trips

| Parameter | Mean values | Max values |
|---|---|---|
| Trip duration | 02:26 | 05:39 |
| Fuel consumption | 751 liter | 1698 liter |
| Full gas percentage | 52.3% | 84.0% |
| Maximum speed | 26.5 kts | 29.7 kts |

The L-class pilot boats are propelled by waterjets. To maneuver effectively with waterjets, a constant water pressure is required. This constant water pressure or flow is directed by a bucket, which can be oriented both backward for propulsion or to the sides for precise steering. As shown in Figure 4.5, the Lynx operates at nearly maximum power consistently. Figure 4.6 shows the sailed speeds, this is not in line with the power distribution. The actual power delivered to the propeller in a propeller-driven ship is adjusted by the engine load factor. However, in a waterjet-propelled vessel, this influence is minimal since the impeller in the jet consistently pumps water. This constant energy output differs significantly from the sailed speeds, this results in an energy loss.

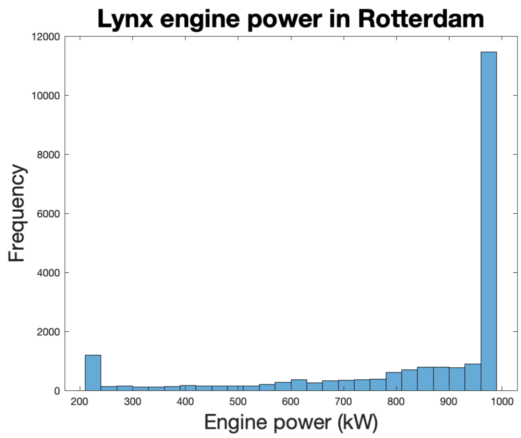


Figure 4.5: Power distribution Lynx in Rotterdam

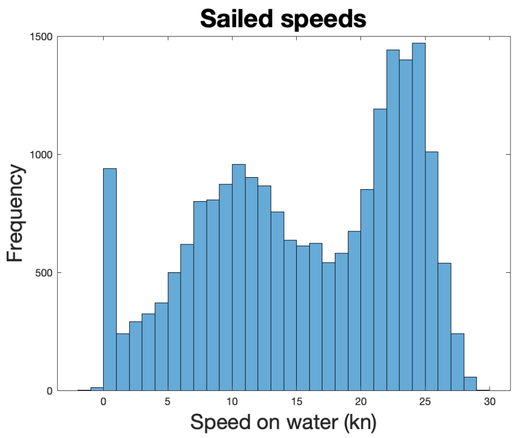


Figure 4.6: Sailed speeds Lynx in Rotterdam

To meet the full operational profile, the longest journey serves as a good benchmark. When this journey can be completed, all other shorter and less fuel-consuming trips can also be executed within the ship's specifications. Table 4.4 provides the specifications of the longest trip conducted in Rotterdam. To gain insight into the ship's usage and the progression of this trip, power and speed over time are plotted in figure A.1 in the appendix. Additionally, the GPS data of the trip is presented in figure A.2. The trip duration and engine operating hours do not align, with the engines running only 87.9% of the time. This discrepancy is due to a 40-minute stop in the harbor. Consequently, this trip falls just short of the 45-minute break threshold between different trips resulting in a relatively long trip. As can be seen in figure 4.2, the trips times are centered around the two and a half hour. The number of trips above four hours is limited. However, to fulfill the complete operational profile of the Lynx in Rotterdam the maximum trip should be taken as benchmark.

**Table 4.4:** Specifications longest trip Lynx in Rotterdam

| Specification | Value | Unit |
|---|---|---|
| Trip duration | 05:25 | hh:mm |
| Fuel consumption | 1698 | liter |
| Sailed distance | 83.3 | NM |
| Above 25 kts | 8.05 | % |
| Max rpm | 61.07 | % |
| Sailing | 87.90 | % |

## 4.4. Speed reduction

The Lynx is designed to sail 29 knots, and based on the data analysis, a required fuel capacity of 1700 litres is determined. This fuel capacity is rounded up to 1800 litres for a 5% margin. The required power to achieve a certain speed increases rapidly in a third order, as shown in equation 4.1. Reducing the maximum speed results in a lower required installed power and subsequently in less energy consumption.

$$P_E = c \cdot v_s^3 \tag{4.1}$$

Figure 4.7 shows the percentage of time the Lynx operates at various speeds. It indicates that the design speed of 29 knots is achieved less than 1% of the time. The Lynx travels at 25 knots or faster 8.7% of the time. During pilotage, the top speed is only briefly reached in peak moments; thus, reducing the maximum speed can decrease power demand without significantly altering the operational profile. This can be verified by calculating the total distance traveled at different speeds. By replacing all data points above 25 knots with 25 knots and the corresponding RPM, the new total distance traveled can be calculated. The old distance, new distance, and the difference are presented in table 4.5. Changing the top speed from 29 knots to 25 knots results in a reduced traveled distance of only 34 NM out of a total of over 5000 NM, indicating that higher speeds yield minimal time savings.

The question is why the Lynx is not reaching its design speed. Several factors contribute to this issue. Personal communications indicate that the vessels are heavier than originally delivered due to additional equipment. Furthermore, as discussed in paragraph 4.1, wave conditions reduce the maximum operating speed in order to maintain ship motions within comfortable limits for the crew.

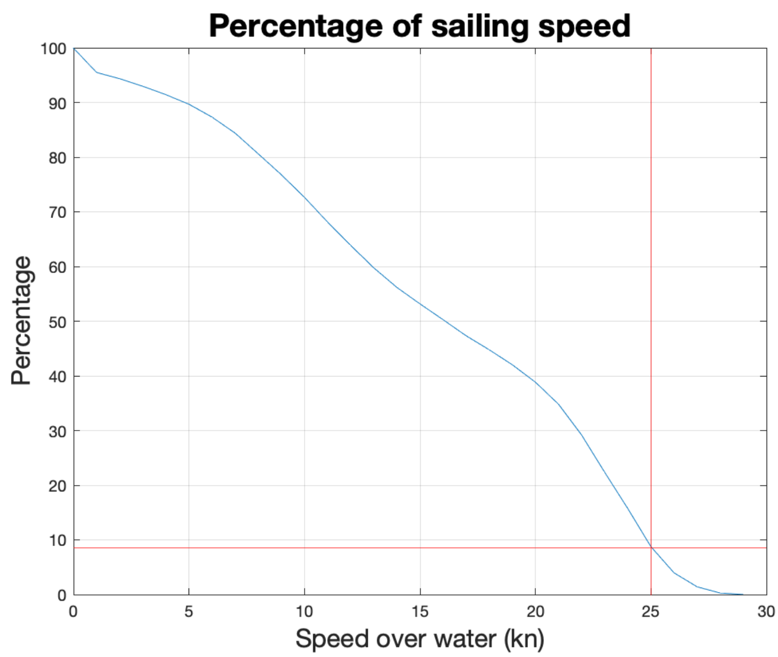


**Figure 4.7:** The percentage sailing at each speed of the Lynx.

**Table 4.5:** Sailed distance on different maximum speeds.

| Parameter | Distance NM |
|---|---|
| Max speed of 29 kts | 5468 |
| Max speed of 25 kts | 5434 |
| Difference | 34 |

Reducing the maximum speed reduces the required installed power, the difference can be determined using the Propulsion Selection Diagram (PSD) of the Damen SPi 2205 FRP. Figure 4.8 shows a reduction of more than 200 kW per engine. The SPi 2205's engine has 10 cylinders, MTU provides in the same engine family a version with 8 cylinders. This engine produces 720 kW instead of 900 kW, with a fuel consumption of 186 l/hr instead of 231 l/hr at maximum RPM. The red lines show the initial required power for a speed of 29 kn, the blue lines present the lower required power for a speed of 25 kn. This results in a fuel saving of roughly 20%.

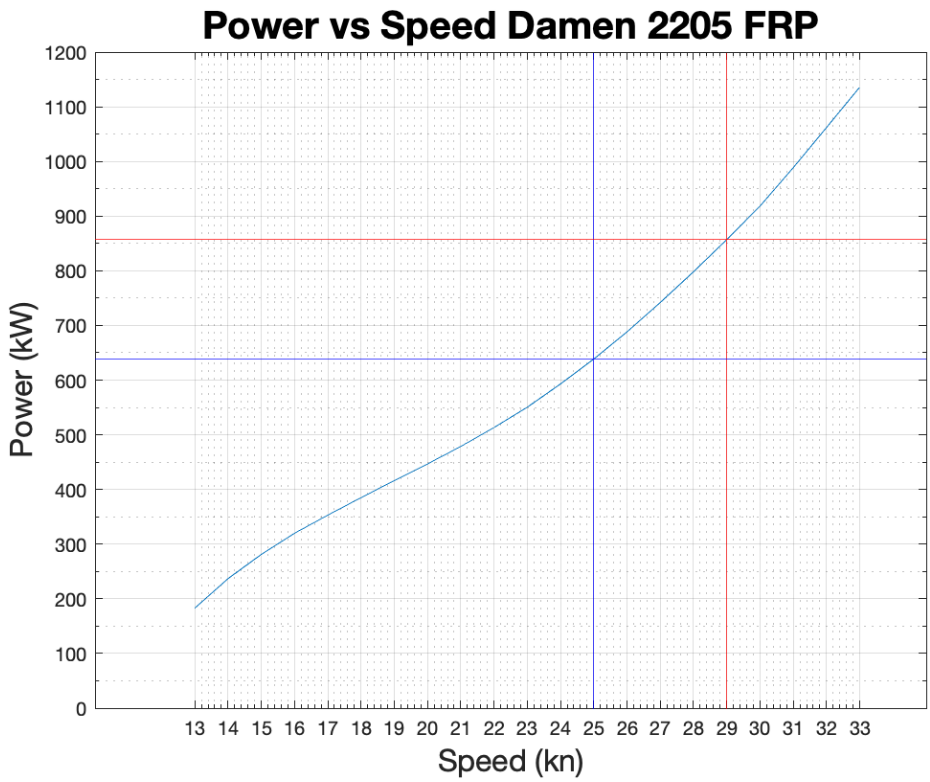


**Figure 4.8:** Resistance curve Damen SPi 2205 FRP.

## 4.5. Data conclusions

To match the current operational profile of the Lynx in the Port of Rotterdam, a maximum speed of 29 knots and 1800 liters of diesel equivalent are required. Reducing the maximum speed affects the required installed power and stored energy capacity. Lowering the maximum speed to 25 knots results in only a 0.26% reduction in traveled nautical miles, but achieves a 20% fuel savings due to a smaller installed engine. The operational profile can then be maintained with a maximum speed of 25 knots and a fuel capacity of 1400 liters.

# 5

# Class regulations

The application of alternative fuels necessitates additional safety measures mandated by classification societies due to the increased risks of hazardous situations for both the crew and the environment. The standard regulations for ships, which apply to conventional ship designs, are enforced but not expanded upon. Several classification societies require adherence to the same standards, with the most relevant ones being applied to the layout. Additionally, key aspects necessary for the use of alternative fuels—though not impacting the design layout—are identified and addressed. With this the following question will be answered:

- How do the necessary safety regulations affect the vessel design?

## Fuel tank placement

Methanol, ammonia, and hydrogen are classified as hazardous materials due to their volatility, flammability, and toxicity, necessitating additional safety measures. According to classification societies [15], various requirements apply to hazardous substances used as fuel. A cofferdam around the tank is required to mitigate the risk of leakage. This cofferdam forms a second barrier in two directions against an incident with the tank or a collision that might rupture the outer hull. Fuel tanks and pipelines must maintain a required distance of B/5 or 800 mm from the ship's side, whichever is less. From the bottom of the ship, a minimum distance of B/15 or 2000 mm, whichever is less, must be maintained. Furthermore, the fuel tanks are not to be placed before the collision bulkhead.

## Fuel preparation room

Ships equipped with methanol, ammonia, or hydrogen are required by class to have a fuel preparation room [15]. This room is sealed to be both water- and airtight, isolating it from other compartments on board, especially the tank room and the combustion engine or fuel cell room. This water- and airtight requirement is for all compartments handling this fuels, the engine-, fuel cell-, and storage rooms need to meet this requirement. The fuel preparation room houses all systems located between the tank and the engine/fuel cell, including the fuel pump, compressor, heat exchanger, and vaporizers. Each fuel tank has its own preparation room to create redundancy; if there is an issue with tank 1, tank 2 remains available, allowing the ship to continue operating. The fuel preparation room, fuel storage room and fuel cell room are all required to have a sufficient ventilation system to prevent a built up of leakage gas when a leakage occurs.

## Fuel inerting

For methanol and ammonia, it is mandatory to have an inerting system [15]. An inerting system ensures a stable environment in the fuel tank when it is not fully filled. The fuel tank is filled with a liquid or gas to provide counter pressure against the fuel, preventing further evaporation that could lead to dangerously high pressures in the gaseous phase. This liquid or gas must not react with the original fuel; in most cases, nitrogen is used for this purpose.

# 6

# Design inputs

The design of a pilot vessel based on alternative fuels—methanol, ammonia, and hydrogen—must meet a set of requirements. The designs can then be evaluated based on their adherence to these requirements. The criteria range from technical specifications determined by data analysis to the spatial configuration on board. The various requirements do not carry equal weight; some are mandatory for class certification to permit the construction of the vessel, while others are necessary for achieving the operational profile and are not directly related to the vessel's construction approval. A summery of the design requirements is shown figure 6.1

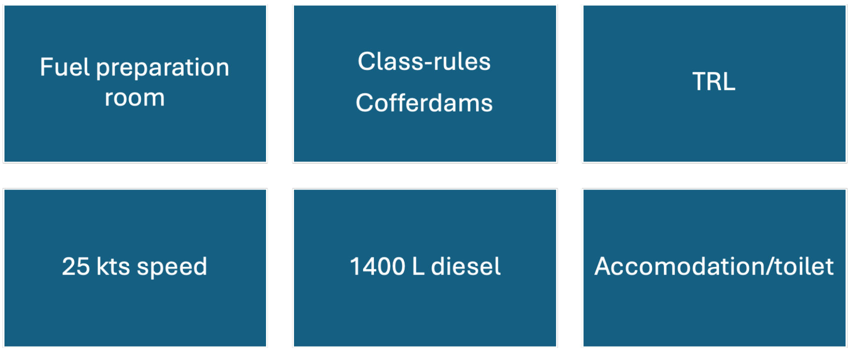


**Figure 6.1:** Overview design requirements

### Technical Readiness Level

In the designs, the TRL of the entire system is crucial. To obtain a comprehensive understanding of overall feasibility, the designs must consider worst-case scenarios. The choice of specific engines is a part of this consideration. Single-fuel engines are still under development, and current research indicates that these engines require extremely high compression ratios. The technical feasibility of these engines is therefore uncertain. However, incorporating single-fuel engines in the design necessitates a complete reliance on alternative fuels, eliminating any fallback on diesel. This requires a larger and heavier fuel tank, and the weight and volume differences of the combustion engine will not be proportionate. Consequently, the TRL of the systems, in addition to that of the fuels, is a critical requirement for the feasibility of the designs.

### Accommodation

Data analysis has shown that the L-Class operates for only short durations. As a result, a full accommodation is unnecessary, and only a restroom and refrigerator have been installed. The Damen SPi 2205 FRP design is derived from the SPa 2205. As a patrol boat, it sometimes operates for several days, necessitating accommodation. Having a restroom or full accommodation below deck is not a strict requirement as a restroom in the superstructure can always be added later. However, maximizing the accommodation space enhances the vessel's operational versatility.

### Design speed

As discussed in Chapter 4, the required operational speed can be reduced from 29 to 25 knots. This reduction results in a lower power demand, allowing the installed power to be decreased from 2*900 kW to 2*720 kW. The new designs must therefore be capable of operating at a speed of 25 knots.

### Fuel capacity

The original designs, both the L-Class and the Damen SPi 2205 FRP, were conceived with an approximate capacity of 5000 liters of diesel to sustain 10 hours of full-throttle operation. However, operational profiles indicate that only 1400 liters are sufficient to match the pilot boat's usage at a speed of 25 knots. Reducing the required fuel capacity presents opportunities for switching to alternative fuels. Given the lower energy density of methanol, ammonia, and hydrogen, additional space is necessary. To maintain the required energy levels, the amount of diesel will be replaced with an equivalent quantity of alternative fuel based on the LHV and drive train efficiency.

### Fuel preparation room

As discussed in chapter 5, applying alternative fuels requires a fuel preparation room to store all systems that are necessary between the combustion engine or fuel cell and the storage tank. For redundancy a preparation room per propulsion line is recommend.

## Cofferdam spacing

To reduce leakages both from tank failure or collisions, a cofferdam spacing around the fuel storage tanks is required. With minimal distance of B/5 or 800 mm to the side and B/15 or 2000 mm to the bottom of the vessel.

# Part III

# Design method & final designs

# 7

# Design method

The six different designs can now be developed based on the design input, considering several important aspects, each of which will be addressed. This chapter will focus on the methodology for each step in the design process, with the outcomes presented in Chapter 8. First, the hull and propulsion system are established in paragraph 7.1. Then, the system components and corresponding energy schematics are detailed in paragraph 7.2. Subsequently, the weight calculation is detailed in paragraph 7.3. Lastly, the resistance calculation and stability are addressed in paragraphs 7.5 and 7.6, respectively. Together with the results in Chapter 8, this chapter will address the following four sub-questions:

- What is the effect of a speed or range reduction on the feasibility of an alternative fuel propulsion system?
- What is the size and weight of an alternative fuel propulsion system for a required power and range?
- What is the impact of an alternative fuel propulsion system on the resistance and speed of the pilot vessel?

## 7.1. Selection of Hull and Propulsion System

In addition to design inputs, various components of the design for a new pilot boat featuring a power generation system must include an alternative fuel to define a comprehensive design. This includes the selection of the hull and the propulsion system, with both component choices being substantiated.

### 7.1.1. Hull selection

The hull shape is a critical aspect of the design of a high-speed vessel. The hull must have sufficient surface area to facilitate planing, which significantly reduces water resistance. Additionally, the bow shape plays a crucial role in seakeeping behaviour. A flared bow is adequate for pleasant seakeeping in calm seas. However, in larger waves, the bow induces significant vertical forces, caused by accelerations, which greatly diminish seakeeping performance. In collaboration with the Delft University of Technology, Damen has designed an alternative hull form, the axe bow, which maintains good seakeeping in higher sea states [32]. The deepened vertical bow slices through waves and provides sufficient additional buoyancy to compensate for movements over waves. The hull is fundamentally semi-planing rather than fully planing, as reflected in the resistance curve shown in figure 4.8. The outflow of the Maas river, combined with onshore winds, generates large waves. Given that the river mouth and the surrounding nautical miles constitute the operational area for pilot boats, managing the short, large waves is a critical aspect of hull design. Therefore, the axe bow design is the superior hull choice over a conventional flared bow design.

### 7.1.2. Propulsion system

The L-class, such as the Lynx, is equipped with waterjets, while the Damen SPi 2205 FRP is designed with propellers. The preference for a waterjet or propeller depends on several factors. The primary factor is cruising speed; at hull speeds above 30 knots, cavitation becomes an issue with conventional propellers. Waterjets do not have this problem as they are more effective above 25 knots and can operate up to 70 knots. Furthermore, waterjets facilitate excellent maneuverability, even at low speeds, reducing the need for a bow thruster. However, the downside is that a constant water flow from the waterjet is required, necessitating a consistently high RPM and thus higher fuel consumption. Additionally, a waterjet-driven vessel has no rotating parts underwater, creating a safer situation if a pilot falls overboard during embarkation.

As discussed in chapter 4, a design speed of 25 knots is sufficient, therefore, a propeller will be more efficient than a waterjet. Furthermore, the rpm can be matched to the actual propulsive power needed, rather than being constantly high as required by a waterjet. This can lead to greater fuel savings, especially when an electric motor is used. Therefore, all six designs are equipped with two propellers.

## 7.2. System Components

The different power generation systems have a distinct set of components, the required components per conversion method are given below. As discussed in chapter 3, the original diesel engine used in the ICE design is employed, assuming that these engines maintain the same size and energy density. The total installed power matches required power of 2*720 kW, as discussed in chapter 4. To calculate the required fuel the LHV and engine efficiency, determined in chapters 2 and 3, are used. The resulting formula is given in equation 7.1. Since only the ICE varies, the remaining efficiencies, as shown in table 7.1, remain constant and are therefore not pertinent to the determination of fuel capacity.

**Internal Combustion Engine layout**

- Fuel tank
- Internal combustion engine
- Gearbox
- Propeller

**Fuel Cell layout**

- Fuel tank
- Fuel cell
- Fuel preparation room
- Battery
- Electric motor
- Propeller

$$Volume_{fuel} = Volume_{diesel} \cdot \frac{\eta_{diesel}}{\eta_{fuel}} \cdot \frac{LHV_{diesel}}{LHV_{fuel}} \tag{7.1}$$

The FC layout requires an alternative determination of required fuel due to different component efficiencies. The resulting power on the propellers should be equal in the ICE and FC layout. Therefore the efficiencies of both systems are needed to determine the required fuel capacity. The efficiency of each component is known, for the three fuels the precise values differ. Using the efficiencies of the ICE layout, the power and consequently the energy on the propeller shaft can be determined. This can then be back-calculated using the efficiencies of the FC layout, provided in table 7.1, to ascertain the required installed power and fuel capacity. The electric motor is mounted on top of the pod, resulting in a L-drive with a single gear.

**Table 7.1:** Power generation system component efficiencies

| Component | Methanol | Ammonia | Hydrogen |
|---|---|---|---|
| Combustion engine | 39% | 37% | 40% |
| Gearbox | 97% | 97% | 97% |
| Shaft seal | 98% | 98% | 98% |
| Drive shaft | 98% | 98% | 98% |
| **Total** | 36% | 34% | 37% |

| Component | Methanol | Ammonia | Hydrogen |
|---|---|---|---|
| Fuel cell | 45% | 45% | 51% |
| Battery | 99% | 99% | 99% |
| Electric motor | 96% | 96% | 96% |
| Gear in pod | 97% | 97% | 97% |
| Shaft seal | 98% | 98% | 98% |
| **Total** | 40% | 40% | 46% |

### 7.2.1. Design layout

The six designs are divided based on the power generation method, with each of the three different fuels. The differences between the system principles are elaborated with a Single Line Diagram (SLD) and an Energy Flow Diagram (EFD). The SLD of the ICE, shown in figure 7.1, is similar to the original installed system with diesel fuel. The SLD of the FC system, given in figure 7.2, differs as the propulsion is electric and fuel cells and batteries are installed. All of these different components are separated by water- and air-tight bulkheads. The abbreviations, used in the SLDs and EFDs are elaborated in table 7.2.

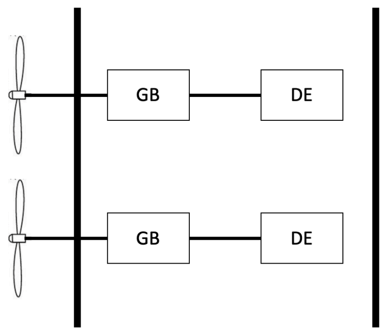


**Figure 7.1:** Single Line Diagram combustion engine layout

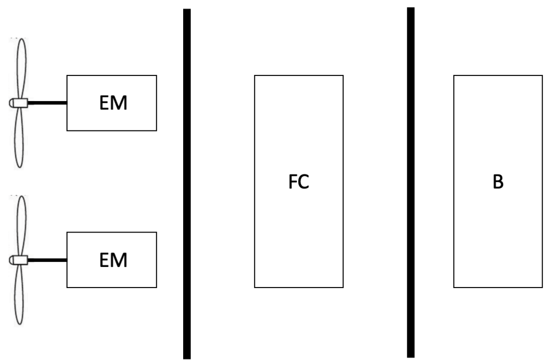


**Figure 7.2:** Single Line Diagram fuel cell layout

The EFD shows the energy path from the source in the fuel to mechanical energy in the propeller. The EFD of the ICE layout, given in figure 7.3, shows the relatively simple layout from fuel to the combustion engine to propeller via the gearbox. This system is parallel without crossovers as each engine drives a single propeller.

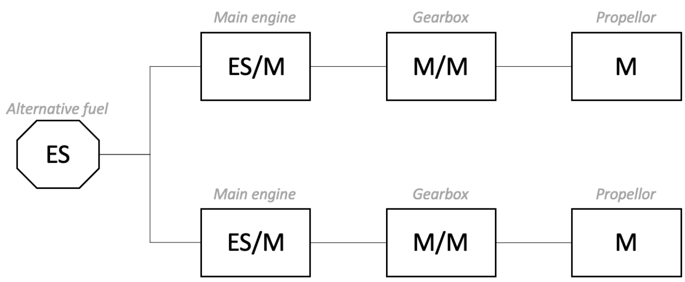


**Figure 7.3:** Energy Flow Diagram combustion engine layout

The EFD of the FC layout, shown in figure 7.4, is a more complex system. The fuel cells provide DC electrical energy that is stored in the batteries or directly used by the electric motors via a DC/AC converter. The batteries can store electricity given by the fuel cell and release electricity to the electric engines based on the engine load. In both EFDs, a redundancy is achieved by separate power flows. In the case of the FC designs; each propeller has its own fuel cell stack, battery pack and electric motor. For the ICE designs the system is simple, each propeller has an own ICE with gearbox.

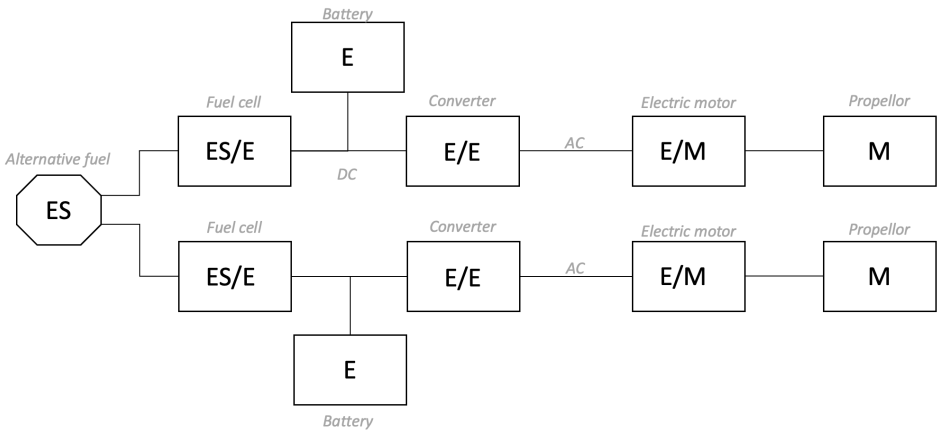


**Figure 7.4:** Energy Flow Diagram fuel cell layout

**Table 7.2:** Abbreviation legend for figures 7.1 to 7.4

| Abbreviation | Meaning |
|---|---|
| AC | Alternating current |
| B | Battery |
| DC | Direct current |
| DE | Diesel engine |
| E | Electrical energy |
| EM | Electric motor |
| ES | Chemical energy |
| FC | Fuel cell |
| GB | Gearbox |
| M | Mechanical energy |

## 7.3. Weight calculation

The ship's weight significantly impacts the required power to achieve high speeds, making this a crucial factor for pilot vessels. To ensure that the performance of all six designs approximates that of the original diesel design, the weight must remain within the same range. Significant deviations in weight necessitate adjustments in the installed power. The ship's weight can be divided into two main components: lightship weight and deadweight. The lightship weight can be further subdivided into several parts, with the hull & superstructure, propulsion & steering, primary systems, electrical system, and joinery & equipment being the largest components. Compared to the diesel design, the fuel tank adds extra weight for all three fuel types. In the FC designs, the engine room can be removed and replaced with new compartments. To achieve this, the initial design is stripped down to a bare ship, into which only the new components need to be integrated.

## 7.4. General arrangement

The placement of the tanks in ICE designs and the complete new systems in the FC designs must meet two class requirements. Safety margins around the fuel tanks and a closed fuel preparation room as discussed in chapter 5. Additionally, the trim must match that of the original diesel design to ensure comparable sailing behavior. By placing the components into the hull using the 3D-CAD software

Rhinoceros, the center of gravity of the entire ship can be determined. The longitudinal center of gravity (LCG) for the remaining components is known from Damen. By redistributing the weight, particularly in the fuel cell designs, the buoyancy point may also change. Using the Grasshopper plug-in, the center of buoyancy of the underwater hull can be found. The hull shape is set in the original trim. Then, the underwater volume changes with the vessel's weight, as the vessel is longitudinal asymetrical, the buyancy point shifts. To keep the trim similar to the original diesel design, the longitudinal coordinate of the buoyancy point (LCB) of the submerged hull and the combined LCG should match. A margin of 100 mm is acceptable as this is easily achieved by movement of crew or additional cargo.

## 7.5. Resistance calculation

The installed power must be sufficient to achieve the design speed, with weight playing a crucial role in this calculation. Increased displacement results in higher resistance, and insufficient power will prevent reaching the design speed. Using the resistance curve provided by Damen from their Propulsion Selection Diagram (PSD), the required power for each speed can be determined based on the ship's weight. An example of these resistance curves is given in figure 4.8 in chapter 4. The installed power must exceed the required power with a margin of 5% to compensate for weather conditions and additional resistance factors, such as hull fouling or increased onboard equipment.

## 7.6. Stability

The designs must comply with the stability requirements set by Bureau Veritas, which stipulate that the initial metacentric height (GM) must be greater than 0.15 m [37]. However, due to the dynamic behavior of the pilot vessel at high speeds, a higher GM is necessary, with a rule of thumb being a minimum of 1.5 m. Especially the risk of broaching with astern waves is severe with a GM lower than 1.5 m. The vertical center of gravity (VCG) of all components are known through the use of Rhinoceros software. The VCG points of the already installed components onboard have been provided by Damen.

# 8

# Designs results

The design inputs established in chapter 6, along with the methodology outlined in chapter 7, form the foundation for the designs. In paragraph 8.1, the required amount of fuel is detailed. Subsequently, all components necessary for both systems are discussed in paragraph 8.2. The weight and trim of the designs are then outlined in paragraph 8.3. In paragraph 8.4, all six designs are presented and described. This is followed by a resistance check in paragraph 8.5 and an assessment of transverse stability in paragraph 8.6. Finally, the designs are compared and evaluated in paragraph 8.7.

## 8.1. Fuel capacity

To achieve the 1400 liter diesel energy equivalent, the efficiencies described in table 7.1 are used. The required volume, weight, and energy are given in table 8.1. These weights and volumes are the net values, the tank and additional required volume in the tank are yet not taken into account. This is in contrast to the summarising values in chapter 2 where the hydrogen tank weight and size is taken into account. As now the fuel tanks for methanol and ammonia are taken into account as well, the weight and size of the tank is separated from the fuel itself. The required tank volume and weight are calculated separately as the fuel tanks contribute to the lightweight ship, the fuel is part of the deadweight.

**Table 8.1:** The required fuel capacity

| | Weight (kg) | Volume ($m^3$) | LHV (MJ) |
|---|---|---|---|
| Diesel ICE | 1176 | 1.400 | 50568 |
| Methanol ICE | 2516 | 3.180 | 50568 |
| Ammonia ICE | 2835 | 4.164 | 53301 |
| Hydrogen ICE | 410.9 | 17.333 | 49304 |
| Methanol FC | 2271 | 2.871 | 45652 |
| Ammonia FC | 2428 | 3.567 | 45652 |
| Hydrogen FC | 335.7 | 14.161 | 40920 |

## 8.2. System Components

The system components introduced in paragraph 7.2 are detailed in terms of size, weight, and power. By combining these building blocks for both the ICE and FC designs, the specification package for all designs will be clarified.

### Fuel tanks

The mass and volume of both the tanks and net stored fuel are given in table 8.2. The fuel tanks for methanol and ammonia are Type C made of stainless steel with a wall thickness of 10 mm. This thickness is oversized. However, the weight margin will be compensated as these tanks are double-walled and require valves and double-walled piping. For methanol and ammonia, a filling margin of 80% and 85% is considered. The hydrogen tanks are 350 bar, as discussed in chapter 2. The net fuel weight and volume differ from the required values given in table 8.1 due to the designed sizes of the tanks. The hydrogen mass in the ICE design is less than required because of the limited space in the hull. The class regulations limit the usable space in the vessel; only 48 of the required 68 can be placed inside the ship. In the hydrogen FC design all 55 fuel tanks are placed, resulting in the required capacity.

**Table 8.2:** Tank and fuel specifications

| | Tank (kg) | Tank ($m^3$) | Fuel (kg) | Fuel ($m^3$) |
|---|---|---|---|---|
| Methanol ICE | 1546 | 3.976 | 2516 | 3.181 |
| Ammonia ICE | 1934 | 4.280 | 2919 | 3.638 |
| Hydrogen ICE | 6336 | 22.542 | 298 | 12.960 |
| Methanol FC | 1446 | 2.912 | 2304 | 2.330 |
| Ammonia FC | 1542 | 3.582 | 2443 | 3.045 |
| Hydrogen FC | 7260 | 25.829 | 352 | 14.850 |

**Combustion engines**

As discussed in chapter 3, the same engines installed in the original diesel vessel are used for the new designs. The data analysis concluded that a more than 200 kW reduction could be achieved due to the lower operational speed, resulting in the 8-cylinder version instead of the 10-cylinder MTU engine. However, as hydrogen still faces challenges to achieve the energy density in the cylinder, additional cylinders are required to produce the same power output. The hydrogen combustion engine will have the weight and size of the 10-cylinder engine but the power output and fuel consumption of the 8-cylinder engine. Still, it is unknown if single-fuel engines for methanol, ammonia, and hydrogen will be built in this power density range. However, assuming single-fuel engines require more methanol, ammonia, or hydrogen, it will, therefore, present the worst scenario for total vessel weight and required volume. All fuels in comparison to diesel require more volume, substituting diesel for a partition of the alternative fuel will result in a more feasible design. The resulting engine specifications per fuel type are given in table 8.3

**Table 8.3:** Engine specifications per fuel type

| | Methanol | Ammonia | Hydrogen | |
|---|---|---|---|---|
| Type | 8V 2000 M72 | 8V 2000 M72 | 10V 2000 M72 | - |
| Mass | 4760 | 4760 | 5580 | kg |
| Volume | 2.644 | 2.644 | 3.216 | $m^3$ |
| Power | 720 | 720 | 720 | kW |
| Fuel rate | 186 | 186 | 186 | l/hr |

**Fuel cells**

The installed fuel cell type differs per fuel, as discussed in chapter 3. HT-PEMFC is the best solution for methanol and ammonia with an integrated hydrogen extraction system. Hydrogen can be used in the more efficient LT-PEMFC. The specifications of the installed fuel cells are given in table 8.4. The output per fuel cell differs, resulting in a few LT-PEMFC and many HT-PEMFC to achieve the total required power of 1500 kW. The fuel cells are stacked in towers with enough surrounding space for ventilation and maintenance.

**Table 8.4:** Fuel cell specifications per fuel type

| | Methanol | Ammonia | Hydrogen | |
|---|---|---|---|---|
| Type | HT-PEMFC | HT-PEMFC | LT-PEMFC | - |
| Brand | Blue.World [11] | Blue.World [11] | Zepp.Solutions [93] | - |
| Mass | 57 | 57 | 355 | kg |
| Volume | 0.052 | 0.052 | 0.595 | $m^3$ |
| Power | 18.0 | 18.0 | 150 | kW |
| Amount | 88 | 88 | 10 | - |
| Total mass | 5016 | 5016 | 3550 | kg |
| Total volume | 4.574 | 4.574 | 5.950 | $m^3$ |
| Total power | 1584 | 1584 | 1500 | kW |

**Electric motors & Pods**

The electric motors are placed on top of the Hydromaster pods. The Danfoss motor is a Synchronous reluctance assisted permanent magnet running on AC voltage with an aluminium casing. With 2 electric motors and the 360-degree rotating pods the manoeuvrability and acceleration are better than with the combustion engine. The further specifications of the electric motors are given in table 8.5. The electric motors produce more power than necessary; however, these engines are evenly effective at the lower required power. The specifications of the pods, azimuth thrusters, are given in table 8.6. The datasheet is made available by Damen; further specifications are not publicly accessible.

**Table 8.5:** Electric motor specifications [22]

| Specification | Value | Unit |
|---|---|---|
| Total Power | 1600 | kW |
| Number | 2 | |
| Total Mass | 1900 | kg |
| Total Volume | 0.722 | $m^3$ |
| Length | 1.04 | m |
| Diameter | 0.665 | m |

**Table 8.6:** Azimuth thruster specification

| Specification | Value | Unit |
|---|---|---|
| Number | 2 | |
| Max. duty rating | 800 | kW |
| Mass | 2250 | kg |
| Type | F L-Drive | |

**Batteries**

The battery type used in the fuel cell design was already determined in chapter 2. Putting batteries between the fuel cells and the electric motors can accommodate variations in energy demand. This results in a more efficient fuel cell operation and reduced fuel consumption. Additionally, it reduces wear on the fuel cell. The amount of installed batteries matches the electric motor capacity. With a discharge capacity of 4C, the battery pack is able to match the full power for the electric motors in peak performance. The resulting specifications of the batteries are given in table 8.7.

**Table 8.7:** Battery specifications [28]

| Specification | Value | Unit |
|---|---|---|
| Type | NCM Pouch | - |
| Mass | 385 | kg |
| Volume | 0.312 | $m^3$ |
| Capacity | 69.3 | kWh |
| Amount | 6 | - |
| Total mass | 2310 | kg |
| Total volume | 1.872 | $m^3$ |
| Total capacity | 415.8 | kWh |
| Peak discharge | 1663.2 | kW |

**Fuel preparation room**
As stated in chapter 6, the fuel cell designs require a fuel preparation room by class. This room houses the pumps, sensors, and connection piping between the fuel cells and storage tanks. For redundancy, a preparation room per fuel tank is installed. The spacing of the preparation room changes per design; a mass of 500 kg is set in all designs. A dual fuel preparation room system is installed for redundancy.

**Switchboard**
The fuel cell designs generate significant electrical power throughout the ship, making their controls essential for effective regulation. The precise components and management of the power output fall outside the scope of this research. However, due to the size of these systems, switchboard cabinets have been considered in terms of both their location and weight in the overall layout and total weight of the ship. An estimated weight of 1000 kg per switchboard is used.

**Accommodation**
The original diesel design is designed with a relatively large accommodation below deck. The vessel is also sold as a patrol vessel that requires multi-day deployment. The pilot vessel is more versatile with the accommodation but can operate without. A small below-deck accommodation with a toilet is, therefore, also sufficient. The total weight of the original accommodation is 2776 kg, and the small accommodation with a toilet is set at 500 kg. The weight estimation of the original accommodation is based on the by Damen given weight calculation. Furthermore, the fresh and waste water tanks are reduced from 1.0 $m^3$ to 0.2 $m^3$.

## 8.3. Weight calculation

The total weight assessment of the six designs is based on the original design, from which the key weights and corresponding centers of gravity have been summarized. All other systems remain in their original locations and have therefore not been included in the calculation. The calculation for the methanol ICE design is presented in table 8.8. The calculations for the other five designs are provided in Appendix B.

At the top of the table, the original lightship is displayed. For the ICE designs, the engines and the accommodation have been removed to obtain the empty lightship, with these components being re-installed later. In the case of the engines, they are shifted aft to adjust the trim in the ammonia and hydrogen ICE designs. The accommodation is not be feasible in all designs. For the FC designs, the remaining engine room components have also been removed. The necessary components are added to the empty lightship, resulting in the new lightship. Both the lightship and full load weights are critical for assessing power requirements and stability. The added deadweight components are based on the provided stability booklet. If a accommodation or bathroom is included in the design, the water tanks are adjusted accordingly. Both the lightship and full load designs have been converted to submerged hull volume. These volumes were measured using a Rhinoceros plug-in, Grasshopper, allowing for the determination of the buoyancy point of the vessels. For all components, a center of gravity in the middle of the designed blocks is assumed.

**Table 8.8:** Weight calculation methanol ICE design

| | **Weight (kg)** | **LCG (m)** | **VCG (m)** |
|---:|---|---|---|
| Original lightship | 40241 | 8.061 | 1.908 |
| Engines | 5580 | 5.797 | 1.206 |
| Accommodation | 2776 | 13.237 | 1.892 |
| Empty Lightship | 31885 | 8.007 | 2.032 |
| Accommodation | 2776 | 13.237 | 1.892 |
| Methanol tank | 1546 | 8.845 | 1.455 |
| Engines | 4760 | 5.797 | 1.206 |
| Fuel prep. Room | 500 | 8.845 | 1.455 |
| **Lightship design** | **41467** | **8.144** | **1.900** |
| Crew & effects | 200 | 11.250 | 4.230 |
| Personel | 680 | 8.860 | 4.230 |
| Sludge tank | 6 | 2.375 | 0.244 |
| Aft deck cargo | 945 | 2.000 | 3.120 |
| Supply owner | 200 | 12.000 | 1.950 |
| Freshwater | 979 | 12.000 | 0.477 |
| Wastewater | 116 | 10.000 | 0.204 |
| Methanol fuel | 2516 | 8.845 | 1.455 |
| **Full load design** | **47109** | **8.182** | **1.910** |
| Lightship displacement ($m^3$) | 40.456 | 8.139 | 0.558 |
| Full load displacement ($m^3$) | 45.960 | 8.182 | 0.599 |

With the known trim value and LCB, the LCG is matched by the component arrangement. Table 8.9 summarises the lightship and full load weights and trim conditions. The initial lightship weights are almost all higher than the original diesel vessel, this is mainly due to the heavy fuel tanks. The Ammonia ICE design has a lower initial weight due to the absence of an accommodation. In full load condition, the weights are in range with the original design. For the trim a margin of 100 mm is accepted, all 12 calculations are within this margin.

**Table 8.9:** Mass and trim overview

| | Lightship design | | Full load design | |
|---|---|---|---|---|
| | Weight (kg) | Trim (mm) | Weight (kg) | Trim (mm) |
| Diesel ICE | 40241 | -20 | 47741 | -1 |
| Methanol ICE | 41467 | -5 | 47109 | 0 |
| Ammonia ICE | 39579 | 98 | 44750 | -47 |
| Hydrogen ICE | 44301 | -21 | 46630 | 61 |
| Methanol FC | 42476 | 23 | 47031 | -35 |
| Ammonia FC | 43654 | -23 | 48128 | 16 |
| Hydrogen FC | 46893 | -96 | 48924 | 5 |

## 8.4. General arrangement

To provide a clear understanding of the design changes to the pilot vessel, the original diesel design layout is shown in figure 8.1. The engine, highlighted in yellow, the gearbox positioned just in front of the engine, the fuel tanks, and the accommodation are all depicted. The fuel tanks are the relatively small gray blocks. The accommodation is the large turquoise block. The location of the gearbox is fixed due to the angle of the propeller shaft for all designs. Altering this angle could result in changes to the vessel's handling characteristics.

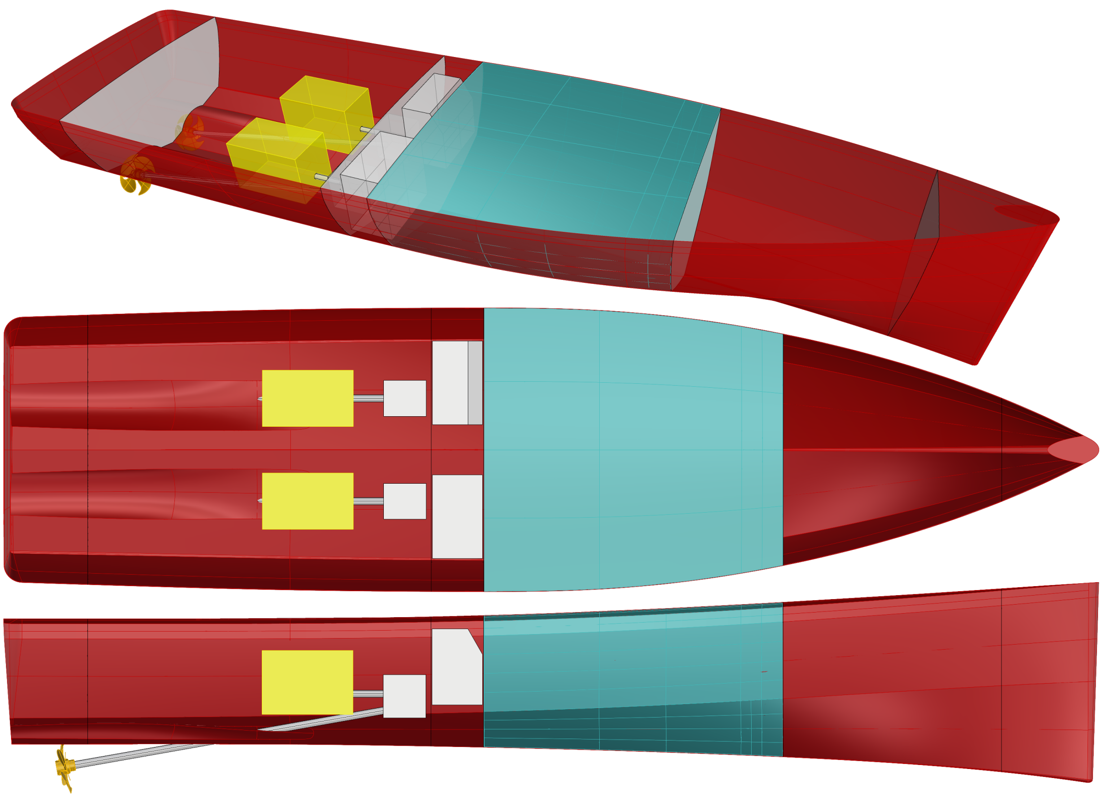

**Figure 8.1:** Original layout diesel ICE design

### 8.4.1. Methanol ICE design

The methanol ICE design, shown in figure 8.2, shares similarities with the original diesel ICE design. The main differences are the size of the fuel tanks (in blue) and the addition of fuel preparation rooms. The tanks retain the shape of the original diesel tanks but are narrower due to the reduced volume required. This has created space between the fuel tanks, in which the fuel preparation rooms are placed. The relatively heavy stainless steel fuel tanks are close to LCB, minimizing their impact on trim. The area surrounding the fuel tanks and fuel preparation rooms is enclosed by water- and airtight bulkheads.

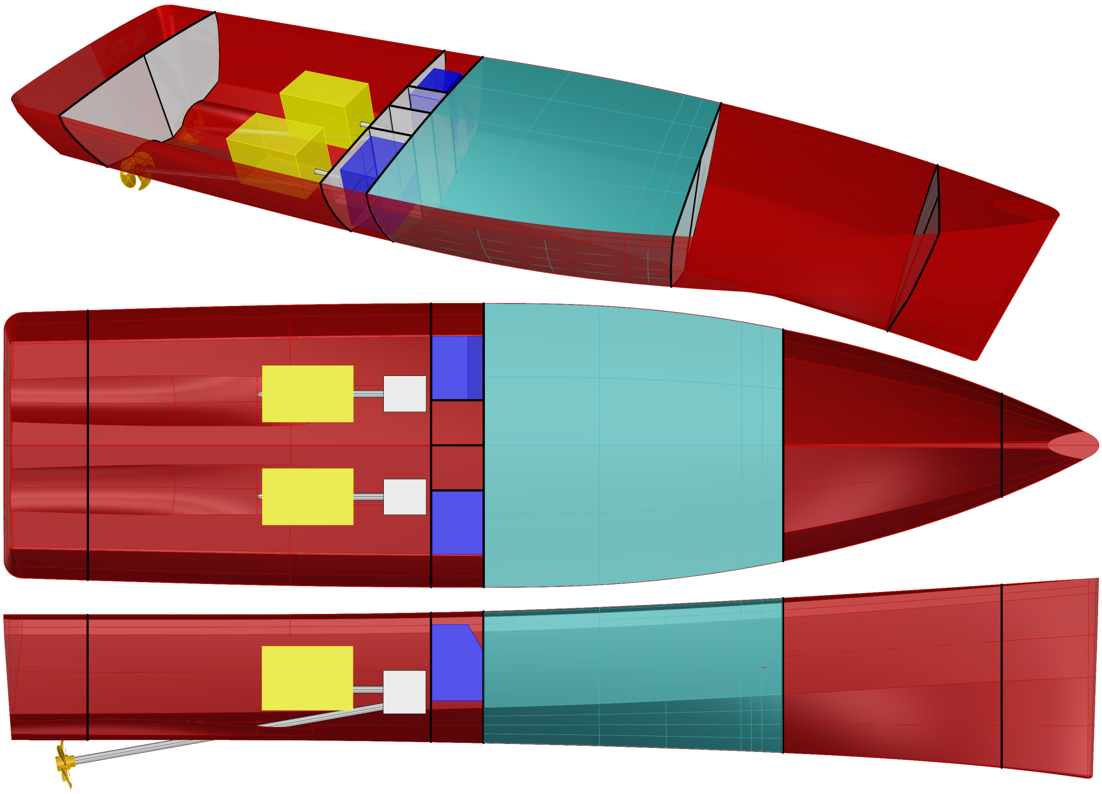

**Figure 8.2:** Layout methanol ICE design

### 8.4.2. Ammonia ICE design

In the ammonia ICE design, there is no space for accommodation; instead, a bathroom is located in the front. The fuel tanks are designed with sufficient surrounding space to meet the class imposed safety margins. Both tanks are placed in water- and airtight compartments and have their own dedicated fuel preparation room. To compensate for the trim caused by the heavy fuel tanks, the engines have been positioned further aft in the engine room as can be seen in figure 8.2.

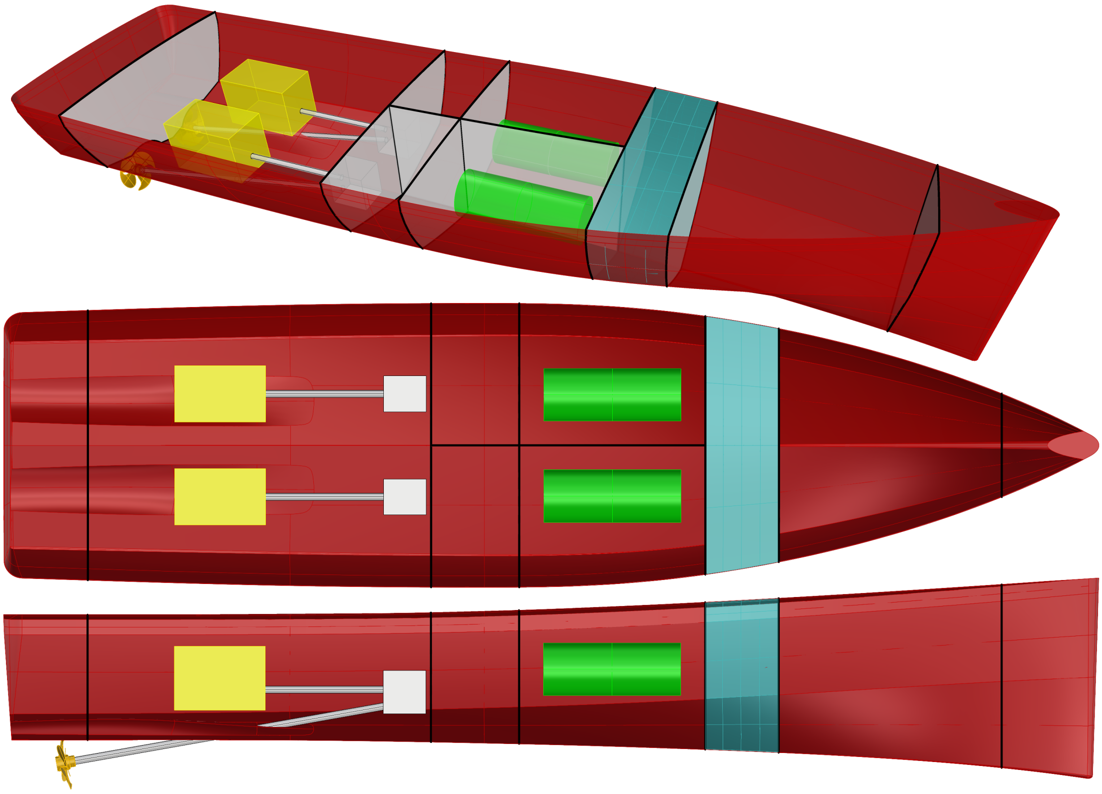

**Figure 8.3:** Layout ammonia ICE design

### 8.4.3. Hydrogen ICE design

In the hydrogen ICE design, shown in figure 8.4, there is not enough space for all required hydrogen tanks due to the imposed class rules. Due to the weight, the hydrogen tanks are positioned in the vessel's middle to reduce impact on the trim. Like the ammonia design, the engines are moved back into the engine room to limit the trim. Due to the central location of the hydrogen tanks, there is no room for accommodation or a bathroom, as the space before the tanks is inaccessible from the superstructure.

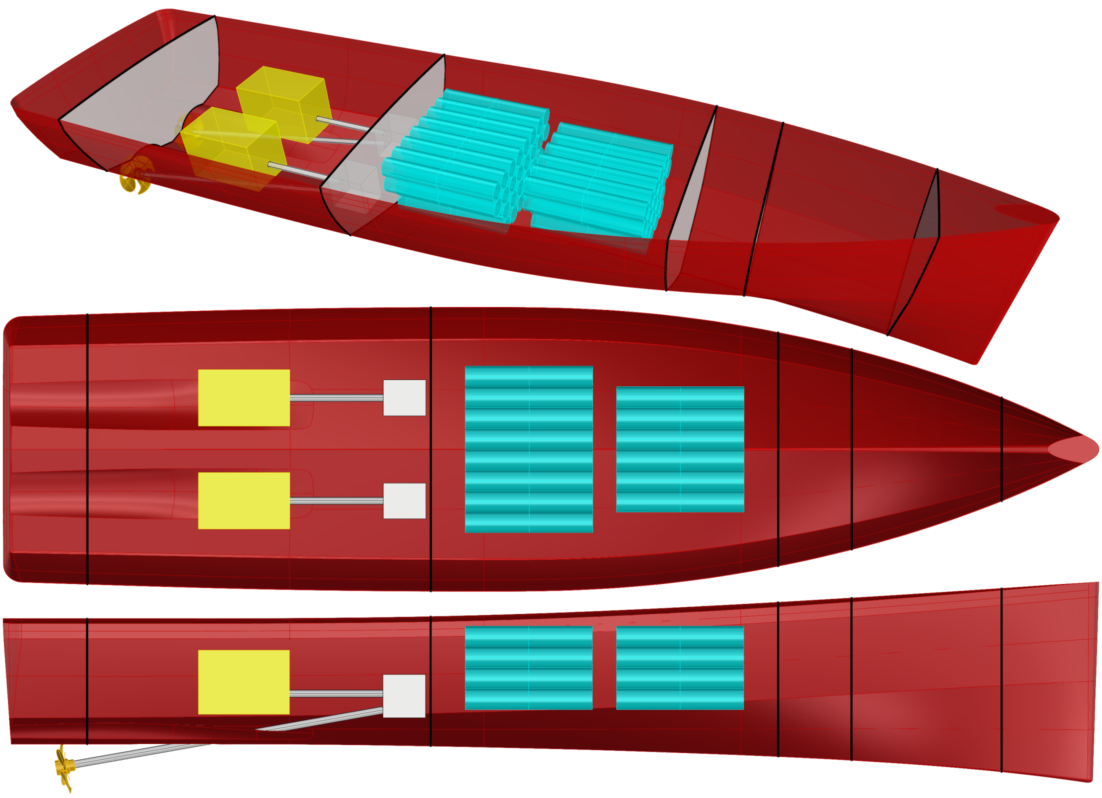

**Figure 8.4:** Layout hydrogen ICE design

### 8.4.4. Methanol FC design

The FC designs are all equipped with pods powered by electric motors, this results in more flexibility in the layout as the combined pod with electric motor is relatively heavy in the aft. In the methanol FC design, shown in figure 8.5, the fuel cells are placed in the front of the vessel to compensate the weight of the pods and electric motors. The methanol tanks have side by side their own fuel preparation room. This preparation room is directly connected with both the fuel cells and fuel tanks. The batteries are placed in the same space with the switchboard close to the electric motor. In the middle of the hull a bathroom is installed.

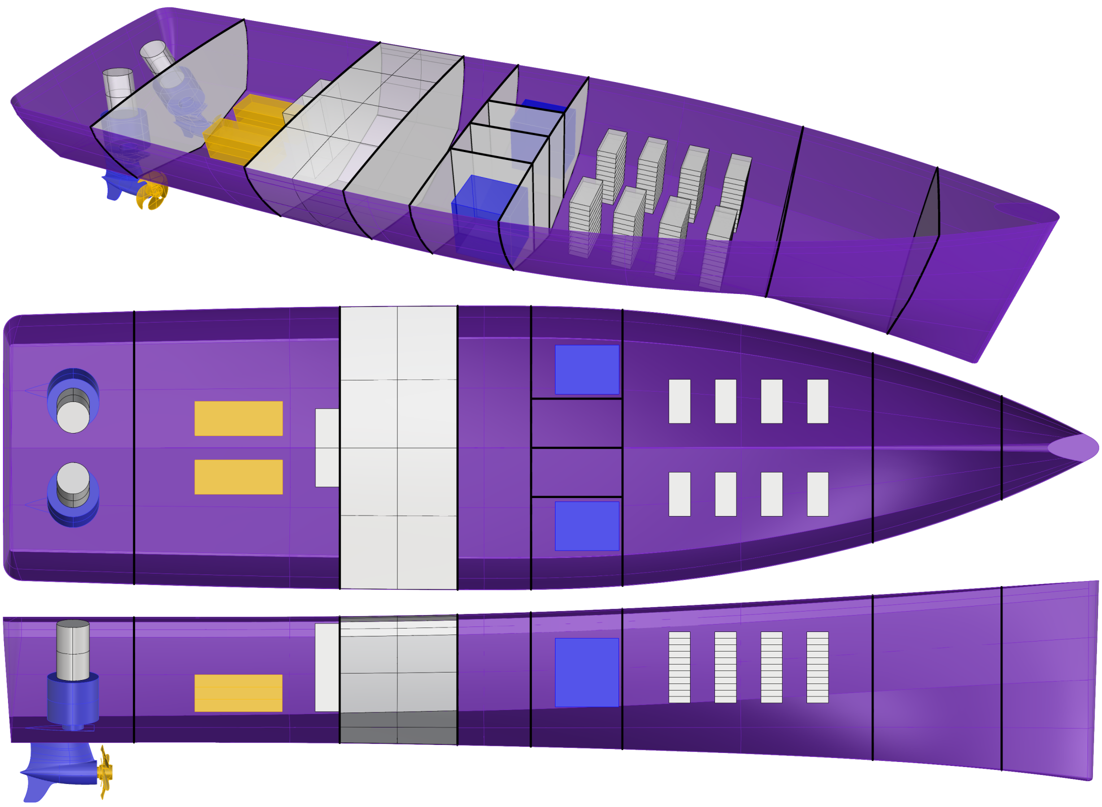

**Figure 8.5:** Layout methanol FC design

### 8.4.5. Ammonia FC design

The Ammonia FC design, shown in figure 8.6, is similar to the arrangement with methanol fuel. The differences are the larger fuel tanks and the absence of a bathroom below deck. This is due to the larger fuel tanks and required safety margins. The fuel preparation rooms are located between the fuel cells and fuel tanks. The batteries, fuel tanks and fuel cells are all divided by water- and airtight bulkheads.

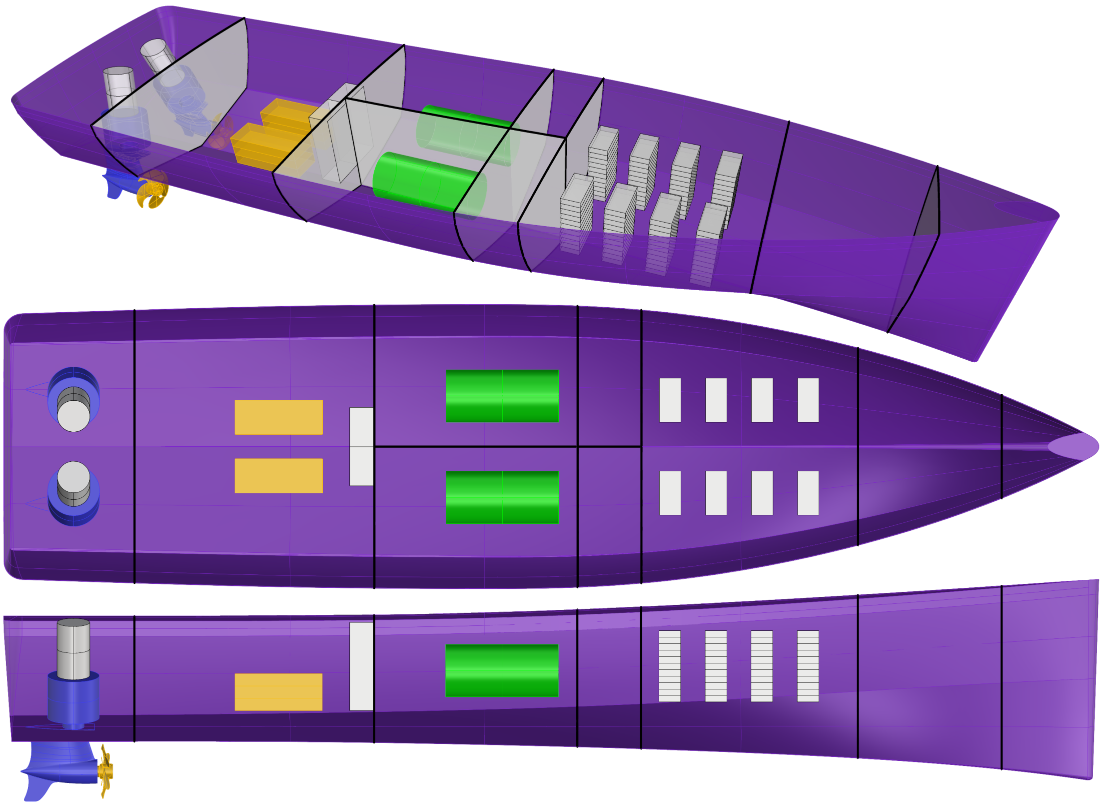

**Figure 8.6:** Layout ammonia FC design

### 8.4.6. Hydrogen FC design

The most unique design is the hydrogen FC design shown in figure 8.7. The LT-PEMFCs are more extensive than those required for methanol and ammonia, but fewer are needed. The fuel cells are placed in the back of the vessel to compensate for the volume and weight of the hydrogen tanks. The fuel preparation room is between the fuel cells and fuel tanks for direct connection. The batteries are located in the front of the vessel. In contrast to the methanol and ammonia design, the switchboard is placed in the same room with the fuel cells instead of the batteries. Due to the large fuel tanks, there is no room for an accommodation or a bathroom inside the hull.

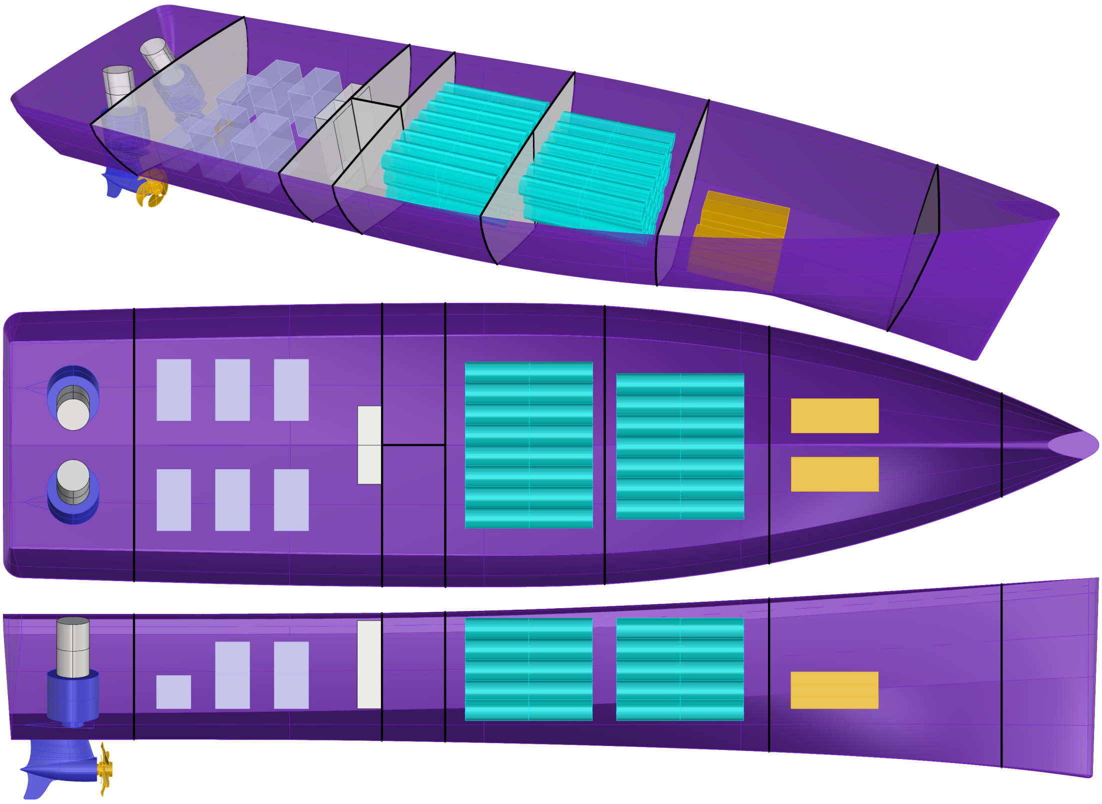

**Figure 8.7:** Layout hydrogen FC design

## 8.5. Resistance calculation

The installed power must achieve the design speed based on the expected resistance. An estimation of the required power has been made based on the installed power in the original diesel ICE design; however, the weight of the ship has changed due to the addition of new system components. By interpolating the resistance data for various ship weights, known to Damen, across different speeds, the resistance for each design can be estimated based on the new weight. Figure 8.8 presents the resistance curve for the methanol ICE design, with resistance expressed in power instead of force. The remaining five resistance curves are provided in appendix B.

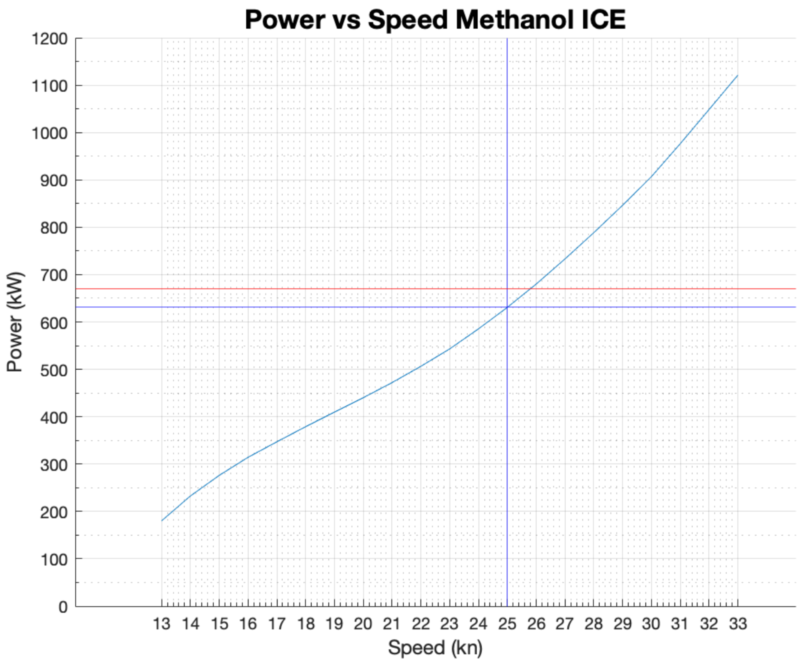


**Figure 8.8:** Resistance curve methanol ICE design

In all figures, the installed power is highlighted by the horizontal red line; this value differs between the ICE and FC designs. A second blue line shows the required power to match the 25 knots. In all six figures, the blue line is below the red line, meaning the installed power is sufficient to achieve 25 knots. The required power is at calm water; in reality, waves and wind occur, and a margin of 5% is therefore necessary. Table 8.10 presents the required power and margin per design. In the last column, the margin is given as a percentage; all designs meet the 5% margin. The installed and required power are both on the propeller shaft, taking all efficiencies into account.

**Table 8.10:** Power margins based on Damen PSD

| | Installed Power (kW) | Required power (kW) | Margin (kW) | Margin (%) |
|---|---|---|---|---|
| Methanol ICE | 670.74 | 630.93 | 38.81 | 5.9 |
| Ammonia ICE | 670.74 | 601.40 | 69.34 | 10.3 |
| Hydrogen ICE | 670.74 | 624.60 | 46.14 | 6.9 |
| Methanol FC | 691.42 | 624.67 | 61.75 | 8.9 |
| Ammonia FC | 691.42 | 643.60 | 47.82 | 6.9 |
| Hydrogen FC | 691.42 | 653.73 | 37.69 | 5.5 |

## 8.6. Stability

The KM value is required to determine the stability of the ship. This value can either be decomposed into KB and BM or calculated directly. Given that BM is challenging to calculate due to the varying drafts of each ship, KM has been determined through interpolation. In this interpolation, the ship's weight and the KM of the original ship, obtained from the stability assessment, are plotted against each other, as shown in figure B.6 in appendix B. The resulting equation 8.1 allows KM to be determined linearly based on the total ship weight. The stability can then be assessed using equation 8.2.

$$KM = -0.00002 \cdot Mass_{Full\ load} + 4.4843 \tag{8.1}$$

$$GM = KM - KG \tag{8.2}$$

Table 8.11 presents the KM, KG, and resulting GM for all six designs. In this calculation the full load conditions are used. The lightweight condition and resulting stability values are given in table B.6 in appendix B. All stability values are above the required 0.15 m and the advised 1.5 m for high speed vessels.

**Table 8.11:** Stability components of the six designs in full load condition

| | **KM (m)** | **KG (m)** | **GM (m)** |
|---|---|---|---|
| ICE methanol | 3.54 | 1.91 | 1.63 |
| ICE ammonia | 3.59 | 1.94 | 1.65 |
| ICE hydrogen | 3.55 | 1.88 | 1.67 |
| FC methanol | 3.54 | 1.78 | 1.76 |
| FC ammonia | 3.52 | 1.77 | 1.75 |
| FC hydrogen | 3.51 | 1.79 | 1.72 |

## 8.7. Design comparison

The ICE designs are similar in layout and system components to the original diesel design. The control techniques on board are largely the same, with only the fuel and engine requiring new systems. By retaining the existing propulsion system, the operation of the vessel will remain comparable. The primary differences in engine room layout and fuel tank placement arise from the need to maintain trim, ensuring consistent vessel performance.

The FC designs differ fundamentally from the ICE designs due to the distinct system components involved. The 360-degree rotatable pods with electric motors at the stern of the vessel provide exceptional maneuverability at both high and low speeds, with propeller efficiency comparable to the fixed propellers in the ICE designs. However, the heavy weight at the stern must be balanced by positioning other components further forward. The location of the fuel preparation rooms is critical, as it must be situated adjacent to both the fuel tanks and FCs. The integration of electric motors, fuel cells, and batteries requires an advanced control system with sufficient redundancy, this results in increased complexity. Emissions from all FC designs are lower than those of the ICE counterparts due to lower operating temperatures and the absence of combustion. However, precise emissions are difficult to determine because the engine is still in the estimation phase. The actual engine has not yet been developed, so its exact emissions cannot currently be accurately assessed.

The six designs can be compared with one another based on design inputs and conclusions drawn from the literature regarding the use of fuels and power generation systems. Not every aspect carries equal weight in the evaluation of the designs. Factors that carry significant weight include range, speed, and class regulations. In contrast, complexity is of lesser importance in defining the technical feasibility. Table 8.12 shows the scores of all six designs on the six most important parameters. All six designs match the class rules. However, the necessary adjustments affect other parameters. In the column headers the weight factor is elaborated.

**Table 8.12:** The six design comparison parameters

| | Range (3) | Accommodation (2) | TRL (2) | Maneuverability (2) | Complexity (1) | Emission(2) | Total |
|---|---|---|---|---|---|---|---|
| Methanol ICE | ++ | ++ | + | + | ++ | – – | ++ |
| Ammonia ICE | ++ | +/– | – – | + | +/– | – | +/– |
| Hydrogen ICE | – – | – – | – | + | +/– | + | – |
| Methanol FC | ++ | +/– | + | ++ | – – | – | + |
| Ammonia FC | ++ | – – | – – | ++ | – – | +/– | +/– |
| Hydrogen FC | ++ | – – | + | ++ | – | ++ | ++ |

## Range

The range, along with the design speed, is the most critical aspect of the design. All vessels achieve the design speed, as demonstrated in paragraph 8.5. Five out of the six designs have sufficient fuel capacity to meet the required range. Only the hydrogen ICE design does not comply, which can be attributed to the strict class regulations regarding cofferdam spacing and the large volume of the hydrogen tanks.

## Accommodation

The placement of the accommodation is challenging in most designs due to the increased required space for fuel tanks. Only the ICE methanol design includes full accommodation. The ICE ammonia and FC methanol designs allow for a smaller accommodation with a toilet. The absence of full accommodation may still be addressed through the design of the superstructure.

## Technical Readiness Level

The TRL of the complete system is a crucial indicator of the technical feasibility of the design. The TRL of the fuels themselves, as detailed in chapter 2, must be combined with that of the power generation system. The ICEs for methanol, ammonia, and hydrogen with the same power output as the diesel variant are still under development. It remains uncertain whether ammonia and hydrogen engines will be available as single-fuel options on the market, which lowers their feasibility. For the FC designs, determining the TRL is more complex, as it depends on the integration of the entire system, not just the FC itself. Unlike the ICEs, the components for FC designs are commercially available. However, the application of HT-PEMFC with an integrated ammonia cracking system is less established, and, combined with the low TRL of the fuel itself, this results in a low overall TRL.

## Maneuverability

The maneuverability of all designs is satisfactory. The ICE designs feature the original propulsion system, which Damen has deemed adequate. The FC designs, equipped with 360-degree rotatable pods, offer enhanced maneuverability, particularly at lower speeds where the rudder of the original propulsion system is less effective.

## Complexity

The complexity of the six designs is related to the Technology Readiness Level (TRL); a lower TRL indicates higher complexity. Consequently, the complete design process will involve greater challenges at both the component and system levels. The complexity of both the ICE ammonia and hydrogen designs is higher than that of the methanol design, primarily due to the repositioning of the main engines and the more intricate fuel tanks. All fuel cell designs exhibit significant complexity due to the comprehensive system integration and control techniques required. There is more established knowledge regarding the application of hydrogen in fuel cells, which slightly reduces the overall complexity.

## Emission

The emissions of the six designs depend on the fuel and processing method employed. Additionally, the actual emissions are influenced by the fuel production method. The use of hydrogen in a LT-PEMFC results in zero emissions, making it the cleanest design. Burning hydrogen in an ICE also produces relatively low emissions, primarily limited to $NO_x$ due to the high temperatures involved. In contrast, ammonia generates high levels of $NO_x$, mainly due to the nitrogen atoms present in the fuel itself. Both combustion and fuel cell applications of methanol release $CO_2$. For ammonia and methanol, the primary method for reducing emissions involves the implementation of EGTS. These systems are described in chapter 3, although they have not been included in the primary designs.

# Part IV

# Conclusion & Discussion

# 9 Conclusion

To conclude the research, the research question will be answered. However, all sub-questions must be answered first as they collectively support the main research question.

## Alternative fuels

The sub-questions of the alternative fuel part are answered below. Table 9.1 shows an overview of all the necessary specifications regarding the used alternative fuels.

- What is the energy density, and how are the storage conditions of the possible alternative fuels?

The energy density, given in the LHV, is volume-based lower for all fuels than diesel. Looking at the gravimetric energy density, hydrogen performs outstandingly. However, considering the storage tank size and weight, hydrogen is the least energy-dense alternative fuel. Methanol can be stored in normal conditions, similar to diesel. Ammonia and hydrogen are stored differently to improve the energy density. Ammonia is cooled to 239.9 kelvin; hydrogen is pressurized to 350 bar. Hydrogen can be stored in liquid or at 700 bar as well. However, the net energy density is lower for storage at 700 bar, and liquid hydrogen requires more advanced systems and is less effective on the scale of a pilot vessel.

- What are the emissions related to the possible alternative fuels?

With the application of methanol, ammonia and hydrogen, the emissions of $SO_x$ and PM are diminished. However, $NO_x$ and $CO_2$ are still emitted. Methanol still results in $NO_x$ and $CO_2$ in both ICE and FC design. Ammonia and hydrogen only emit $NO_x$. Ammonia produces relatively more $NO_x$ as nitrogen is part of the chemical structure. The hydrogen fuel cell system achieves zero emission due to the low operating temperature in the fuel cell. The combustion of hydrogen in the ICE design still emits $NO_x$ due to the high temperatures in the cylinder.

- How is the Technical Readiness Level (TRL) of the possible alternative fuels?

The TRL of methanol and hydrogen is rated at an 8 due to the experience with both fuels. However, more experience with both fuels is needed to reach stage 9. The usage of ammonia as marine fuel still needs to be developed more. With a level of 5, the implementation of ammonia in high-speed vessels is not possible at this moment. However, development and research of ammonia as a fuel must be continued as it is a promising candidate for becoming an alternative fuel in the coming decades.

**Table 9.1:** Applicated alternative fuel specifications

| Specification | Methanol | Ammonia | Hydrogen | Unit |
|---|---|---|---|---|
| Storage temperature | 298 | 239.9 | 298 | K |
| Storage pressure | 101 | 101 | 350000 | kPa |
| LHV | 20.1 | 18.8 | 9.11 | MJ $kg^{-1}$ |
| LHV | 15.9 | 12.8 | 1.58 | MJ $dm^{-3}$ |
| TRL | 8 | 5 | 8 | - |
| Emissions | $CO_2$, $NO_x$ | $NO_x$ | $NO_x$ | - |

## Power generation systems

- What are the operational principles of Internal Combustion Engines (ICE) and fuel cells (FCs)?

The main difference between ICE and FC is the chemical reaction. As the name of the ICE implies, combustion with the fuel and oxygen occurs, whereas, in the fuel cell, an electrochemical reaction betwen hydrogen and oxygen takes place. The ICE produces mechanical energy that can drive the propeller shaft via a gearbox, whereas the FC produces electricity to power an electric motor on the drive shaft.

- What are the energy conversion efficiencies associated with ICEs and FCs for alternative fuels?

The used efficiencies for both ICE and FC designs are given in table 9.2. In comparison, the efficiency of the diesel combustion engine is rated at 39%. Thus, almost all designs have a higher conversion efficiency. This efficiency is taken at full power with a constant output. The FC efficiencies are higher at partial loads; however, the full-load condition is used for the FCs as it presents the worst-case efficiency and installing more fuel cells that can operate at a higher efficiency will result in a worse scenario as extra weight and volume is added to the designs.

**Table 9.2:** Energy conversion efficiencies

| | **Methanol** | **Ammonia** | **Hydrogen** |
|---|---|---|---|
| ICE | 39% | 37% | 40% |
| FC | 45% | 45% | 51% |

## Design inputs

- What is the energy demand based on the load profiles of the ’Loodswezen’ pilot vessels?

The energy demand for pilot vessels in the Rotterdam area can be determined based on the required operational speed and range. This is done based on the L-class vessel the Lynx of the Dutch Pilot Association ’Het Loodswezen’. Based on measurements on the Lynx from January till November 2022, a maximum speed of 25 knots is concluded as the sailed speed over water exceeded the 25 knots for 8.5%. Lowering the operational speed from 29 to 25 knots reduces the sailed distance by 34 NM or 0.63%. The sailed trips are divided by a set bunker time of 45 minutes. This results in a required amount of diesel of 1400 litre, considering the 25 knots operational speed. Reducing the required energy from roughly 5000 to 1400 litre diesel equivalent is significant and provides opportunities to use alternative fuel onboard high-speed pilot vessels.

- How do the necessary safety regulations affect the vessel design?

Class regulation asks for two main safety aspects for implementing alternative fuels on marine vessels that influence the design layout. First, cofferdam spacing is required around the fuel tanks. With this cofferdam, an extra safety layer against leakage by both the tank and external impacts is achieved. This affects the design because less space can be used to place the fuel tanks in a compact vessel. Secondly, when alternative fuels are applied, a fuel preparation room is required. All necessary components for the fuel system, such as pumps, valves or sensors, are placed inside the fuel preparation room. Each tank has its fuel preparation room for redundancy, as the fuel system shuts down when a sensor sees an error. The FPR has to be located between the fuel tanks and FCs; the location affects the design layout.

## System and layout design

- What is the effect an alternative fuel propulsion system on the speed and range?

The alternative fuel on board the new designs must replace the energy equivalent of diesel from the original design to match the original operational profile. However, a less energy dense fuel is more spacious, resulting on more required space onboard. Therefore, the implementation of alternative fuels will result in a shorter range, or by reducing the installed power a lower speed as a lower power output consumes less fuel. In the case of the pilot vessel, both principles are executed; less power installed as a lower speed is possible and a smaller fuel capacity is installed.

- What is the size and weight of an alternative fuel propulsion system for a required power and range?

The required fuel capacity and power generation system of five designs fit inside the hull; only the hydrogen ICE design cannot meet the required amount of fuel tanks. The precise size and weight of all the installed components are given in chapter 8. The used engine in the ICE designs is assumed to be equal in size and weight to the initially installed diesel engine. The FC designs require fuel cells, batteries, pods and electro motors, making the total size and weight more extensive than the original design. Removing the accommodation in some designs results in less comfort onboard but leads to more space for the power generation systems and fuel tanks.

- What is the impact of an alternative fuel propulsion system on the resistance and speed of the pilot vessel?

The main impact on the resistance at certain speeds is the vessel's weight. With varying components over the six designs, the weight differs for each design. However, as discussed in paragraph 8.5, all designs have enough installed power to sail the vessel at 25 knots. The required power is at calm water; a margin of 5% for increased resistance due to waves and wind is considered.

Combining the conclusions on the ten sub-questions, an answer can be given to the research question, which is formulated as follows:

**Is it technical feasible to integrate alternative fuel based technologies in pilot vessels, with a particular emphasis on the technical aspects and layout design considerations, using the Stan Pilot 2205 design as a framework for investigation?**

Integrating emission reducing technologies is feasible in the SPi 2205 FRP following the operational profile of the pilot vessel in the Rotterdam harbour. Five out of the six designs, concluded out of the literature part, are technically feasible. Each of the 5 designs has its own features, they are rated in paragraph 8.7. The specifications of the five technical feasible designs are summarised in table 9.3.

**Table 9.3:** Specifications of the five technical feasible designs

| | Fuel (kg) | Weight (kg) | Trim (mm) | Power (kW) | Margin (%) | Accommodation |
|---|---|---|---|---|---|---|
| Methanol ICE | 2516 | 47109 | 0 | 670.74 | 5.9 | Full accommodation |
| Ammonia ICE | 2919 | 44750 | 98 | 670.74 | 10.3 | Bathroom |
| Methanol FC | 2304 | 47031 | -21 | 691.42 | 8.9 | Bathroom |
| Ammonia FC | 2443 | 48128 | 23 | 691.42 | 6.9 | None |
| Hydrogen FC | 352 | 48924 | -23 | 691.42 | 5.5 | None |

Ammonia as a fuel has a TRL of 5, making it a less viable option. Therefore, three out of the six designs are considered realistic options. The hydrogen FC design is the most feasible, as all necessary components are commercially available, and there is considerable experience with them. For the methanol FC design, the HT-PEMFC is still in a development phase and has not yet been applied on the scale of the LT-PEMFC. Regarding the methanol ICE design, the selected single-fuel engine is not yet commercially available. Once this single-fuel ICE reaches the market, the methanol ICE design will be the best option. Until then, the hydrogen FC design is a viable and immediately implementable alternative. However, determining the best result for all situations is not possible. The best alternative fuel with power generation method is different per customer, shipyard, and operational profile and area.

# 10 Discussion

In this chapter, the key assumptions and potential limitations of the research are discussed, organized by topic. First, the use of single-fuel application in ICEs and HT-PEMFC fuel preparation are examined, both of which are components of the system specification. Next, the critical points from the data that define the operational profile and design inputs are reviewed. Furthermore, the distinctions between preliminary design and detailed engineering, as well as the differences in technical feasibility, are explored. Finally, the chapter addresses the contrast between emission reduction and zero-emission, and how the latter can be achieved in further steps. Then, in paragraph 10.1 the recommendations for further research are discussed.

### Single fuel ICE

The assumption is that all three ICEs can run on a single fuel to simplify the design process. As the engines have yet to be built, tested, or used, there is no certainty that single-fuel high-speed engines, mainly for ammonia and hydrogen, will become viable. However, assuming a single-fuel engine only stores less energy-dense fuel is the worst-case scenario. For example, a dual fuel engine with 60% diesel and 40% hydrogen requires less stored hydrogen onboard, making it a more feasible design. On the other hand, this will result in increased emissions, leading to a design that is less effective in reducing emissions. Furthermore, the assumed engine efficiencies are based on single-cylinder tests. The actual efficiency might differ after constructing and testing the multi-cylinder complete engine. The hydrogen ICE efficiency in the literature is given at peak efficiency; for the constant efficiency, 4% less is assumed. This is in line with the differences between constant and peak efficiencies for other fuel types. Even with this high estimated efficiency, the required hydrogen tanks do not fit inside the hull.

### HT-PEMFC fuel preparation

In the HT-PEMFC, utilized in the methanol and ammonia fuel cell design, an integrated MSR system is present. This system, as described in Chapter 3, decomposes methanol into hydrogen and $CO_2$. In the ammonia fuel cell design, it is assumed that the same integrated MSR system can also decompose ammonia into hydrogen and nitrogen. The manufacturer of the fuel cells indicates that the MSR system is integrated but does not specify its application with ammonia. However, considering that a cracker is of similar size to an MSR, the assumption regarding the size and capacity of this system is consistent with that of a PEMFC equipped with an integrated ammonia cracker.

### Operational input

The operational profile is constructed based on engine and AIS data. The recorded data is not consistent; for instance, wave height and wind speed are not known for every data point. This makes it challenging to incorporate these two factors into the analysis, particularly since they are crucial at high speeds. However, it is important to note that a pilot vessel typically travels equally in both directions during a trip, which mitigates the impact of wind and waves on the total trip duration. Nevertheless, achieving top speed is still affected as this is done in peak moments. Furthermore, it is difficult to determine when a piloting operation occurs from the data, making it challenging to specify the exact usage patterns of the vessel during these operations.

The new pilot vessel designs are based on the operating profile in Rotterdam, although the pilot boats operate in areas beyond just Rotterdam. IJmuiden and Vlissingen, for instance, are also significant pilotage areas. Due to incomplete data from these regions, it is difficult to obtain a comprehensive understanding of their specific conditions. In Vlissingen, for example, trips tend to be shorter with shorter intervals, which does not align well with the 45-minute refueling time. An alternative bunker strategy might be more appropriate in this context. The pilot service rotates its fleet across operational areas to maintain consistent vessel usage, which presents challenges when introducing a new pilot boat specifically designed for the Rotterdam area. However, this design increases the boat's effectiveness in its designated area, while pilot boats for IJmuiden and Vlissingen will likely require different specifications.

#### Detail engineering

The technical feasibility in this research is based on a preliminary design. A comprehensive system analysis, detailed engineering of technical spaces, and system testing are necessary to determine whether the application of alternative fuels on pilot boats is truly technically feasible. The designs account for additional weight and volume, with a rough outline that allows for further detailing. For example, the assumption of single-fuel ICEs represents a conservative approach, as single-fuel systems require more space for fuel storage compared to dual-fuel systems.

#### Emission reduction

The application of alternative fuels such as methanol, ammonia, and hydrogen has significantly reduced emissions. $SO_x$ and PM have been completely eliminated from the exhaust gases. However, $NO_x$ and $CO_2$ emissions remain present. To transition from emission reduction to zero emissions, EGTS and CCS, as discussed in chapter 3, must be implemented. The size of these systems needs to be accounted for in the designs, which has not been done in the current process. However, there is available space for these systems to be installed, though their inclusion will increase the overall complexity of the design.

## 10.1. Recommendations

Based on the conclusion and discussion, the following steps can be taken as the next phase of this research.

#### Dynamic system calculations

In this research, only the static power requirements have been determined; the actual dynamic power demands and the interaction between the fuel cell, battery, and electric motor were not addressed. This system integration is a crucial aspect in the further development of an emission-reducing high-speed pilot vessel. While there is extensive knowledge regarding the behavior of diesel in an ICE, this is not the case for alternative fuels. Research into the combustion characteristics, wear and tear, and power output of engines running on alternative fuels is necessary to advance the development of high-speed engines using these fuels.

#### Detail engineering

To gain a more comprehensive understanding of the technical feasibility, detailed engineering needs to be developed within the ship's design. This type of research may not be suitable as a master thesis project but would be better suited for the engineering departments at Damen or another shipbuilder.

#### Emission reducing feasibility study on Stan Patrol vessels

The vessel used in this research, the SPi 2205 FRP, is part of a larger collection of similar ships within the Damen portfolio. The same boat is also sold as a patrol boat (SPa 2205 FRP), but its operational profile differs from that of the pilot boat. This different profile will likely require a greater fuel capacity and accommodation. Consequently, conducting a technical feasibility study for this patrol boat presents a significant challenge.

### Cost estimation

This research focused on technical feasibility, with costs deliberately excluded from consideration. Given the rapidly growing market for alternative fuels and power generation systems, it is challenging to accurately estimate costs. To gain an understanding of the investment required for alternative fuels, a study on the current and projected costs of these fuels and systems is necessary.

# References


[1] International Energy Agency (IEA). *Global EV Outlook 2023*. https://iea.blob.core.windows.net/assets/dacf14d2-eabc-498a-8263-9f97fd5dc327/GEVO2023.pdf. 2023.

[2] International Energy Agency (IEA). *Global Hydrogen Review 2022*. License: CC BY 4.0. IEA. 2022. URL: https://www.iea.org/reports/global-hydrogen-review-2022.

[3] International Energy Agency (IEA). *Global Hydrogen Review 2023*. License: CC BY 4.0. IEA. 2023. URL: https://www.iea.org/reports/global-hydrogen-review-2023.

[4] Auto Upkeep Academy. *Four-Stroke Engine*. 2024. URL: https://academy.autoupkeep.com/courses/how-cars-work/lessons/how-cars-work/topic/four-stroke-engine/.

[5] Joan van den Akker. "Carbon capture onboard LNG-fueled vessels: A feasibility study". MA thesis. Delft University of Technology, 2017. URL: http://resolver.tudelft.nl/uuid:a94741f3-c7cb-4970-80d1-bceebff4e423.

[6] *Alma Clean Power Announces Breakthrough in Direct Ammonia Fuel Cells*. https://almacleanpower.com/news/alma-clean-power-announces-breakthrough-in-direct-ammonia-fuel-cells. Accessed on: 2024-01-29.

[7] Port of Amsterdam. *HS Neo Orbis - Interreg NWEurope*. Accessed: 2024-01-29. June 2021. URL: https://vb.nweurope.eu/media/16834/neo-orbis_en.pdf.

[8] Pablo Ayuso et al. "Optimized profitability of LFP and NMC Li-ion batteries in residential PV applications". In: *Mathematics and Computers in Simulation* 183 (2021), pp. 97–115.

[9] Muhammad Aziz. "Liquid Hydrogen: A Review on Liquefaction, Storage, Transportation, and Safety". In: *Energies* 14.18 (2021). ISSN: 1996-1073. DOI: 10.3390/en14185917. URL: https://www.mdpi.com/1996-1073/14/18/5917.

[10] Francesco Baldi, A. Coraddu, and Maria E. Mondejar, eds. *Sustainable Energy Systems on Ships: Novel Technologies for Low Carbon Shipping*. English. Elsevier, 2022. ISBN: 978-0-32-385990-5. DOI: 10.1016/C2020-0-01975-4.

[11] *Bloom Energy Hydrogen Data Sheet*. https://www.bloomenergy.com/wp-content/uploads/hydrogen-data-sheet.pdf. Accessed on February 8, 2024. 2022.

[12] Alberto Boretti. "Advances in Diesel-LNG Internal Combustion Engines". In: *Applied Sciences* 10.4 (2020). ISSN: 2076-3417. DOI: 10.3390/app10041296. URL: https://www.mdpi.com/2076-3417/10/4/1296.

[13] Alberto Boretti. "Hydrogen internal combustion engines to 2030". In: *International Journal of Hydrogen Energy* 45.43 (2020), pp. 23692–23703. ISSN: 0360-3199. DOI: https://doi.org/10.1016/j.ijhydene.2020.06.022. URL: https://www.sciencedirect.com/science/article/pii/S0360319920321595.

[14] Alberto Boretti. "Technology readiness level of hydrogen storage technologies for transport". In: *Energy Storage* n/a.n/a (), e546. DOI: https://doi.org/10.1002/est2.546. eprint: https://onlinelibrary.wiley.com/doi/pdf/10.1002/est2.546. URL: https://onlinelibrary.wiley.com/doi/abs/10.1002/est2.546.

[15] Bureau Veritas. *Rules for the Classification of Steel Ships - Part B*. Accessed: 2024-08-07. July 2024. URL: https://erules.veristar.com/dy/data/bv/pdf/467-NR_PartB_2024-07.pdf.

[16] Arnab Choudhury, H Chandra, and A Arora. "Application of solid oxide fuel cell technology for power generation—A review". In: *Renewable and Sustainable Energy Reviews* 20 (2013), pp. 430–442.

[17] Giovanni Cinti et al. "System Design and Modeling of a High Temperature PEM Fuel Cell Operated with Ammonia as a Fuel". In: *Energies* 13.18 (2020). ISSN: 1996-1073. URL: https://www.mdpi.com/1996-1073/13/18/4689.

[18] Steelhead Composites. *350 bar hydrogen*. https://www.hannovermesse.de/apollo/hannover_messe_2023/obs/Binary/A1258826/1258826_04076422.pdf. 2018.

[19] Steelhead Composites. *700 bar hydrogen*. https://www.hannovermesse.de/apollo/hannover_messe_2023/obs/Binary/A1258826/1258826_04076419.pdf. 2018.

[20] *Cryogenic Storage of Liquid Hydrogen: Opportunities and Challenges of LH2 Storage*. https://www.sag.at/wp-content/uploads/2021/04/cryogenic-storage-of-lh2_sag.pdf.

[21] Damen. *Marine NOx Reduction System*. https://media.damen.com/image/upload/v1699944799/catalogue/tugs/aftertreatment/product-sheet-aftertreatment-system.pdf. Accessed: February 15, 2024. 2024.

[22] Danfoss. *Data Sheet EM-PMI540-T4000*. Accessed: 2024-09-03. 2024. URL: https://assets.danfoss.com/documents/latest/357594/AI269158146706en-000201.pdf.

[23] Pavlos Dimitriou and Rahat Javaid. "A review of ammonia as a compression ignition engine fuel". In: *International Journal of Hydrogen Energy* 45.11 (2020), pp. 7098–7118. ISSN: 0360-3199. DOI: https://doi.org/10.1016/j.ijhydene.2019.12.209. URL: https://www.sciencedirect.com/science/article/pii/S0360319920300124.

[24] Ahmed G Elkafas et al. "Fuel cell systems for maritime: a review of research development, commercial products, applications, and perspectives". In: *Processes* 11.1 (2022), p. 97.

[25] P. V. Elumalai et al. "Hydrogen in Spark Ignition Engines". In: *Application of Clean Fuels in Combustion Engines*. Ed. by Gabriele Di Blasio et al. Singapore: Springer Nature Singapore, 2022, pp. 195–213. ISBN: 978-981-16-8751-8. DOI: 10.1007/978-981-16-8751-8_10. URL: https://doi.org/10.1007/978-981-16-8751-8_10.

[26] AYK Energy. *Technical Manual: AYK Energy Cygnus Marine Battery System*. 2023. URL: https://www.aykenergy.com/products#cygnus.

[27] *ENGINE TYPE DZ H2 DATASHEET*. Behydro. 2024. URL: https://www.behydro.com/uploads/files/DATASHEETS-Behydro.pdf.

[28] Evoy. *Technical Manual: Evoy Electric Boat Motor System*. 2023. URL: https://www.evoy.no/evoy-faq-electric-boat-motor/.

[29] Maritime Executive. *Record Number of Methanol-Fueled Ships Ordered Reports DNV*. https://maritime-executive.com/article/record-number-of-methanol-fueled-ships-ordered-reports-dnv. Accessed: 25-Jan-2024. 2023.

[30] *Ferry 2306 E3 Full Electric*. Damen Group. 2024. URL: https://www.damen.com/vessels/ferries/city-ferries/ferry-2306-e3-full-electric.

[31] *Fleet – Future Proof Shipping*. https://futureproofshipping.com/about/fleet/. Accessed: March 25, 2024.

[32] JL Gelling. "the Axe Bow: the shape of Ships to Come". In: *The 19th International HISWA Symposium on Yacht Design and Yacht Construction, Amsterdam*. 2006, pp. 1–10.

[33] William Robert Grove. "VIII. On the gas voltaic battery. —Experiments made with a view of ascertaining the rationale of its action and its application to eudiometry". In: *Philosophical Transactions of the Royal Society of London* 133 (1843), pp. 91–112. DOI: 10.1098/rstl.1843.0009.

[34] Arne Güdden et al. "An experimental study on methanol as a fuel in large bore high speed engine applications–Port fuel injected spark ignited combustion". In: *Fuel* 303 (2021), p. 121292.

[35] H2 MOBILITY Deutschland GmbH & Co KG. *Overview: Hydrogen Refuelling for Heavy-Duty Vehicles*. https://h2-mobility.de/wp-content/uploads/sites/2/2021/08/H2-MOBILITY_Overview-Hydrogen-Refuelling-For-Heavy-Duty-Vehicles_2021-08-10.pdf. 2021.

[36] Methanol Institute. *Marine Methanol Report*. Available online: Accessed on March 21, 2024. 2023. URL: https://www.methanol.org/wp-content/uploads/2023/05/Marine_Methanol_Report_Methanol_Institute_May_2023.pdf.

[37] International Maritime Organization. *International Code on Intact Stability, 2008 (2008 IS Code)*. Resolution MSC.267(85). 2008. URL: https://wwwcdn.imo.org/localresources/en/KnowledgeCentre/IndexofIMOResolutions/MSCResolutions/MSC.267(85).pdf.

[38] IPCC. *Climate Change 2021: The Physical Science Basis. Contribution of Working Group I to the Sixth Assessment Report of the Intergovernmental Panel on Climate Change*. Tech. rep. Intergovernmental Panel on Climate Change, 2021. URL: `https://report.ipcc.ch/ar6/wg1/IPCC_AR6_WGI_FullReport.pdf`.

[39] Haris Ishaq, Ibrahim Dincer, and Curran Crawford. "A review on hydrogen production and utilization: Challenges and opportunities". In: *International Journal of Hydrogen Energy* 47.62 (2022), pp. 26238–26264.

[40] Byongug Jeong et al. "Evaluation of the Lifecycle Environmental Benefits of Full Battery Powered Ships: Comparative Analysis of Marine Diesel and Electricity". In: *Journal of Marine Science and Engineering* 8.8 (2020). ISSN: 2077-1312. DOI: `10.3390/jmse8080580`. URL: `https://www.mdpi.com/2077-1312/8/8/580`.

[41] Yasin Karagöz et al. "Effect of hydrogen–diesel dual-fuel usage on performance, emissions and diesel combustion in diesel engines". In: *Advances in Mechanical Engineering* 8 (Aug. 2016). DOI: `10.1177/1687814016664458`.

[42] Gurbinder Kaur and Gurbinder Kaur. "SOFC technology: Its working and components". In: *Solid Oxide Fuel Cell Components: Interfacial Compatibility of SOFC Glass Seals* (2016), pp. 79–122.

[43] *KEYOU H2 Mobility as a Service*. `https://www.keyou.de/solutions`. Accessed: February 20, 2024.

[44] Rahul Krishna et al. "Hydrogen Storage for Energy Application". In: *Hydrogen Storage*. Ed. by Jianjun Liu. Rijeka: IntechOpen, 2012. Chap. 10. DOI: `10.5772/51238`. URL: `https://doi.org/10.5772/51238`.

[45] Donggeun Lee and Han Ho Song. "Development of combustion strategy for the internal combustion engine fueled by ammonia and its operating characteristics". In: *Journal of Mechanical Science and Technology* 32 (2018), pp. 1905–1925.

[46] Charles Lhuillier et al. "Experimental study on ammonia/hydrogen/air combustion in spark ignition engine conditions". In: *Fuel* 269 (2020), p. 117448. ISSN: 0016-2361. DOI: `https://doi.org/10.1016/j.fuel.2020.117448`. URL: `https://www.sciencedirect.com/science/article/pii/S0016236120304439`.

[47] Na Li et al. "A review of reformed methanol-high temperature proton exchange membrane fuel cell systems". In: *Renewable and Sustainable Energy Reviews* 182 (May 2023), p. 113395. DOI: `10.1016/j.rser.2023.113395`.

[48] Wei Li et al. "Investigations on combustion system optimization of a heavy-duty natural gas engine". In: *Fuel* 331 (2023), p. 125621. ISSN: 0016-2361. DOI: `https://doi.org/10.1016/j.fuel.2022.125621`. URL: `https://www.sciencedirect.com/science/article/pii/S0016236122024516`.

[49] Jingping Liu et al. "Experimental study on the performance, combustion and emission characteristics of a high compression ratio heavy-duty spark-ignition engine fuelled with liquefied methane gas and hydrogen blend". In: *Applied Thermal Engineering* 124 (2017), pp. 585–594.

[50] Yang Liu, Jitian Han, and Huailiang You. "Performance analysis of a CCHP system based on SOFC/GT/CO2 cycle and ORC with LNG cold energy utilization". In: *International Journal of Hydrogen Energy* 44.56 (2019), pp. 29700–29710.

[51] K. Machaj et al. "Ammonia as a potential marine fuel: A review". In: *Energy Strategy Reviews* 44 (2022), p. 100926. ISSN: 2211-467X. DOI: `https://doi.org/10.1016/j.esr.2022.100926`. URL: `https://www.sciencedirect.com/science/article/pii/S2211467X22001201`.

[52] Maersk. *Maersk to deploy first large methanol-enabled vessel on Asia - Europe trade lane*. `https://www.maersk.com/news/articles/2023/12/07/maersk-to-deploy-first-large-methanol-enabled-vessel-on-asia-europe-trade-lane`. Accessed: 25-Jan-2024. 2023.

[53] Jasmina Ovcina Mandra. "Maersk invests in Blue World, orders methanol fuel cell pilot system". In: *Offshore Energy* (Dec. 2023). URL: `https://www.offshore-energy.biz/maersk-invests-in-blue-world-orders-methanol-fuel-cell-pilot-system/`.

[54] A Mercier et al. “Improvement of SI engine combustion with ammonia as fuel: effect of ammonia dissociation prior to combustion”. In: *Fuel Communications* 11 (2022), p. 100058.

[55] Methanex Corporation. *Methanex 2022 Sustainability Report*. https://www.methanex.com/wp-content/uploads/2023/04/Methanex-2022-Sustainability-Report.pdf. 2023.

[56] Christine Mounaïm-Rousselle et al. “Operating Limits for Ammonia Fuel Spark-Ignition Engine”. In: *Energies* 14.14 (2021). ISSN: 1996-1073. DOI: 10.3390/en14144141. URL: https://www.mdpi.com/1996-1073/14/14/4141.

[57] MTU. *Series 2000 M72 Marine Diesel Engines for Fast Vessels with High Load Factors (1B)*. Accessed: 2024-01-16. 2020. URL: https://www.mtu-solutions.com/content/dam/mtu/products/defense/marine-and-offshore-service-and-supply/main-propulsion/mtu-series-2000/3231471_Marine_spec_8V10V2000M72_1B.pdf/_jcr_content/renditions/original./3231471_Marine_spec_8V10V2000M72_1B.pdf.

[58] Merck Life Science N.V. *Safety Data Sheet for Sodium borohydride 452882*. Accessed: 2024-01-29. Jan. 2024. URL: https://www.sigmaaldrich.com/NL/en/sds/aldrich/452882?userType=undefined.

[59] Ebrahim Nadimi et al. “Effects of using ammonia as a primary fuel on engine performance and emissions in an ammonia/biodiesel dual-fuel CI engine”. In: *International Journal of Energy Research* 46.11 (2022), pp. 15347–15361. DOI: https://doi.org/10.1002/er.8235. eprint: https://onlinelibrary.wiley.com/doi/pdf/10.1002/er.8235. URL: https://onlinelibrary.wiley.com/doi/abs/10.1002/er.8235.

[60] Helder X Nunes et al. “Rehydrogenation of sodium borates to close the NaBH4-H2 cycle: A review”. In: *Energies* 14.12 (2021), p. 3567.

[61] Sebastian Ohneseit et al. “Thermal and Mechanical Safety Assessment of Type 21700 Lithium-Ion Batteries with NMC, NCA and LFP Cathodes–Investigation of Cell Abuse by Means of Accelerating Rate Calorimetry (ARC)”. In: *Batteries* 9.5 (2023). ISSN: 2313-0105. DOI: 10.3390/batteries9050237. URL: https://www.mdpi.com/2313-0105/9/5/237.

[62] International Maritime Organization. *IMO 2020 – Cutting Sulphur Oxide Emissions*. https://www.imo.org/en/MediaCentre/HotTopics/Pages/Sulphur-2020.aspx. Accessed: February 15, 2024. 2020.

[63] International Maritime Organization. *Nitrogen Oxides (NOx) – Regulation 13*. https://www.imo.org/en/OurWork/Environment/Pages/Nitrogen-oxides-(NOx)---Regulation-13.aspx. Accessed: February 15, 2024. 2020.

[64] Volvo Penta. “Volvo Penta Case Study on HVO Fuel in All Demo and Test Boats”. In: *Volvo Penta News* (June 2022). URL: https://www.volvopenta.com/about-us/news-page/2022/jun/volvo-penta-case-study-on-hvo-fuel-in-all-demo-and-test-boats/.

[65] Mike L Perry and Tom F Fuller. “A historical perspective of fuel cell technology in the 20th century”. In: *Journal of the electrochemical society* 149.7 (2002), S59.

[66] B. Ramne et al. *GreenPilot – Pilot Boat with Minimal Environmental Impact*. Tech. rep. Version 20181128 with appendices. Swedish Maritime Technology Forum, Nov. 2018. URL: https://smtf.se/wp-content/uploads/2019/02/D8.3-Final-Report-ver20181128-with-appendices2.pdf.

[67] B. Ramne et al. *GreenPilot – Pilot Boat with Minimal Environmental Impact*. https://smtf.se/wp-content/uploads/2019/02/D8.3-Final-Report-ver20181128-with-appendices2.pdf. 2018.

[68] Shambhu Singh Rathore et al. “Direct ammonia solid-oxide fuel cells: A review of progress and prospects”. In: *International Journal of Hydrogen Energy* 46.71 (2021), pp. 35365–35384. ISSN: 0360-3199. DOI: https://doi.org/10.1016/j.ijhydene.2021.08.092. URL: https://www.sciencedirect.com/science/article/pii/S0360319921032870.

[69] Hegazy Rezk et al. “Optimal Parameter Identification of a PEM Fuel Cell Using Recent Optimization Algorithms”. In: *Energies* 16.14 (2023). ISSN: 1996-1073. URL: https://www.mdpi.com/1996-1073/16/14/5246.

[70] P. Ribeirinha et al. “Synergetic integration of a methanol steam reforming cell with a high temperature polymer electrolyte fuel cell”. In: *International Journal of Hydrogen Energy* 42.19 (2017). Special Issue on The 21st World Hydrogen Energy Conference (WHEC 2016), 13-16 June 2016, Zaragoza, Spain, pp. 13902–13912. ISSN: 0360-3199. DOI: https://doi.org/10.1016/j.ijhydene.2017.01.172. URL: https://www.sciencedirect.com/science/article/pii/S0360319917303397.

[71] Etienne Rivard, Michel Trudeau, and Karim Zaghib. “Hydrogen Storage for Mobility: A Review”. In: *Materials* 12.12 (2019). ISSN: 1996-1944. DOI: 10.3390/ma12121973. URL: https://www.mdpi.com/1996-1944/12/12/1973.

[72] *RSD Tug 2513 Electric*. Damen Group. 2024. URL: https://www.damen.com/vessels/tugs/electric-tugs/rsd-tug-2513-electric.

[73] Scania. *OC16 071A 372-411kW*. 2024. URL: https://www.scania.com/content/dam/scanianoe/market/master/products-and-services/engines/pdf/specs/power-gen/OC16-071A_372-411kW.pdf.

[74] Zhiwei Shi et al. “Mechanism, performance and modification methods for NH3-SCR catalysts: A review”. In: *Fuel* 331 (2023), p. 125885.

[75] Krzysztof Jan Siczek. “Chapter 2 - Principles of valve train operation”. In: *Tribological Processes in the Valve Train Systems with Lightweight Valves*. Ed. by Krzysztof Jan Siczek. Butterworth-Heinemann, 2016, pp. 3–18. ISBN: 978-0-08-100956-7. DOI: https://doi.org/10.1016/B978-0-08-100956-7.00012-6. URL: https://www.sciencedirect.com/science/article/pii/B9780081009567000126.

[76] Power Sonic. *Technical Manual: Sealed Lead-Acid Batteries*. 2018. URL: https://www.power-sonic.com/wp-content/uploads/2018/12/Technical-Manual.pdf.

[77] Ana-Irina Stan et al. “Lithium ion battery chemistries from renewable energy storage to automotive and back-up power applications—An overview”. In: *2014 International Conference on Optimization of Electrical and Electronic Equipment (OPTIM)*. IEEE. 2014, pp. 713–720.

[78] D. Stapersma and Maritieme Techniek en Technische Materiaalwetenschappen. (3mE) TU Delft Faculteit Werktuigbouwkunde. *Diesel Engines: A Fundamental Approach to Performance Analysis, Turbocharging, Combustion, Emissions and Heat Transfer : Including Thermodynamical Principles. Pt. 1. Diesel Engines A : Performance Analysis and Turbocharging : WB4408A. Performance analysis*. v. 1. TU Delft, 2009. URL: https://books.google.nl/books?id=Bpq7nQEACAAJ.

[79] DNV B.V. Energy Systems. *External Safety Study - Bunkering of Alternative Marine Fuel for Seagoing Vessels*. Tech. rep. 10288905-1. Port of Amsterdam, Apr. 2021. URL: https://www.portofamsterdam.com/sites/default/files/2021-11/DNV%20POA%20%20Final%20Report_External%20safety%20study%20-%20bunkering%20of%20alternative%20marine%20fuels%20for%20seagoing%20vessels_Rev0_2021-04-19.pdf.

[80] Wai Szeto and Dennis YC Leung. “Is hydrotreated vegetable oil a superior substitute for fossil diesel? A comprehensive review on physicochemical properties, engine performance and emissions”. In: *Fuel* 327 (2022), p. 125065.

[81] Blue World Technologies. *HT PEM Fuel Cell Stack*. https://www.blue.world/wp-content/uploads/2023/11/20231031_Stack_data-sheet_ENG.pdf. 2023.

[82] Muhammad R. Usman. “Hydrogen storage methods: Review and current status”. In: *Renewable and Sustainable Energy Reviews* 167 (2022), p. 112743. ISSN: 1364-0321. DOI: https://doi.org/10.1016/j.rser.2022.112743. URL: https://www.sciencedirect.com/science/article/pii/S1364032122006311.

[83] *Value Maritime: Sustainable Solutions for the Maritime Industry*. https://valuemaritime.com/. Accessed: February 13, 2024.

[84] M.C. van Benten, J.T. Padding, and D.L. Schott. “Towards Hydrogen-Fuelled Marine Vessels using Solid Hydrogen Carriers”. English. In: ICBMH 2023: 14th International Conference on Bulk Materials Storage, Handling and Transportation ; Conference date: 11-07-2023 Through 13-07-2023. 2023.

[85] E Van Rheenen et al. “A review of the potential of hydrogen carriers for zero emission, low signature ship propulsion systems”. In: *Conference Proceedings of INEC*. 2022.

[86] Berend van Veldhuizen et al. “Solid Oxide Fuel Cells for Marine Applications”. In: *International Journal of Energy Research* 2023 (2023).

[87] Sebastian Verhelst et al. “Methanol as a fuel for internal combustion engines”. In: *Progress in Energy and Combustion Science* 70 (2019), pp. 43–88.

[88] *Wärtsilä Engine Configurator*. https://www.wartsila.com/marine/engine-configurator. Accessed: 16 January 2024.

[89] Huang Wei et al. “Evaluating the Readiness of Ships and Ports to Bunker and Use Alternative Fuels: A Case Study from Brazil”. In: *Journal of Marine Science and Engineering* 11.10 (2023), p. 1856.

[90] Windy.app. *Maasvlakte 2, Netherlands Wind and Weather Statistics*. Accessed: 2024-08-19. 2024. URL: https://windy.app/forecast2/spot/285524/Maasvlakte+2+Netherlands/statistics.

[91] Nora Wissner et al. *Methanol as a marine fuel*. 2023.

[92] Hossein Ali Yousefi Rizi and Donghoon Shin. “Green Hydrogen Production Technologies from Ammonia Cracking”. In: *Energies* 15.21 (2022). ISSN: 1996-1073. DOI: 10.3390/en15218246. URL: https://www.mdpi.com/1996-1073/15/21/8246.

[93] Zepp.solutions. *DS-X150-S1.2: Zepp.solutions Fuel Cell System Data Sheet*. https://zepp.solutions/wp-content/uploads/2022/09/DS-X150-S1.2.pdf. 2022.

[94] Jianlu Zhang et al. “Chapter 1 - PEM Fuel Cell Fundamentals”. In: *Pem Fuel Cell Testing and Diagnosis*. Ed. by Jianlu Zhang et al. Amsterdam: Elsevier, 2013, pp. 1–42. ISBN: 978-0-444-53688-4. DOI: https://doi.org/10.1016/B978-0-444-53688-4.00001-2. URL: https://www.sciencedirect.com/science/article/pii/B9780444536884000012.

[95] Jieyang Zhou et al. “Optimization of a 30 kW SOFC combined heat and power system with different cycles and hydrocarbon fuels”. In: *International Journal of Hydrogen Energy* 47.6 (2022), pp. 4109–4119.

# Part V

# Appendices

# A

# Trip specifications

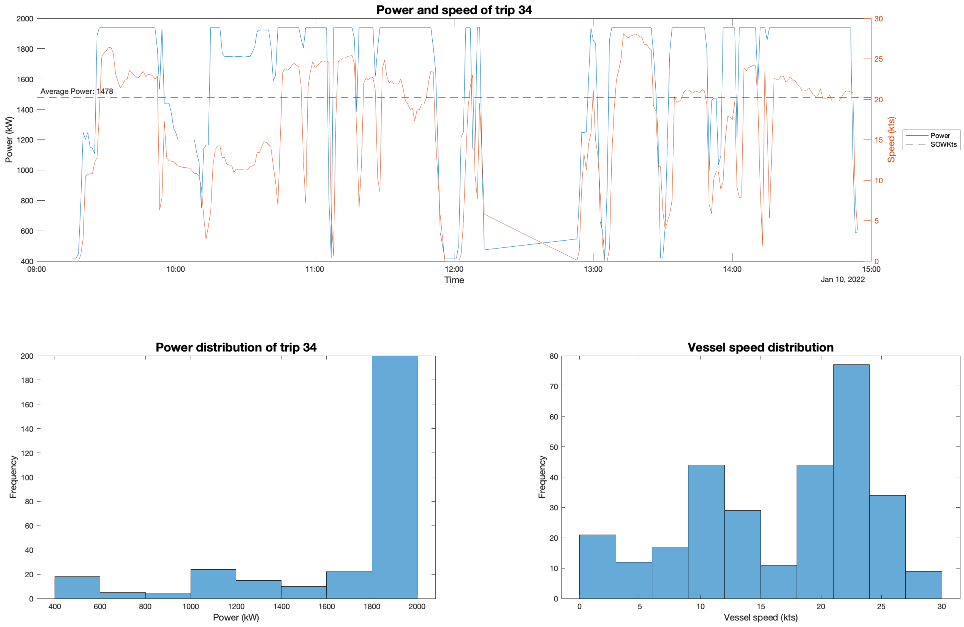


**Figure A.1:** Summary longest trip Lynx in Rotterdam

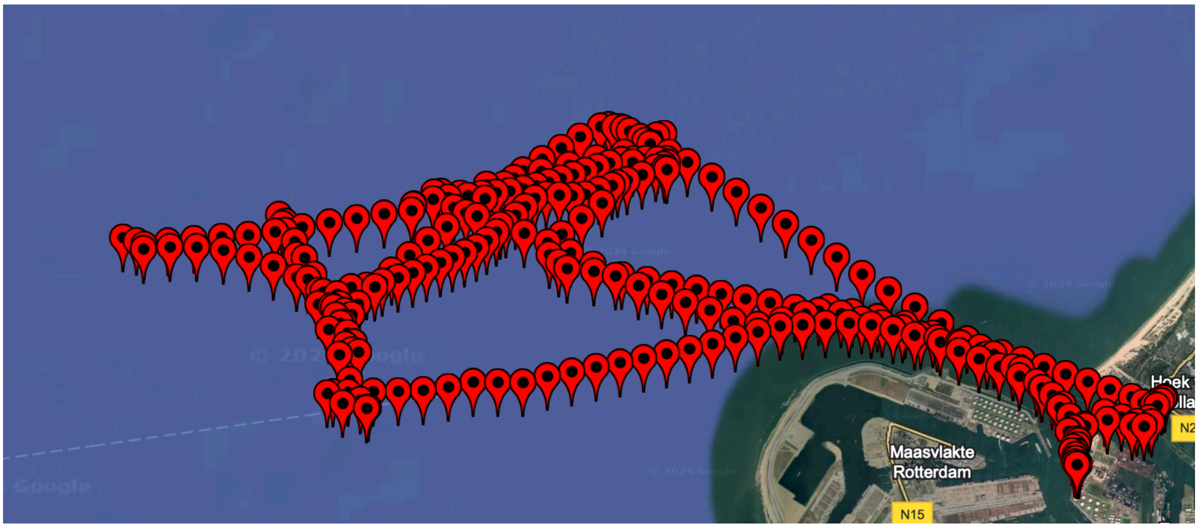


**Figure A.2:** GPS data longest trip Lynx in Rotterdam

# B
# Designs

## B.1. weight calculations

**Table B.1:** Weight calculation methanol FC design

| | **Weight kg** | **LCG m** | **VCG m** |
|---|---|---|---|
| Original lightship | 40241 | 8.061 | 1.908 |
| Engines | 5580 | 5.797 | 1.206 |
| Engine room systems | 8804 | 5.768 | 1.298 |
| Accommodation | 2776 | 14.315 | 1.892 |
| Empty lightship | 23081 | 8.731 | 2.312 |
| Fuel prep Room | 550 | 11.500 | 1,263 |
| Pods | 4950 | 1.011 | -0.324 |
| Electric motors | 1890 | 1.011 | 2.384 |
| Switchboard | 2200 | 6.200 | 1.615 |
| Fuel cells | 5518 | 14.800 | 1.483 |
| Batteries | 2541 | 4.388 | 1.040 |
| Methanol tanks | 1446 | 11.500 | 1.263 |
| Toilet | 300 | 10.000 | 1.892 |
| **Lightship design** | **42476** | **8.024** | **1.736** |
| Crew & effects | 200 | 11.250 | 4.230 |
| Personnel | 680 | 8.860 | 4.230 |
| Sludge tank | 6 | 2.375 | 0.244 |
| Aft deck cargo | 945 | 2.000 | 3.120 |
| Supply owner | 200 | 12.000 | 1.950 |
| Fresh water | 200 | 10.000 | 0.477 |
| Waste water | 20 | 10.000 | 0.204 |
| Methanol fuel | 2304 | 11.500 | 1.263 |
| **Full load design** | **47031** | **8.125** | **1.782** |
| Lightship displacement (m3) | 41.440 | 8.047 | 0.562 |
| Full load displacement m3 | 45.883 | 8.090 | 0.594 |

**Table B.2:** Weight calculation ammonia ICE design

| | **Weight (kg)** | **LCG (m)** | **VCG (m)** |
|---|---|---|---|
| Original lightship | 40241 | 8.061 | 1.908 |
| Engines | 5580 | 5.797 | 1.206 |
| Accommodation | 2776 | 13.237 | 1.892 |
| Empty lightship | 31885 | 8.007 | 2.032 |
| Toilet | 500 | 9.210 | 1.892 |
| Ammonia tanks | 1934 | 12.010 | 1.534 |
| Engines | 4760 | 5.797 | 1.206 |
| Fuel prep. room | 500 | 14.000 | 1.534 |
| **Lightship design** | **39579** | **8.027** | **1.900** |
| Crew & effects | 200 | 11.250 | 4.230 |
| Personnel | 680 | 8.860 | 4.230 |
| Sludge tank | 6 | 2.375 | 0.244 |
| Aft deck cargo | 945 | 2.000 | 3.120 |
| Supply owner | 200 | 12.000 | 1.950 |
| Fresh water | 200 | 9.000 | 0.477 |
| Waste water | 20 | 15.000 | 0.204 |
| Ammonia fuel | 2919 | 12.010 | 1.534 |
| **Full load design** | **44750** | **8.211** | **1.941** |
| Lightship displacement ($m^3$) | 38.614 | 8.125 | 0.545 |
| Full load displacement ($m^3$) | 43.658 | 8.164 | 0.582 |

**Table B.3:** Weight calculation ammonia FC design

| | Weight (kg) | LCG (m) | VCG (m) |
|---|---|---|---|
| Original lightship | 40241 | 8.061 | 1.908 |
| Engines | 5580 | 5.797 | 1.206 |
| Engine room systems | 8804 | 5.768 | 1.298 |
| Accommodation | 2776 | 13.237 | 1.892 |
| Empty lightship | 23081 | 8.860 | 2.312 |
| Fuel prep. room | 600 | 11.950 | 1.571 |
| Pods | 5400 | 1.011 | -0.324 |
| Electric motors | 1840 | 1.011 | 2.384 |
| Switchboard | 2400 | 6.900 | 1.615 |
| Fuel cells | 6019 | 14.600 | 1.483 |
| Batteries | 2772 | 5.200 | 1.040 |
| Ammonia tanks | 1542 | 9.700 | 1.327 |
| **Lightship design** | **43654** | **8.082** | **1.711** |
| Crew & effects | 200 | 11.250 | 4.230 |
| Personnel | 680 | 8.860 | 4.230 |
| Sludge tank | 6 | 2.375 | 0.244 |
| Aft deck cargo | 945 | 2.000 | 3.120 |
| Supply owner | 200 | 12.000 | 1.950 |
| Ammonia fuel | 2443 | 9.700 | 1.327 |
| **Full load design** | **48128** | **8.084** | **1.766** |
| Lightship displacement ($m^3$) | 42.59 | 8.059 | 0.571 |
| Full load displacement ($m^3$) | 46.95 | 8.100 | 0.602 |

**Table B.4:** Weight calculation hydrogen ICE design

| | Weight (kg) | LCG (m) | VCG (m) |
|---|---|---|---|
| Original lightship | 40241 | 8.061 | 1.908 |
| Engines | 5580 | 5.797 | 1.206 |
| Accommodation | 2776 | 13.237 | 1.892 |
| Empty lightship | 31885 | 8.007 | 2.032 |
| Hydrogen tanks | 6336 | 11.767 | 1.610 |
| Engines | 5580 | 4.400 | 1.206 |
| Fuel prep. room | 500 | 16.151 | 1.571 |
| **lightship design** | **44301** | **8.182** | **1.863** |
| Crew & effects | 200 | 11.250 | 4.230 |
| Personnel | 680 | 8.860 | 4.230 |
| Sludge tank | 6 | 2.375 | 0.244 |
| Aft deck cargo | 945 | 2.000 | 3.120 |
| Supply owner | 200 | 12.000 | 1.950 |
| Hydrogen fuel | 298 | 11.767 | 1.610 |
| **Full load design** | **46630** | **8.118** | **1.931** |
| Lightship displacement ($m^3$) | 43.22 | 8.161 | 0.579 |
| Full load displacement ($m^3$) | 45.49 | 8.179 | 0.596 |

**Table B.5:** Weight calculation hydrogen FC design

| | Weight (kg) | LCG (m) | VCG (m) |
|---|---|---|---|
| Original lightship | 40241 | 8.061 | 1.908 |
| Engines | 5580 | 5.797 | 1.206 |
| Engine room systems | 8804 | 5.768 | 1.298 |
| Accommodation | 2776 | 13.237 | 1.892 |
| Empty lightship | 23081 | 8.860 | 2.312 |
| Fuel prep. room | 550 | 8.000 | 1.571 |
| Pods | 4950 | 1.011 | -0.324 |
| Electric motors | 1680 | 1.011 | 2.384 |
| Switchboard | 2200 | 7.066 | 1.292 |
| Fuel cells | 3905 | 4.506 | 1.369 |
| Batteries | 2541 | 16.500 | 1.090 |
| Hydrogen tanks | 7986 | 11.662 | 1.617 |
| **Design lightship** | **46893** | **8.185** | **1.717** |
| Crew & effects | 200 | 11.250 | 4.230 |
| Personnel | 680 | 8.860 | 4.230 |
| Sludge tank | 6 | 2.375 | 0.244 |
| Aft deck cargo | 945 | 2.000 | 3.120 |
| Supply owner | 200 | 12.000 | 1.950 |
| Hydrogen fuel | 352 | 11.662 | 1.617 |
| **Full load design** | **48924** | **8.102** | **1.790** |
| Lightship displacement ($m^3$) | 45.75 | 8.089 | 0.594 |
| Full load displacement ($m^3$) | 47.73 | 8.107 | 0.608 |

## B.2. Resistance graphs

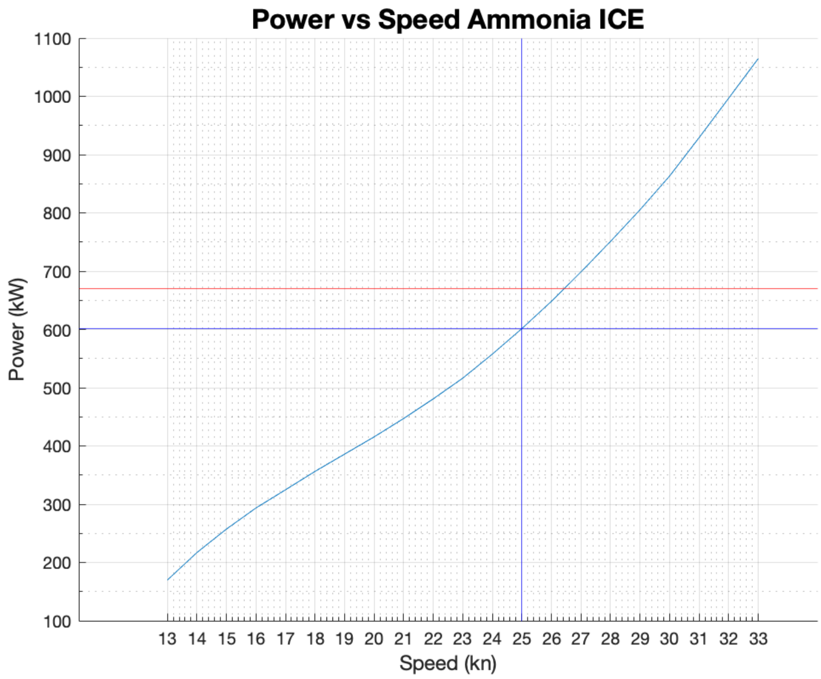


**Figure B.1:** Resistance curve ammonia ICE design

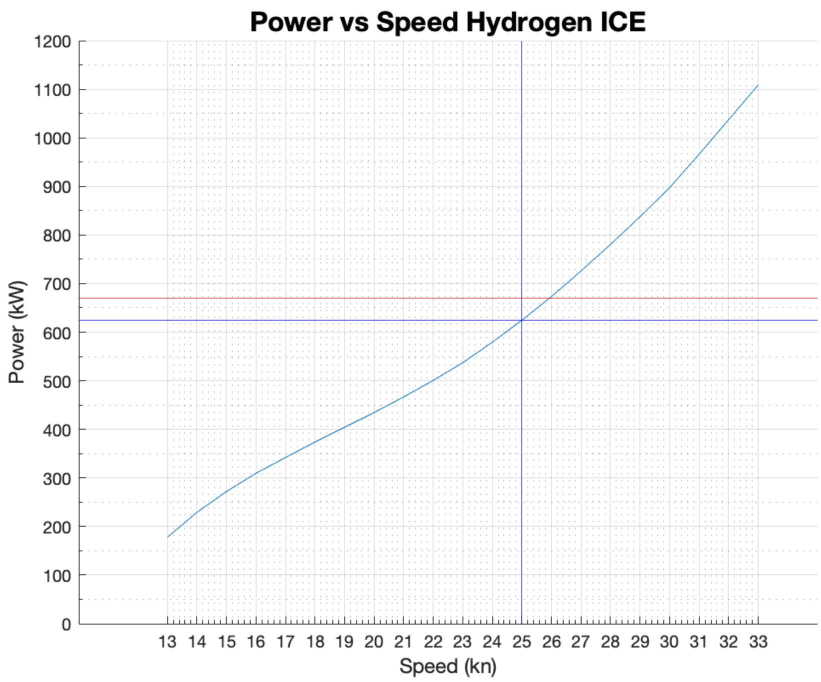


**Figure B.2:** Resistance curve hydrogen ICE design

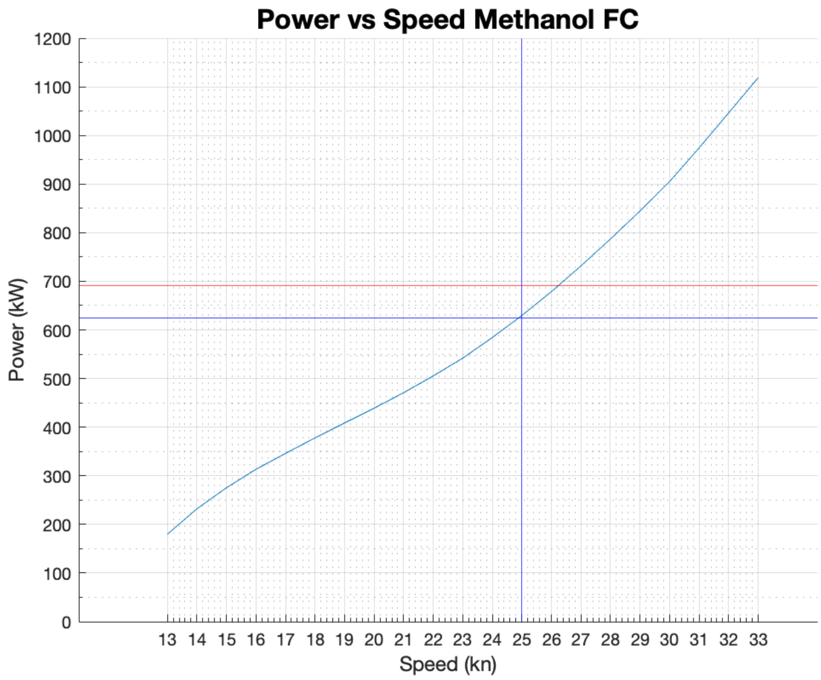


**Figure B.3:** Resistance curve methanol FC design

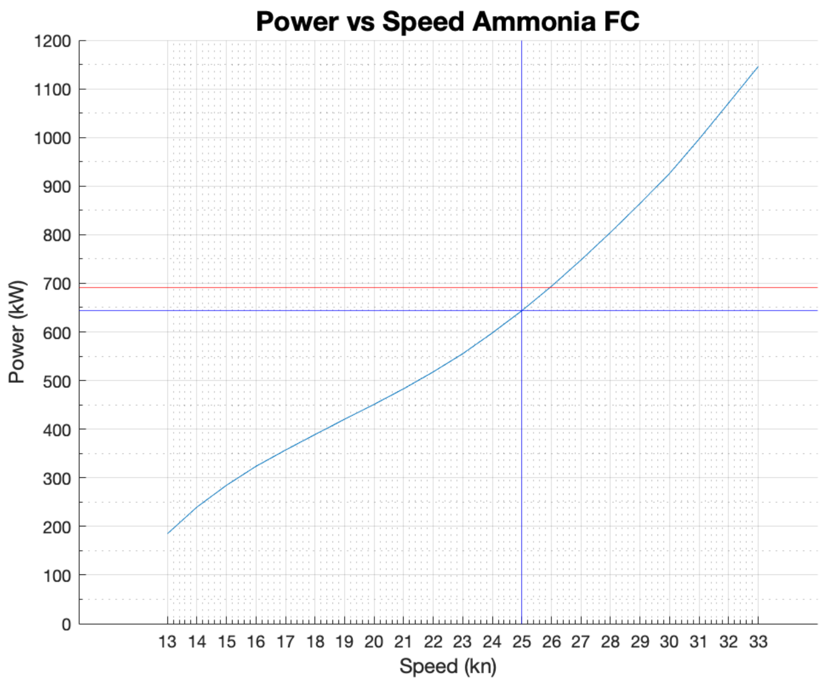


**Figure B.4:** Resistance curve ammonia FC design

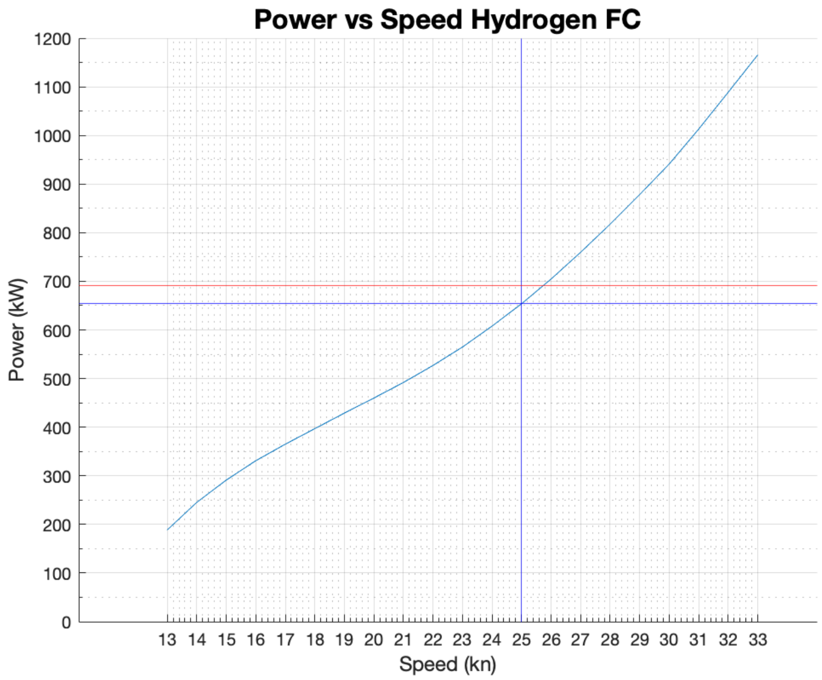


**Figure B.5:** Resistance curve hydrogen FC design

## B.3. Stability

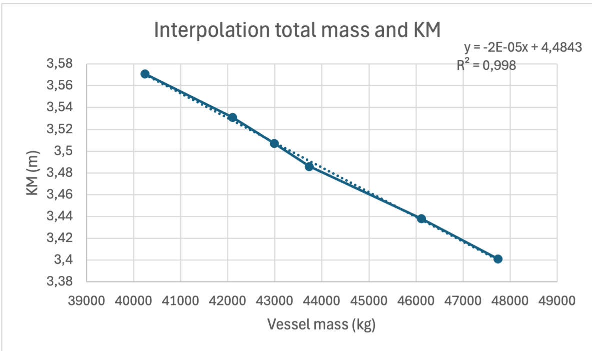


**Figure B.6:** KM interpolation based on Damen 2205 FRP

**Table B.6:** Stability components of the six designs in lightweight condition

| | KM (m) | KG (m) | GM (m) |
|---|---|---|---|
| ICE methanol | 3.65 | 1.90 | 1.76 |
| ICE ammonia | 3.69 | 1.90 | 1.79 |
| ICE hydrogen | 3.60 | 1.86 | 1.74 |
| FC methanol | 3.63 | 1.74 | 1.90 |
| FC ammonia | 3.61 | 1.71 | 1.90 |
| FC hydrogen | 3.55 | 1.72 | 1.83 |